2021-01-15

The effects of diketopiperazines on the virulence of Burkholderia cepacia complex species

Jervis, Nicole Marie

UNIVERSITY OF CALGARY

The effects of diketopiperazines on the virulence of *Burkholderia cepacia* complex species

by

Nicole Marie Jervis

A THESIS

SUBMITTED TO THE FACULTY OF GRADUATE STUDIES

IN PARTIAL FULFILMENT OF THE REQUIREMENTS FOR THE

DEGREE OF MASTER OF SCIENCE

GRADUATE PROGRAM IN BIOLOGICAL SCIENCES

CALGARY, ALBERTA

JANUARY, 2021

Abstract

Recognized as a novel class of quorum sensing inhibitors (QSIs), 2,5-diketopiperazines (DKPs) are small, organic molecules that hold many important physiochemical properties which has led to recent inquiries into their effects towards limiting the pathogenicity of multi-drug resistant bacterial pathogens. Species within the *Burkholderia cepacia* complex (Bcc) are one such group of pathogens that require attention towards the development of alternative therapeutic strategies given their detrimental clinical outcomes, particularly in patients with cystic fibrosis. By targeting Bcc QS regulation, our data demonstrated DKPs, cyclo(-D-ala-val), cyclo(-pro-val), cyclo(-leu-pro), and cyclo(-phe-pro) to alter the production of extracellular virulence factors and to decrease the production of biofilm-associated factors which comprise the protective extracellular matrix of Bcc biofilms. Further analysis demonstrated these DKPs to also possess antibiotic potentiator activity, enhancing the antimicrobial activity of ceftazidime, meropenem, and tobramycin. Taken together, the data collected in this study offers an initial step towards understanding the potential role of DKPs in the development of alternative therapeutics.

Acknowledgements

Foremost, I would like to acknowledge my supervisor Dr. Douglas Storey. Thank you for all your careful guidance, helpful advice and unwavering support that you have provided me throughout the years. After taking me on as an eager undergraduate research student, I am grateful for your belief in my abilities to continue on in graduate studies where your kindness and mentorship has helped shaped me into the researcher I am today. I am especially thankful for the opportunity I had to attend conferences, work as a teaching assistant, and learn the art of backyard croquet. Above all, your patience and understanding in allowing me the freedom to navigate through my project while also offering your valuable knowledge and encouragement will always be appreciated. I would also like to thank my committee members Dr. J. Harrison and Dr. M. Parkins, as well as Dr. A. Savchenko for all of their guidance and dedication towards helping me improve as a scientist.

To all the members of the Storey lab, I will always be grateful for the memorable times we shared, both in the lab brainstorming ideas for experiments, as well as outside the lab gift wrapping at the mall, attending concerts, and wandering unknown areas of campus in search of Pokémon. To the Harrison lab, thank you for including me as an unofficial member by generously offering lab space to carry out experiments and for all your help and advice when said experiments did not turn out. To my labmate Nabiha Mehina, your support and friendship has been immeasurable throughout our time together. From our first day as new graduate students collecting an abundance of free pens at orientation, to our final days of jamming to BTS while scrambling to finish our theses, I owe you my deepest debt of gratitude that will no doubt carry on as we continue forward into the next chapters of our lives.

To my partner, Daniel Aschauer, for everything you have done unconditionally to take care of my happiness and to support me throughout my studies, thank you. I am grateful to

have shared these experiences with you and will forever hold them close as we continue to share more together in the future.

Above all, I would like to thank my family for all their love and constant support in my academic endeavours. To my parents, Jennifer and Rocky, your encouragement to take on new challenges never ceases to motivate me to do better and I will eternally be grateful for your care in my well-being. To my sister, Vanessa, your energy and passion for life will always be a true inspiration that I will forever admire, thank you for sharing your light with me every day.

Dedication

To my parents, who provided me with the ability to find my own way.

Table of Contents

Abstract ii
Acknowledgements iii
Dedication v
Table of Contents vi
List of Tables ix
List of Figures and Illustrations x
List of Symbols, Abbreviations and Nomenclature xi

CHAPTER ONE: INTRODUCTION 1
1.1 2,5-Diketopiperazines (DKPs) 1
1.1.1 Physiochemical properties 1
1.1.2 Biological significance 3
1.1.3 DKPs as quorum sensing inhibitors 4
1.1.4 DKPs of interest 5
1.2 The *Burkholderia cepacia* complex (Bcc) 6
1.2.1 An important group of cystic fibrosis pathogens 6
1.2.2 Pathogenic traits 8
1.2.2.1 Extracellular virulence factors 8
1.2.2.2 Biofilm formation 10
1.2.3 Quorum sensing regulation 14
1.2.4 Treatment of Bcc infections 16
1.3 Project Overview 19
1.3.1 Hypothesis 19
1.3.2 Objectives 19

CHAPTER TWO: MATERIALS AND METHODS 20
2.1 Bacterial Strains and Growth Conditions 20
2.1.1 Maintenance and growth 20
2.1.2 Synthetic cystic fibrosis sputum media 20
2.2 Preparation of 2,5-Diketopiperazines 22
2.3 Growth Assessments 24
2.3.1 Growth curves 24
2.3.2 Viable cell enumeration 24
2.4 Extracellular Virulence Factor Assessments 25
2.4.1 Isolation of cell-free spent media 25
2.4.2 Protease production 26
2.4.3 Lipase production 27
2.4.4 Siderophore production 27

2.5 Biofilm Assessments 31
2.5.1 Growth conditions 31
2.5.2 Crystal violet staining assay 31
2.5.3 Viable biofilm cell enumeration 34
2.6 Antibiotic Susceptibility Testing 35
2.6.1 MBEC of antibiotics to treat Bcc biofilms 35
2.6.2 MBEC of antibiotics in combination with DKPs to treat Bcc biofilms 36
2.7 Statistical Analyses 37

CHAPTER THREE: DKPS AS ANTVIRULENCE AGENTS 38
3.1 Introduction 38
3.2 Results 40
3.2.1 DKPs do not affect the growth rate or viability of Bcc species 40
3.2.2 Extracellular virulence factor production of Bcc species 45
3.2.3 DKPs alter extracellular virulence factor production of Bcc species 50
3.2.3.1 Protease production 50
3.2.3.2 Lipase production 55
3.2.3.3 Siderophore production 60
3.3 Summary 65

CHAPTER FOUR: DKPS AS ANTIBIOFILM AGENTS 67
4.1 Introduction 67
4.2 Results 68
4.2.1 Bcc biofilm biomass production over time 68
4.2.2 DKPs limit Bcc biofilm biomass production 72
4.2.3 Bcc viable biofilm cell count over time 83
4.2.4 DKPs do not affect the viability of Bcc species 86
4.3 Summary 90

CHAPTER FIVE: DKPS AS ANTIBIOTIC POTENTIATORS 92
5.1 Introduction 92
5.2 Results 94
5.2.1 Bcc biofilms have a high level of tolerance to antibiotics 94
5.2.2 DKPs potentiate antibiotic activity in the treatment of Bcc biofilms 98
5.2.2.1 Ceftazidime 98
5.2.2.2 Meropenem 101
5.2.2.3 Tobramycin 104
5.3 Summary 107

CHAPTER SIX: DISCUSSION 109
6.1 DKPs alter the virulence phenotype of Bcc species 111

6.2 DKPs limit the production of biofilm-associated factors....115
6.3 DKPs potentiate the activity of antibiotics....119
6.4 Summary of Findings....122
6.5 Future Directions....124
6.5.1 Transcriptomic analyses to assess the effects of DKPs at the molecular level....124
6.5.2 Confocal laser scanning microscopy to visualize Bcc biofilms....124
6.5.3 Examining the potentiating activity of DKPs in vivo....125
6.5.4 Investigating different treatment combinations on a larger panel of clinical isolates....126
6.5.5 Evolutionary trajectory assessment of DKPs as antibiotic potentiators 126
6.6 Concluding Remarks....127

REFERENCES....128

SUPPLEMENTARY INFORMATION....148

List of Tables

Table 2.1: Bacterial strains used in this study 21

Table 2.2: Amino acids added to synthetic cystic fibrosis sputum media 23

Table 3.1: DKPs decrease Bcc protease production at early stationary phase 51

Table 3.2: DKPs decrease Bcc protease production at late stationary phase 53

Table 3.3: DKPs decrease Bcc lipase production at early stationary phase 56

Table 3.4: DKPs decrease Bcc lipase production at late stationary phase 58

Table 3.5: DKPs increase Bcc siderophore production at early stationary phase 61

Table 3.6: DKPs increase Bcc siderophore production at late stationary phase 63

Table 4.1: DKPs limit Bcc biofilm biomass production after 4 hours of incubation 73

Table 4.2: DKPs limit Bcc biofilm biomass production after 8 hours of incubation 76

Table 4.3: DKPs limit Bcc biofilm biomass production after 12 hours of incubation 78

Table 4.4: DKPs limit Bcc biofilm biomass production after 24 hours of incubation 81

Table 4.5: DKPs do not affect Bcc viable biofilm cell counts over time 87

List of Figures and Illustrations

Figure 1.1: 2,5-Diketopiperazines (DKPs) 2

Figure 1.2: The biofilm life cycle and biofilm extracellular matrix of Bcc species 11

Figure 1.3: A schematic of AHL-based quorum sensing regulation in Bcc species 15

Figure 2.1: Representative images of extracellular virulence factor assessments 28

Figure 2.2: Representative images of the crystal violet staining assay 33

Figure 3.1: DKPs do not affect the growth rate of Bcc species 41

Figure 3.2: DKPs do not affect the viable cell count of Bcc species 43

Figure 3.3: Extracellular virulence factor production of Bcc species at early and late stationary phases of bacterial growth 46

Figure 4.1: Bcc biofilm biomass production over time 70

Figure 4.2: Bcc viable biofilm cell count over time 84

Figure 5.1: Antibiotic treatment of Bcc biofilms, *in vitro* 95

Figure 5.2: DKPs potentiate the activity of ceftazidime in the treatment of Bcc biofilms 99

Figure 5.3: DKPs potentiate the activity of meropenem in the treatment of Bcc biofilms 102

Figure 5.4: DKPs potentiate the activity of tobramycin in the treatment of Bcc biofilms 105

Supplementary Figure 1: Growth curves of Bcc species 149

Supplementary Figure 2: Biofilm equivalency test 151

List of Symbols, Abbreviations and Nomenclature

Symbol	Definition
AHL	*N*-acyl-homoserine lactone
BapA	biofilm-associated protein A
Bcc	*Burkholderia cepacia* complex
BH	baicalin hydrate
˚C	degree Celsius
C6-HSL	*N*-hexanoyl-homoserine lactone
C8-HSL	*N*-octanoyl-homoserine lactone
CAS	chrome azurol S
cci	cenocepacia pathogenicity island
CDPS	cyclodipeptide synthase
CF	Cystic Fibrosis
CFU	colony forming units
CV	crystal violet
ddH_2O	double distilled water
DKP	2,5-Diketopiperazine
ECM	extracellular matrix
e-DNA	extracellular DNA
EPS	extracellular polymeric substance
g	gram
h	hours
L	litre
M	molar
mg	milligram
MHA	Mueller Hinton agar
mL	millilitre
mM	millimolar
MVCC	mean viable cell count

n	number of replicates
NRPS	non-ribosomal peptide synthetase
OD	optical density
PB	phosphate buffer
PBS	phosphate-buffered saline
pH	potential of hydrogen
PNAG	poly-β-1,6-N-acetylglucosamine
QS	quorum sensing
QSI	quorum sensing inhibitor
ROS	reactive oxygen species
rpm	revolutions per minute
SCFM	synthetic cystic fibrosis sputum media
SD	standard deviation
Sig.	significance
TCA	trichloroacetic acid
v/v	volume/volume
w/v	weight/volume
Δ	change
µL	microlitre
µM	micromolar

Chapter One: Introduction

1.1 2,5-Diketopiperazines (DKPs)

1.1.1 Physiochemical properties

2,5-Diketopiperazines (DKPs) are a highly diverse and abundant group of biologically active cyclic dipeptides that carry important chemical and medicinal properties (Ressurreicao *et al.* 2011; Ortiz and Sansinenea, 2017). Consisting of two amide groups bound together in a heterocyclic six-membered-ring formation as depicted in Figure 1.1a, DKPs are characterized as having a conformationally semi-rigid backbone that provides a great amount of stability against both heat and proteolytic activity (Corey, 1938; Borthwick, 2012). Recognized as privileged structures, these molecules not only maintain a stable core ring, but they also hold many other chemical advantages that label them as attractive scaffolds for drug discovery (Giessen and Marahiel, 2015; Ortiz and Sansinenea, 2017).

The synthesis of DKPs can occur through a number of processes given the level of reactivity at each position of their core. Chemical methods including amide bond formation, *N*-alkylation, *C*-acylation, and tandem cyclization of amino acids are all utilized in their formation (Borthwick, 2012). Following initial assembly, modifying enzymes can then be employed as a means of adding different types of substituent groups to the DKP core, giving rise to the high degree of variation that is seen among these molecules (Lautru *et al.* 2002; Saruwatari *et al.* 2014; Giessen and Marahiel, 2015). Diversity can be introduced at all six positions of their core, being the C3 and C6 carbon positions, the N1 and N4 nitrogen positions, or at the C2 and C5 carbonyl carbon positions (Figure 1.1a) (Borthwick, 2012). Of these, the C3 and C6 positions are considered as the most readily available positions to be functionalized, where the addition of substituent groups can range from the simplest form of a single amino acid, such as in the

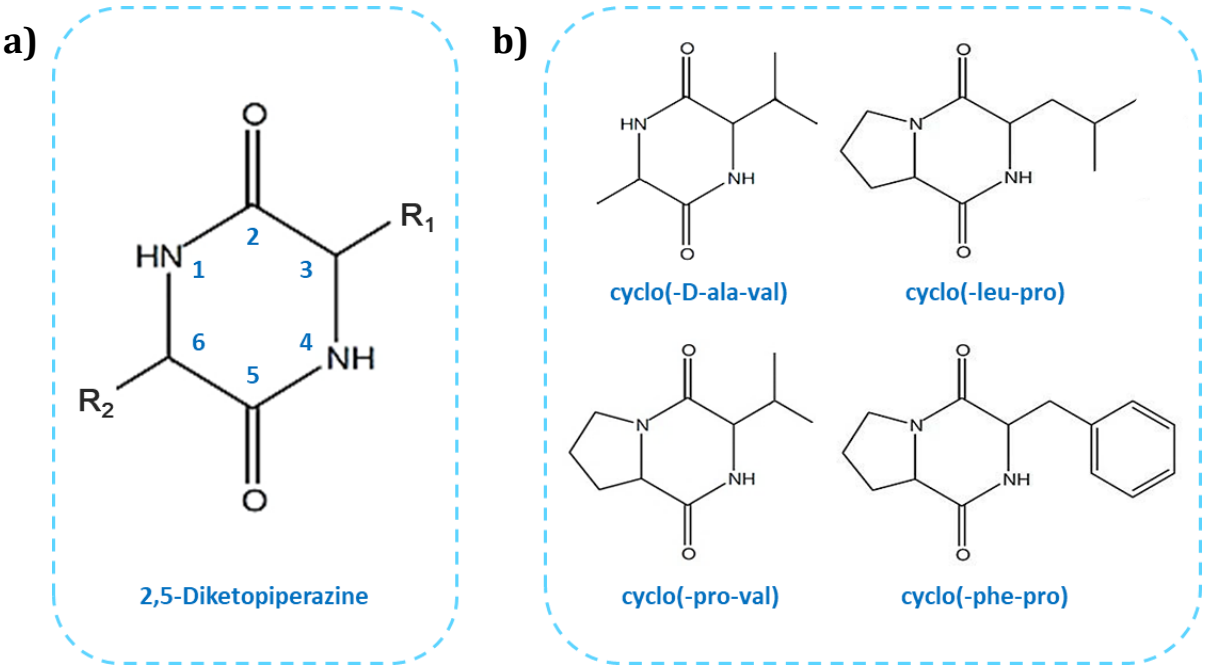

Figure 1.1: 2,5-Diketopiperazines (DKPs)

(a) The primary DKP core structure (blue numbers indicate the different positions of the ring), **(b)** The DKPs under investigation in this study, including cyclo(-D-ala-val), cyclo(-pro-val), cyclo(-leu-pro) and cyclo(-phe-pro).

case of the DKPs represented in Figure 1.1b, to much larger and more complex structures that possess multiple functional groups (Borthwick, 2012; Ortiz and Sansinenea, 2017). With their ease of synthesis, conformationally strong core, and highly diverse substituent groups, the physiochemical nature of DKPs has allowed for great scientific inquiry into their biologically significant roles in several applications (Giessen and Marahiel, 2015).

1.1.2 Biological significance

DKPs hold several important properties that have over time been incorporated in many biologically and clinically significant applications (Ressurreicao *et al.* 2011; Giessen and Marahiel, 2015). Although DKPs are naturally abundant as secondary metabolites produced by species from all kingdoms of life, a large majority of the DKPs used as therapeutic compounds were originally isolated from *Aspergillus* and *Penicillium* species (Campbell *et al.* 2009; Gonzalez *et al.* 2012; Ortiz and Sansinenea, 2017). In many cases, these naturally secreted molecules were further exploited with the aim of generating derivatives that possess higher potencies and enhanced abilities to interact with different biological targets (Gonzalez *et al.* 2012). This has ultimately led to identifying DKPs that can act as anti-inflammatory agents, oxytocin antagonists, neuroprotective agents, and even as anti-cancer drugs (Borthwick, 2012; Liao *et al.* 2014).

Some pronounced examples of DKPs in therapeutics can include the oxytocin antagonist Retosiban, a DKP-based drug administered for the prevention of preterm birth (McCafferty *et al.* 2007; Borthwick and Liddle, 2011), or the use of Tadalafil, a distinctly annulated DKP prescribed for treating erectile dysfunction and pulmonary arterial hypertension (Daugan *et al.* 2003; Galie *et al.* 2008). One drug that is currently undergoing stage III clinical trials for its use in treating non-small cell lung cancer and preventing chemotherapy-induced neutropenia is the

DKP now referred to as plinabulin (Kanoh *et al.* 1999; Singh *et al.* 2011). Originally isolated from *Aspergillus ustus* as (-)-phenylahistin, plinabulin is a derivative that functions as a tubulin depolymerizing agent, inhibiting tumor cell proliferation and inducing apoptosis (Nicholson *et al* 2006). Quite notably, Ding and colleagues (2020) recently synthesized and screened a large panel of plinabulin derivatives and identified some to have even greater potency profiles and cytotoxicity towards several human cancer cell lines.

In addition to the advancements that have been made in human therapeutics, DKPs have also demonstrated the capacity to hold various anti-pathogenic properties by targeting microbial entities (Borthwick, 2012; Gonzalez *et al.* 2012). DKP molecules such as bicyclomycin (Miyoshi *et al.* 1972; Vior *et al.* 2018), brevianamide F (Bringmann *et al.* 2004), and aplaviroc (Maeda *et al.* 2004), have all been shown to carry anti-viral, anti-fungal and/or anti-bacterial activities. These DKPs along with their respective derivatives have therefore been extensively studied in terms of their potential clinical applications (Borthwick, 2012; Zhao *et al.* 2019). Taken together, the multitude of studies that have been dedicated towards characterizing the various properties of DKPs has led to their incorporation in several drugs and has also ignited special interest in continued research towards identifying other clinically significant functions.

1.1.3 DKPs as quorum sensing inhibitors

A relatively new subset of DKPs that has recently been under investigation includes those capable of limiting the pathogenicity of bacterial species by functioning as quorum sensing inhibitors (QSIs), such as those represented in Figure 1.1b (Holden *et al.* 1999; Campbell *et al.* 2009). This group of DKPs were first identified as secondary metabolites naturally secreted from different Gram-negative bacteria, such as *Escherichia coli* and *Pseudomonas aeruginosa,* and have since been identified in ~90% of Gram-negative bacterial species as well as in other

microbes and higher organisms (Holden *et al.* 1999; Carvalho and Abraham, 2012; Gonzalez *et al.* 2012). While their wide-spread abundance has led to detailed documentation of their non-ribosomal peptide synthetase (NRPS) and cyclodipeptide synthase (CDPS) biosynthetic pathways, the biological role behind their production is still largely unclear (Belin *et al.* 2012; Gonzalez *et al.* 2012). Based on their structural properties, however, it is hypothesized that their production is part of an uncharacterized form of intra- and inter-species communication (Gu *et al.* 2013).

When exposed to unnaturally high concentrations, these DKP molecules exhibit antagonistic effects towards LuxIR-mediated QS systems, which are recognized as global regulatory systems employed by many bacterial species as a means of regulating genes linked to their pathogenicity (Campbell *et al.* 2009; Carvalho and Abraham, 2012; Scoffone *et al.* 2016). A recent study by Buroni and colleagues (2018) provided evidence towards the possible mechanism behind this inhibitory activity, identifying a site on the LuxI-based autoinducer synthase in which DKPs are likely interacting. Specifically, by binding near a stabilizing loop that holds the two precursor molecules, DKPs interfere with the initial step in the synthesis of the N-acyl homoserine lactone (AHL) signalling molecules that are responsible for activating its cognate LuxR-based transcriptional regulator (Buroni *et al.* 2018). With a great reliance on QS regulation for the active expression of several virulence factor determinants and antibiotic resistance mechanisms, utilizing DKPs that function as QSIs offers an ideal approach for sensitizing multi-drug resistant pathogens to antibiotic treatments (Scoffone *et al.* 2016, 2017).

1.1.4 DKPs of interest

Previous work conducted in our lab by Purighalla (2011), identified four DKP molecules as having antagonistic effects towards species of the *Burkholderia cepacia* complex (Bcc), an

important group of human bacterial pathogens, particularly in regard to their clinical manifestations in patients with cystic fibrosis (CF) (Figure 1.1b). Using *lux*-reporter assays, DKPs cyclo(-D-ala-val), cyclo(-pro-val), cyclo(-leu-pro) and cyclo(-phe-pro) were all shown to be inhibitory towards the expression of the gene coding for the autoinducer synthase, *cepI,* as well as the gene coding for the transcriptional regulator, *cepR,* of the CepIR QS system of Bcc species. Additionally, Purighalla also showed this inhibition to be non-competitive in nature as the addition of exogenous AHL molecules to the *cepI-luxABCE* reporter system did not rescue the expression of *cepI* while in the presence of each of the four DKP molecules.

Not a lot is known about these particular DKPs in the context of their specific mode of action or their anti-pathogenic properties towards species of the Bcc. Given the results that have already been reported for other DKPs acting as QSIs (Scoffone *et al.* 2016, Buroni *et al.* 2018), it is possible that these four DKPs of interest could share similar inhibitory properties towards the pathogenic phenotype of Bcc species. Therefore, further scientific investigation is needed to gain a greater understanding of their potential role in the field of alternative therapeutic research, particularly in the treatment of infections caused by species of the Bcc.

1.2 The *Burkholderia cepacia* complex (Bcc)

1.2.1 An important group of cystic fibrosis pathogens

Cystic fibrosis (CF) is an autosomal recessive disorder that is characterized by the build-up of complex, viscid mucus lining multiple organs of the body with the greatest clinical complications seen primarily in the lungs (Cohen and Prince, 2012; Elborn, 2016). Caused by a genetic mutation in the cystic fibrosis transmembrane conductance regulator (CFTR), the movement of ions and water across epithelial cell membranes is severely impaired, resulting in the excess accumulation of dehydrated mucus that is unable to be expelled by the normal

process of mucociliary clearance (Riordan *et al.* 1989; Matsui *et al.* 1998; Gadsby *et al.* 2006; Munkholm and Mortensen, 2014). This in turn creates an opportunity for a multitude of microorganisms and infecting agents to colonize and elicit damage to the lungs through their production of various virulence factor determinants and subsequent stimulation of a severe inflammatory response (Delhaes *et al.* 2012; Bragonzi *et al.* 2018). There are several notable bacterial pathogens, including *Staphylococcus aureus, Haemophilus influenza* and *Pseudomonas aeruginosa,* that make up most of the early colonizers and are therefore largely responsible for initial damage to the lung tissue (Cystic Fibrosis Canada, 2018). While other opportunistic pathogens, such as those within the *Burkholderia cepacia* complex (Bcc), take advantage of these already highly compromised conditions and increase in prevalence later in adulthood (Courtney *et al.* 2004; Coutinho *et al.* 2011; Cystic Fibrosis Canada, 2018).

Species of the Bcc are an important group of CF pathogens that are particularly threatening due to their highly variable and unpredictable clinical outcomes (Sousa *et al.* 2011). Of the 24 closely related species that currently comprise the Bcc, *B. cenocepacia, B. multivorans, B. cepacia, B. vietnamensis* and *B. stabilis,* are the most isolated species found to infect patients with CF (Coutinho *et al.* 2011; Cystic Fibrosis Canada, 2018). Although the incidence of Bcc infection currently remains low among CF patients, the outcome of infection can be detrimental, including a progressive decline in lung function and the development of a necrotizing pneumonia known as cepacia syndrome (Isles *et al.* 1984; Courtney *et al.* 2004). Thus, long-term pulmonary colonization is typically associated with a worse prognosis that requires complex, intensive treatment interventions (Coutinho *et al.* 2011) (more in section 1.2.4). These clinical manifestations are largely the result of damage caused by the excessive

inflammatory response stimulated by the various pathogenic traits that Bcc species employ as a means of establishing infection.

1.2.2 Pathogenic traits

Upon initial colonization, Bcc species express a number of pathogenic traits that contribute to their high level of adaptability within the complex polymicrobial environment of the CF lung (Sousa *et al.* 2011; Delhaes *et al.* 2012). As opportunistic intracellular pathogens, Bcc species possess various mechanisms involved in lung epithelial cell invasion and translocation, enabling their spread and the evasion of host immunity effectors (McClean and Callaghan, 2009; David *et al.* 2015; Ganesh *et al.* 2020). The production of extracellular virulence factors and the formation of highly tolerant biofilms collectively play a critical role in initial colonization and the establishment of persistent, chronic infections (Coutinho *et al.* 2011; Mariappan *et al.* 2011; Scoffone *et al.* 2017). The pathogenicity of Bcc species is therefore greatly defined by these characteristics.

1.2.2.1 Extracellular virulence factors

Species of the Bcc produce several proteases that play a significant role in both acute and chronic infections (Sokol *et al.* 2003). Two zinc-dependent metalloproteases, ZmpA and ZmpB, account for the majority of total proteases produced, serving as the primary factors involved in the cleavage of several important host defense proteins (Gingues *et al.* 2005; Kooi *et al.* 2006; Ganesh *et al.* 2020). Secreted by the type-3-secretion system of Bcc species, both ZmpA and ZmpB actively degrade host fibrinogen, causing damage to lung epithelium and consequently supporting the spread of infection (Reihill *et al.* 2017). Furthermore, their importance as a pathogenic trait has been previously demonstrated using the *Drosophila melanogaster* chronic infection model where mutations in either *zmpA* or *zmpB* genes were shown to lead to the

attenuation of *B. cenocepacia* K56-2 virulence, resulting in increased fly survival (Casonguay-Vanier *et al.* 2010).

In addition to proteases, Bcc species, particularly *B. multivorans* and *B. cenocepacia,* also exhibit lipase activity that contributes to the dysregulation of airway haemostasis and the spread of infection (Carvalho *et al.* 2007). The activity of lipases includes both the LipA lipase as well as the LipB chaperone, which, like proteases, help to mediate host cell invasion as well as the evasion of host immunity (Jorgensen *et al.* 1991). By catalyzing the hydrolysis of esters in long chain fatty acids, lipases play a considerable role in the ability of Bcc species to invade lung cell epithelia, thereby disrupting mucosal integrity (Mullen *et al.* 2007). Lipolytic activity has also been shown to inhibit the phagocytic function of macrophages in the host, providing protection from innate host defense mechanisms (Straus *et al.* 1992; Mullen *et al.* 2007).

In response to low iron conditions, Bcc species also produce and release an array of siderophores as a means of sequestering iron that is required for many different metabolic processes (Lewenza and Sokol, 2001; Visser *et al.* 2004; Mathew *et al.* 2014). Of the different siderophores that have been identified, ornibactin is the key siderophore that is highly conserved among Bcc species as it demonstrates the highest level of affinity towards iron compared to secondary siderophores such as cepaciachelin and pyochelin (Butt and Thomas, 2017). The production of ornibactin is crucial for Bcc pathogenicity. As demonstrated with a rat lung chronic infection model, mutation in the *pvdA* gene required for ornibactin synthesis was shown to attenuate the virulence of *B. cenocepacia* K56-2, resulting in a significantly reduced amount of inflammation (Sokol *et al.* 1999). The role of siderophores in disease progression has since been further expanded by additional studies that characterized the non-specific toxic

effects of the siderophore pyochelin towards eukaryotic cells and other bacterial pathogens through the generation of reactive oxygen species (ROS) (Adler *et al.* 2012).

1.2.2.2 Biofilm formation

In addition to the wide range of extracellular virulence factors that are largely associated with the initial colonization and establishment of infection, Bcc species are also known for their adaptive ability to form highly tolerant biofilms that contribute to antibiotic resistance and recurrent infection (Ferreira *et al.* 2019). The formation of biofilm is a tightly regulated, multistep process that includes the coordinated production of various factors throughout its development (Ferreira *et al.* 2011; Koo *et al.* 2017). This development consists of distinct stages, each involving unique changes that occur over time as illustrated in Figure 1.2a. In general, the different stages of the Bcc biofilm life cycle include initial adhesion, early biofilm development, biofilm maturation, and late-stage dispersal.

Initial adhesion to lung epithelial cells includes the expression of various cell-surface associated components, including type-1 fimbriae, lectins and large surface proteins that work together to help mediate cell-cell interactions (Holden *et al.* 2009; McClean and Callaghan, 2009; Fazli *et al.* 2014). Different species of the Bcc are known to produce different variants of each of these adhesins. For example, while *B. cenocepacia* codes for *fimA,* which is a fimbria homologous to the major subunit of *Escherichia coli* type-1 fimbriae (Inhulsen *et al.* 2012), *B. multivorans* relies on fimbriae of the filamentous hemagglutinin family and the HecB-like fimbrial usher proteins for cell-cell interaction (Denman and Brown, 2013). In addition to fimbriae, Bcc species also utilize a wide variety of soluble lectins for initial adhesion. Specifically, lectins BclA, BclB and BclC, each function by binding to fucosylated or mannosylated glycoproteins of lung epithelia (Lameignere *et al.* 2008; Sulak *et al.* 2010;

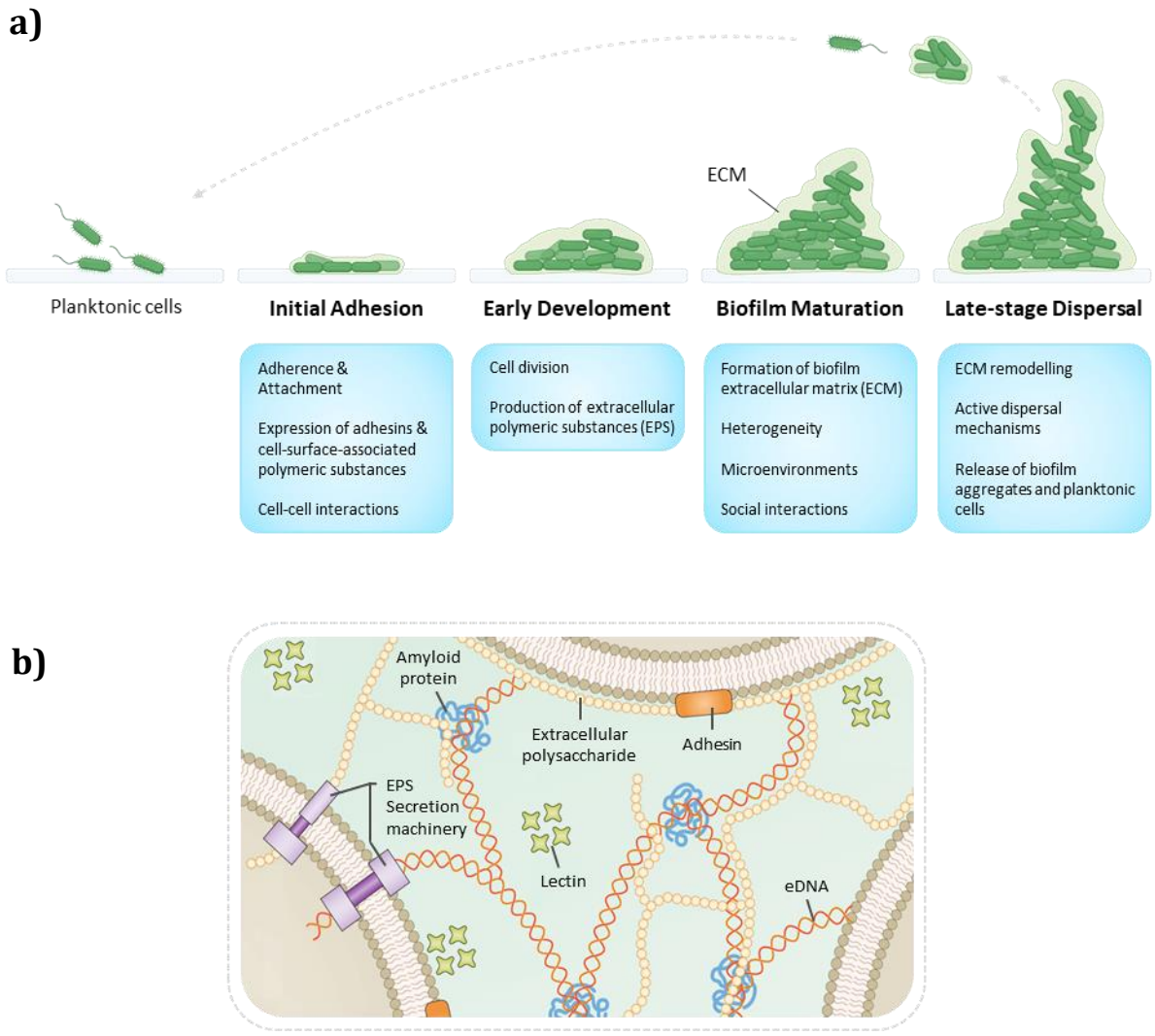

Figure 1.2: The biofilm life cycle and biofilm extracellular matrix of Bcc species

(a) The different stages of biofilm development in Bcc species, highlighting some of the distinct physiological changes that occur during initial adhesion, early development, biofilm maturation, and late-stage dispersal. **(b)** A simplified depiction of the biofilm extracellular matrix (ECM), highlighting some key components that comprise the majority of its biomass. Images adapted from Koo *et al.* (2017) and created with BioRender.com.

Inhulsen *et al.* 2012). Although the role of these factors has shown to have some level of redundancy, one factor that is indispensable for successful Bcc biofilm formation is the biofilm-associated protein A (BapA) (Huber *et al.* 2002; Inhulsen *et al.* 2012). BapA belongs to a diverse family of large surface proteins that have been shown to be major players in the formation of biofilm in other species as well, such as *S. aureus* and *E. coli* (Lasa and Penades, 2006). Transported to the surface by a type-1-secretion system, BapA aids in both primary attachment to host cells as well as intercellular adhesion between bacterial cells (Hinsa *et al.* 2003; Lasa and Penades, 2006). Together these different cell-associated adhesins bring Bcc species and lung epithelia in tight association, mediating irreversible attachment and thus initiating the next stage of biofilm development.

Following attachment, early biofilm development begins as Bcc cells begin to proliferate and produce a large amount of extracellular polymeric substances (EPS) that function to maintain structural integrity of the growing extracellular matrix (ECM) (Figure 1.2b) (Ferreira *et al.* 2011). The presence of EPS also provides Bcc species with increased protection against the activity of both antibiotics and host immune determinants by acting as a physical barrier and by also holding the capacity to scavenge ROS (Bylund *et al.* 2006; Cuzzi *et al.* 2012). Some EPS substrates that have been identified within Bcc biofilms include cellulose, poly-β-1,6-N-acetylglucosamine (PNAG) and the gene cluster Bcam1330-1341 (Messiaen *et al.* 2014; Fazli *et al.* 2013, 2014). The major EPS that comprises the majority of the Bcc ECM however is cepacian, a carbohydrate polymer consisting of acetylated heptasaccharide repeating units that polymerize to give rise to high-molecular-weight polysaccharide chains (Cerantola *et al.* 1999; Cescutti *et al.* 2000). Cepacian plays a major role in the protective nature of Bcc biofilms by inhibiting neutrophil chemotaxis, neutralizing ROS, and by shielding Bcc cells from exposure to

metal ion stress and arid conditions (Cunha *et al.* 2004; Bylund *et al.* 2006; Ferreira *et al.* 2010). Additionally, the production of cepacian has been shown to be highly involved in facilitating the persistence of Bcc infections in the lungs as demonstrated in multiple murine chronic infection models (Conway *et al.* 2004; Sousa *et al.* 2007).

With an increasing production of EPS, the Bcc biofilm continues to grow and mature, enduring several physiochemical changes as more biofilm-associated components are incorporated (Koo *et al.* 2017). Continued production of adhesins and EPS promotes further adherence and cell-cell aggregation, leading to the formation of a highly evolved three-dimensional scaffold (Ferreira *et al.* 2011). At this time, the inclusion of extracellular DNA (e-DNA) becomes an important component, particularly in *B. multivorans* biofilms, as it offers additional structural stability to support the ECM biomass (Messiaen *et al.* 2014). With its growing complexity, this stage of development also includes the formation of multiple water channels and microenvironments of varying physical and chemical properties.

From here, the final stage of dispersal occurs which includes the release of biofilm aggregates as well as the cellular switch back to planktonic motility (Silva *et al.* 2016; Koo *et al.* 2017). Biofilm dispersal is a necessary part of the Bcc biofilm life cycle as it allows for the ability to separate and colonize new areas of the CF lung (Traverse *et al.* 2012). This action largely occurs in response to environmental cues, such as a limited amount of space, a significant decrease in nutrient availability, as well as other stress inducing conditions like sudden fluctuations in oxygen and other elements (Saucer *et al.* 2004; Kostakioti *et al.* 2013; Guilhen *et al.* 2017). Late-stage dispersal of Bcc biofilms plays an important role in enabling their spread of infection which can present itself as symptoms of exacerbation and promote their continued persistence within the host (Traverse *et al.* 2012; Silva *et al.* 2016).

1.2.3 Quorum sensing regulation

Many pathogenic traits of Bcc species are largely regulated by quorum sensing (QS), the population-dependent form of cell-to-cell communication that allows for the coordinated expression of many virulence genes (Subsin *et al.* 2007; O'Grady *et al.* 2009; Suppiger *et al.* 2013). Analogous to the LasIR QS system of *P. aeruginosa,* the CepIR QS system of Bcc species consists of a regulatory protein, CepR, which acts as a transcriptional regulator under high population densities by binding to the N-acyl-homoserine lactone (AHL) signalling molecules that are produced by the inducer synthase, CepI (Figure 1.3) (Lewenza *et al.* 1999; Sokol *et al.* 2003; Slinger *et al.* 2019). The AHLs involved in this regulatory system includes the *N*-octanoyl-homoserine lactone (C8-HSL) and in smaller amounts, the *N*-hexanoyl-homoserine lactone (C6-HSL) (Malott *et al.* 2005). In a similar manner to this system, Bcc isolates that carry the cenocepacia pathogenicity island (cci), such as the highly transmissible *B. cenocepacia* K56-2 strain, also carry a secondary AHL-mediated QS system, CciIR (Baldwin *et al.* 2004; Malott *et al.* 2005). This secondary system works under the CepIR system to assist in co-regulating or reciprocally regulating many genes required for Bcc virulence as shown in Figure 1.3 (O'Grady *et al.* 2009; Subramoni and Sokol, 2012).

To varying extents, extracellular virulence factors including proteases, lipases and siderophores, as well as biofilm-associated factors, like adhesins and EPS, have all been shown to be under the control of QS regulation (O'Grady *et al.* 2009; Inhulsen *et al.* 2012). Given the role that these traits play in CF pulmonary infections, the loss or interference of QS regulation in Bcc species is detrimental to their ability to establish a chronic infection. Indeed, several infection models including *Caenorhabditis elegans* (Kothe *et al.* 2003), *Drosophila melanogaster* (Castonguay-Vanier *et al.* 2010), *Galleria mellonella* (Uehlinger *et al.* 2009) and various murine

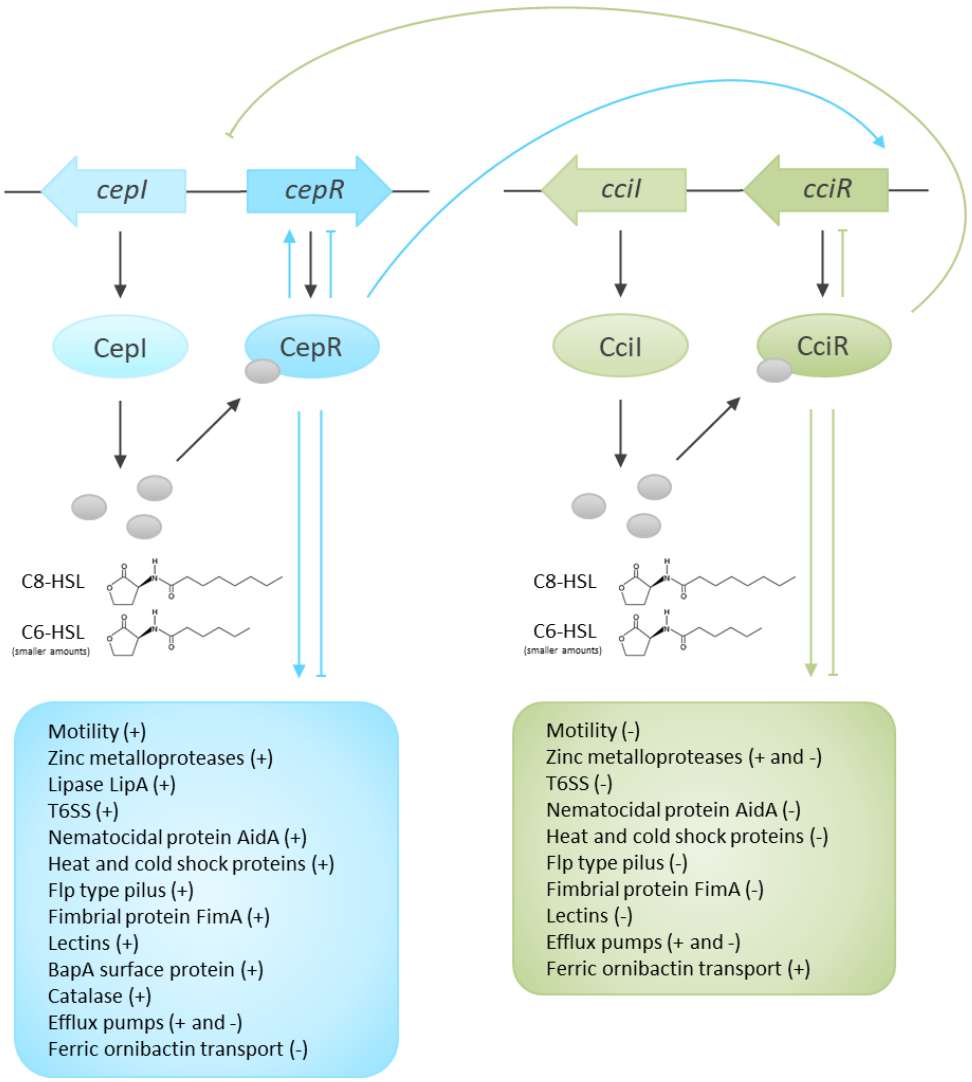

Figure 1.3: A schematic of AHL-based quorum sensing regulation in Bcc species

The CepI synthase of the CepIR QS system (shown in blue) produces HSL molecules that bind to and activate the transcriptional regulator, CepR, which regulates the activation (+) and/or suppression (-) of target genes as well as influences the expression of *cepR,* both positively (pointed arrow) and negatively (flattened arrow). The CciIR QS system (shown in green) of *B. cenocepacia* strains harbouring the cepacia pathogenicity island functions in a highly similar manner to the CepIR QS system. Image adapted from Subramoni and Sokol (2012).

species (Sokol *et al.* 2003; McKeon *et al.* 2011), have all demonstrated CepIR and/or CciIR QS mutants to exhibit competitive disadvantages, reduced induction of the host inflammation, and a limited ability to maintain an infection, *in vivo*.

The importance of QS in Bcc species can be further demonstrated by its maintenance throughout infection. In contrast to what has been observed in other CF pathogens, like *P. aeruginosa,* where loss of QS function is typically selected for in long-term colonization (Smith *et al.* 2006; D'Argenio *et al.* 2007), functional QS regulation is highly maintained throughout all stages of Bcc infection (Chambers *et al.* 2005; McKeon *et al.* 2011). In an experiment conducted by McKeon and colleagues (2011), only a single isolate out of 45 samples (2.2%) collected from CF patients chronically infected with *B. cenocepacia* or *B. multivorans* exhibited a loss in QS function. Interestingly, strains which lacked a proper QS system also showed to rarely exhibit the ability to out-compete the wild-type strain in both *in vitro* and *in vivo* analyses (McKeon *et al.* 2011). As a highly conserved global regulator of several genes that mediate the pathogenicity of Bcc species, QS systems offer ideal targets in the development of alternative therapeutic strategies (Wopperer *et al.* 2006; Scoffone *et al.* 2019).

1.2.4 Treatment of Bcc infections

Treatment of Bcc infections can be a highly challenging process as there are a number of factors associated with determining an effective course of treatment. In addition to the unpredictable nature of clinical outcomes, species of the Bcc are also known to be intrinsically resistant to many antibiotics used in clinical practice (Mahenthiralingam *et al.* 2005; Tseng *et al.* 2014). This is highly attributed to the multitude of resistance mechanisms that they possess, including the production of efflux pumps, various drug modifying enzymes and reduced membrane permeability (Pope *et al.* 2008; Hamad *et al.* 2012; Rushton *et al.* 2013). The

formation of biofilm also plays a significant role in contributing to resistance given the protective nature of the ECM towards the antimicrobial activity of host immune effectors and antibiotics (Messiaen *et al.* 2014; Ernst *et al.* 2018; Sharma *et al.* 2019). Therefore, supressing pre-existing Bcc biofilm infections often requires the use of complex combination methods that involve high dosage antibiotics over extended periods of time (Zhou *et al.* 2007; Abbott *et al.* 2016; Garcia *et al.* 2018). Administration of the combination antibiotic trimethoprim-sulfamethoxazole is generally recommended for Bcc infections, however, other combinations involving different classes of antibiotics, such as ceftazidime + tobramycin or meropenem + tobramycin have also been used depending on their *in vitro* susceptibility patterns (Avgeri *et al.* 2009). Consequently, the overuse of these antibiotics has over time resulted in an increased prevalence of multi-drug resistant strains and therefore the need for alternative treatment strategies has also exponentially increased (Scoffone *et al.* 2017).

With the goal of improving treatment of Bcc infections, a number of alternative therapeutic approaches are actively being researched (Scoffone *et al.* 2017). One method involves the use of natural products that possess antimicrobial activity, such as an arginine derivative of the glycopolymer PNAG which has been shown to electrostatically bind to the outer membrane of bacterial cells resulting in depolarization and cell death (Narayanaswamy *et al.* 2017, 2019). Furthermore, this PNAG derivative was also shown to target Bcc biofilms, disrupting their structural integrity and increasing their susceptibility to antibiotic treatment. Another alternative method includes investigating the use of molecules that are already in use to treat other diseases, like cysteamine which is prescribed as a therapeutic agent for individuals with nephropathic cystinosis (Gahl *et al.* 2007). Recently, Fraser-Pitt and colleagues (2016) demonstrated cysteamine to also enhance the antimicrobial activity of various

antibiotics towards species of the Bcc by possessing mucolytic activity that selectively disrupts disulphide bonds and thus that allows for greater biofilm penetration.

In addition to these alternative strategies, the use of quorum sensing inhibitors (QSIs), such as DKPs, has also been considered as it offers a unique approach of enhancing antibiotic treatment by interfering with the regulation of pathogenic traits without possessing any antimicrobial activity on its own (Allen *et al.* 2014; Scoffone *et al.* 2017; Shaw and Wuest, 2020). By limiting traits such as the production of extracellular virulence factors, biofilm formation and the expression of factors associated with resistance mechanisms, QSIs leave the target pathogen more susceptible to antimicrobial interventions. However, efforts into understanding the potential role of this strategy to hold significance within the evolving field of alternative therapeutics is quite limited with only a few reported studies investigating their effects on species of the Bcc (Scoffone *et al.* 2017; Slinger *et al.* 2019).

One well known and researched QSI for its activity against the CepIR QS system is baicalin hydrate (BH) (Brackman *et al.* 2009). Its effect on Bcc species as antibiotic potentiators has been demonstrated through both *in vitro* and *in vivo* studies, highlighting an increasing interest in their continued analysis and that of other QSIs (Brackman *et al.* 2011, 2012; Slachmuylders *et al.* 2018). Recently, the potential for DKPs to act in this manner has also been under similar investigation, as described previously (Scoffone *et al.* 2016; Buroni *et al.* 2018). Given the diverse functions that DKPs have been shown to carry and their involvement in a wide range of applications, continued research into understanding their anti-pathogenic properties as QSIs could uncover new insights towards improving the treatment of Bcc infections.

1.3 Project Overview

The use of QSIs as a means of decreasing the pathogenicity of Bcc species offers a new and evolving area of research towards improving treatment options of Bcc infections. Specifically, DKPs have been shown to hold biologically significant properties in various applications, including their function as QSIs. Therefore, continuing from the work of Purighalla (2011), we were interested in further investigating the extent to which DKPs cyclo(-D-ala-val), cyclo(-pro-val), cyclo(-leu-pro) and cyclo(-phe-pro) could affect the pathogenic phenotype of Bcc species as the next step towards understanding their potential use in alternative therapeutics. Specifically, this included observing their influence on QS-regulated traits, including the production of extracellular virulence factors and the formation of biofilm, as well as their ability to potentiate the activity of different antibiotics in the treatment of Bcc biofilms.

1.3.1 Hypothesis

By interfering with QS regulation, we hypothesized that DKPs would alter the production of extracellular virulence factors and the formation of biofilm in Bcc species, resulting in a subsequent increase in their susceptibility to antibiotic treatment when grown as biofilms.

1.3.2 Objectives

1. **Assess the effects of DKPs on the production of proteases, lipases and siderophores of Bcc species over time.**
2. **Quantify the changes in Bcc biofilm biomass and viability over time while exposed to DKPs.**
3. **Determine the extent to which DKPs can potentiate antibiotic activity in the treatment of Bcc biofilms, *in vitro.***

Chapter Two: Materials and Methods

2.1 Bacterial Strains and Growth Conditions

2.1.1 Maintenance and growth

Bacterial strains used in this study are listed in Table 2.1. Frozen stocks of all strains were prepared by inoculating sterile 10% (w/v) skim milk (Difco) and were stored at -80 ˚ C. Bacterial strains were routinely grown on sterile Mueller Hinton agar (MHA) media plates (38g MHA (Difco) per litre of double distilled water (ddH_2O)). Unless otherwise stated, all media used in this study was sterilized by autoclaving. Primary streak plates were grown at 37 ˚ C overnight and stored at 4 ˚ C for a maximum of 10-14 days. Prior to each experimental procedure, fresh secondary streak plates were prepared by transferring a single colony from the primary plates onto sterile MHA plates and grown overnight at 37 ˚ C.

Unless otherwise stated, initial bacterial cultures were obtained by inoculating a single colony from fresh secondary streak plates into 3mL culture tubes containing synthetic cystic fibrosis sputum media (SCFM), a complex media that mimics the nutrient availability typically found in the lungs of individuals with CF (Palmer *et al.* 2007). These cultures were routinely grown at 37 ˚ C in an incubator shaker (New Brunswick Scientific I24 series) for 2-12 hours prior to experimental setup.

2.1.2 Synthetic cystic fibrosis sputum media

The highly defined synthetic cystic fibrosis sputum media (SCFM) was prepared following a slightly modified procedure from Palmer *et al.* (2007). Briefly, the buffered base (6.50mL of 0.2M NaH_2PO_4, 6.25mL of 0.2M Na_2HPO_4, 0.35mL of 1.0M KNO_3, 1.08mL of 0.25M K_2SO_4, 0.122g NH_4Cl, 1.114g KCl, 3.030g NaCl, 2.093g MOPS and 780mL of ddH_2O per litre of

Table 2.1: Bacterial strains used in this study

Strain	Description	Reference
Burkholderia cepacia		
15862	CF respiratory isolate	(ABMR)*
16192	CF respiratory isolate	(ABMR)*
Burkholderia multivorans		
C5393	CF respiratory isolate (Canada)	(Mahenthiralingam *et al.* 2000)
LMG13010	CF respiratory isolate (Belgium)	(Mahenthiralingam *et al.* 2000)
Burkholderia cenocepacia		
H111	CF respiratory isolate (Germany)	(Romling *et al.* 1994)
K56-2	CF respiratory isolate, ET-12 lineage (Canada)	(Mahenthiralingam *et al.* 2000)
K56-*R2*	Δ*cepR* derivative of K56-2	(Malott *et al.* 2005)
K56-*I2*	Δ*cepI* derivative of K56-2	(Malott *et al.* 2005)
K56-*cciIR*	Δ*cciI, cciR* derivative of K56-2	(Malott *et al.* 2005)
K56-*cepR,cciIR*	*ΔcepR, cciI, cciR,* derivative of K56-2	(Malott *et al.* 2005)

* Isolates generously provided by the Alberta Microbiota Repository (ABMR) and IMPACTT, the Canadian Microbiome Core (https://www.impactt-microbiome.ca/)

media) was autoclaved prior to addition of the various amino acids (Amresco Inc., USA) listed in Table 2.2. Each amino acid stock (100mM) was sterilized through a 0.2µm syringe filter (PES filter; VWR) and added to the buffered base accordingly (Table 2.2). The media was then adjusted to a pH of 6.8 (through the addition of concentrated NaOH or HCl) and passed through a 0.2µm vacuum filter (PES filter; VWR). Stocks of additional components were sterilized through 0.2µm syringe filters and carefully added to the media (3.00mL of 1.0M D-glucose, 9.30mL of 1.0M L-lactate, 1.75mL of 1.0M $CaCl_2$, 0.61mL of 1.0M $MgCl_2 \bullet 6H_2O$ and 1.00mL of 3.6mM $FeSO_4 \bullet 7H_2O$). A small aliquot of the media was grown at 37 ˚C and 250 rpm (New Brunswick Scientific I24 series) overnight as a sterility control check. For long-term storage, the media and all amino acid stocks (Table 2.2) were covered in tinfoil and stored at 4 ˚C while all other stocks were stored at room temperature.

2.2 Preparation of 2,5-Diketopiperazines

Synthetic 2,5-diketopiperazines (DKPs): cyclo(-D-ala-val), cyclo(-pro-val), cyclo(-leu-pro), and cyclo(-phe-pro) were purchased from Bachem, USA, and stored at -20 ˚C. For experimental use, DKPs were suspended in heated 50mM sodium phosphate buffer (PB) (0.39g of $NaH_2PO_4 \bullet H_2O$ and 1.36g of Na_2HPO_4 per 250mL of ddH_2O) (pH 7.5) and passed through 0.2µm syringe filters (PES filter; VWR) to sterilize (Perzborn *et al.* 2013). Suspended DKP stocks (4mM) were stored at 4 ˚C for short-term storage. When necessary, diluted stocks of different concentrations of DKPs were prepared in PB in order to keep the volume of DKPs added consistent across all experimental samples.

Table 2.2: Amino acids added to synthetic cystic fibrosis sputum media

Amino Acid		Stock Preparation (100mM)		Volume of stock added per litre of media (mL)
		Amount (g)	Solvent (25mL)	
Lys	L-Lysine	0.457	ddH_2O	21.28
Ala	L-Alanine	0.223	ddH_2O	17.80
Pro	L-Proline	0.288	ddH_2O	16.61
Leu	L-Leucine	0.328	ddH_2O	16.09
Glu	L-Glutamate	0.459	0.5M HCl	15.49
Ser	L-Serine	0.263	ddH_2O	14.46
Gly	L-Glycine	0.188	ddH_2O	12.03
Ile	L-Isoleucine	0.328	ddH_2O	11.20
Val	L-Valine	0.293	ddH_2O	11.17
Thr	L-Threonine	0.298	ddH_2O	10.72
Asp	L-Aspartate	0.333	0.5M NaOH	8.27
Tyr	L-Tyrosine	0.453	1.0M NaOH	8.02
Orn	L-Ornithine	0.422	ddH_2O	6.76
Met	L-Methionine	0.373	ddH_2O	6.33
Phe	L-Phenylalanine	0.413	ddH_2O	5.30
His	L-Histidine	0.479	ddH_2O	5.19
Arg	L-Arginine	0.527	ddH_2O	3.06
Cys	L-Cystine	0.692	ddH_2O	1.60
Trp	L-Tryptophan	0.511	0.2M NaOH	0.13

2.3 Growth Assessments

2.3.1 Growth curves

To measure the effects of DKPs on the growth rate of Bcc species, individual bacterial cultures of *B. cepacia* (15862 and 16192), *B. multivorans* (C5393 and LMG13010), and *B. cenocepacia* (H111, K56-2, K56-*cciIR* and K56-*cepR,cciIR*) were prepared as described in section 2.1.1 and grown overnight (~12 hours) in a shaking incubator (New Brunswick Scientific I24 series) set at 37 ° C and 150 rpm. These cultures were then normalized in SCFM to an optical density at 600nm (OD_{600}) of 0.05 (~ 5.0 x10^7 CFU/mL) and aliquoted (135µL) into the wells of 96-well flat bottom microplates (Nunc, Denmark) with the addition of either PB (15µL) as an untreated control or one of the four DKPs (15µL) to a final concentration of 400µM. Sterile media control wells were filled with SCFM (150µL), while the outer edge wells were filled with ddH_2O (200µL) to help limit evaporation of the culture wells over the duration of the experiment. Plates were sealed with a layer of parafilm and grown at 120 rpm on a platform orbital shaker (New Brunswick Scientific, C2 Classic Series) that was placed inside of an incubator (VWR, model 1535) set at 37 ° C. Humidified conditions were maintained by placing small containers of water in the incubator. The OD_{600} was recorded every 2 hours for 24 hours using a Perkin Elmer Victor X4 (model 2030) plate reader. This procedure was carried out twice in triplicate (n=6).

2.3.2 Viable cell enumeration

In addition to collecting OD_{600} measurements every two hours, the number of viable bacterial cells was also determined every eight hours over the 24-hour growth curve procedure. This was done by transferring 5µL of culture from each well into new 96-well microplates containing 45µL of 1x phosphate-buffered saline (PBS) (4.30mM Na_2HPO_4, 2.70mM

KCl, 1.37mM NaCl and 1.47mM KH_2PO_4) and carrying out ten-fold serial dilutions. Diluted wells were then spotted (5μL) onto MHA plates and the resulting colony forming units (CFUs) were recorded following incubation at 37 ° C for 40-48 hours. This procedure was carried out twice in triplicate (n=6).

2.4 Extracellular Virulence Factor Assessments

2.4.1 Isolation of cell-free spent media

To evaluate the effect of DKPs on the production of extracellular virulence factors of Bcc species, cell-free spent media was isolated from both treated and untreated bacterial cultures and analysed using various detection methods. Individual bacterial cultures of *B. cepacia* (15862 and 16192), *B. multivorans* (C5393 and LMG13010), and *B. cenocepacia* (H111, K56-2, K56-*cciIR* and K56-*cepR,cciIR*) were prepared and grown as outlined in section 2.1.1. Following incubation, 1.5mL of culture was transferred to a microtube and the spent media was removed by centrifugation at 13,000 rpm for 3 minutes (Eppendorf, 5425 R). Pelleted cells were resuspended in fresh SCFM and standardized to an OD_{600} of 0.01 (~ 1.0 x10^7 CFU/mL). Experimental cultures were prepared by aliquoting standardized culture (2.7mL) into 15mL culture tubes (VWR) along with either PB (0.3mL) as an untreated control or one of the four DKPs (0.3mL) to a final concentration of 25, 100 or 400μM. A culture tube containing 3mL of SCFM was used as a sterile media control. All samples were grown at 37 ° C in an incubator shaker (New Brunswick Scientific I24 series) set at 250 rpm.

To observe the effects of DKPs on extracellular virulence factor production over time, cell-free spent media was isolated at both the early and late stationary phases of bacterial growth. Based on their individual growth rates in SCFM (Supplementary Figure 1), early stationary phase occurred after 12 hours of incubation for the *B. multivorans* strains and at 14

hours for the *B. cepacia* and *B. cenocepacia* strains. The late stationary time points were taken after an additional six hours of growth, being 18 and 20 hours, respectively. At each time point, a 1mL sample was removed from the culture tubes and transferred to a microtube where 0.1mL was used to measure the OD_{600}, while the remaining 0.9mL was centrifuged at 13,000 rpm for 3 minutes (Eppendorf, 5425 R). The spent media was then filtered through a 0.2µm syringe filter (PES filter; VWR) to obtain a cell-free sample used in the extracellular virulence factor assays. When necessary, the cell-free spent media samples were stored at 4 ° C prior to assessment.

2.4.2 Protease production

Protease production by Bcc species was measured following a procedure outlined by Scoffone and colleagues (2016), with slight modifications. Cell-free spent media (section 2.4.1) was added to a microtube containing a non-specific, chromogenic protease substrate, azocasein (5mg of azocasein (Sigma) per 1mL of 100mM TrisHCL pH 8) in a 1:1 ratio (200µL + 200µL). The microtubes were incubated for 2 hours rotating at 120 rpm on a platform orbital shaker (New Brunswick Scientific, C2 Classic Series) that was placed inside of an incubator (VWR, model 1535) set at 37 ° C. Following incubation, 10% (w/v) trichloroacetic acid (TCA) (25µL) was added to the microtubes and lightly vortexed to mix prior to centrifugation at 15,000 rpm for 2 minutes (Eppendorf, 5425 R). The spent media was then aliquoted (100µL) in triplicate into the wells of a 96-well microplate with the addition of 0.525M NaOH (70µL). The resulting color change was detectable at an optical density of 420nm using a Perkin Elmer EnSpire® Multimode plate reader, where a higher OD_{420} reading indicated a higher amount of proteolytic cleavage of the azocasein substrate. The change in OD_{420} compared to the sterile media control was determined for each experimental sample and further standardized to bacterial growth

($\Delta OD_{420}/OD_{600}$). This experiment was carried out two times in triplicate (n=6). An example of the protease production by each Bcc strain (untreated controls) at both early and late stationary phase is pictured (Figure 2.1a).

2.4.3 Lipase production

The lipase production by Bcc species was quantified following a procedure outlined by Lonon and colleagues (1988). Briefly, all media stocks required for this assay were prepared and sterilized by passage through 0.2µm filters and were stored at room temperature. Cell-free spent media (section 2.4.1) (33.33µL) was then added to the wells of a 96-well microplate containing 50mM TrisHCl pH 7.6 (153.33µL), 1M $CaCl_2$ (6.66µL) and 10% (v/v) Tween-20 (10.00µL). The microplate was incubated for 2 hours rotating at 120 rpm on a platform orbital shaker (New Brunswick Scientific, C2 Classic Series) that was placed inside of an incubator (VWR, model 1535) set at 37 ˚C. Following incubation, the optical density at 400nm was recorded using a Perkin Elmer EnSpire® Multimode plate reader, where a higher OD_{400} reading indicated a higher amount of lipase activity. The change in OD_{400} compared to the sterile media control was determined for each experimental sample and further standardized to bacterial growth ($\Delta OD_{400}/OD_{600}$). This experiment was carried out two times in triplicate (n=6). An example of the lipase production by each Bcc strain (untreated controls) at both early and late stationary phase is pictured (Figure 2.1b).

2.4.4 Siderophore production

Siderophore production by Bcc species was determined using the chrome azurol S (CAS) assay, a universal colorimetric method for detecting siderophores (Schwyn and Neilands 1987). In place of the traditional CAS-agar plate method, a modified microplate method utilizing liquid CAS media was used following a procedure described by Arora and Verma

Figure 2.1: Representative images of extracellular virulence factor assessments

Cell-free spent medium from bacterial cultures grown in SCFM was isolated at early stationary phase (*B. cepacia* and *B. cenocepacia* strains = 12 h, *B. multivorans* strains = 14 h) and late stationary phase (*B. cepacia* and *B. cenocepacia* strains = 18 h, *B. multivorans* strains = 20 h) and utilized in the analysis of extracellular virulence factors. **(a)** Protease production as detected through incubation with the chromogenic substrate azocasein (section 2.4.2). **(b)** Lipase production determined through the level of precipitation formed by incubation with Tween-20 (section 2.4.3). **(c)** Siderophore production as detected through the utilization of the colorimetric method of chrome azurol S (CAS) media. The rows labelled as '1:2 dilution' indicate that the cell-free spent media samples were first diluted by 1:2 with SCFM prior to detection (section 2.4.4). All images are representative of two independent experiments performed in triplicate (n=6).

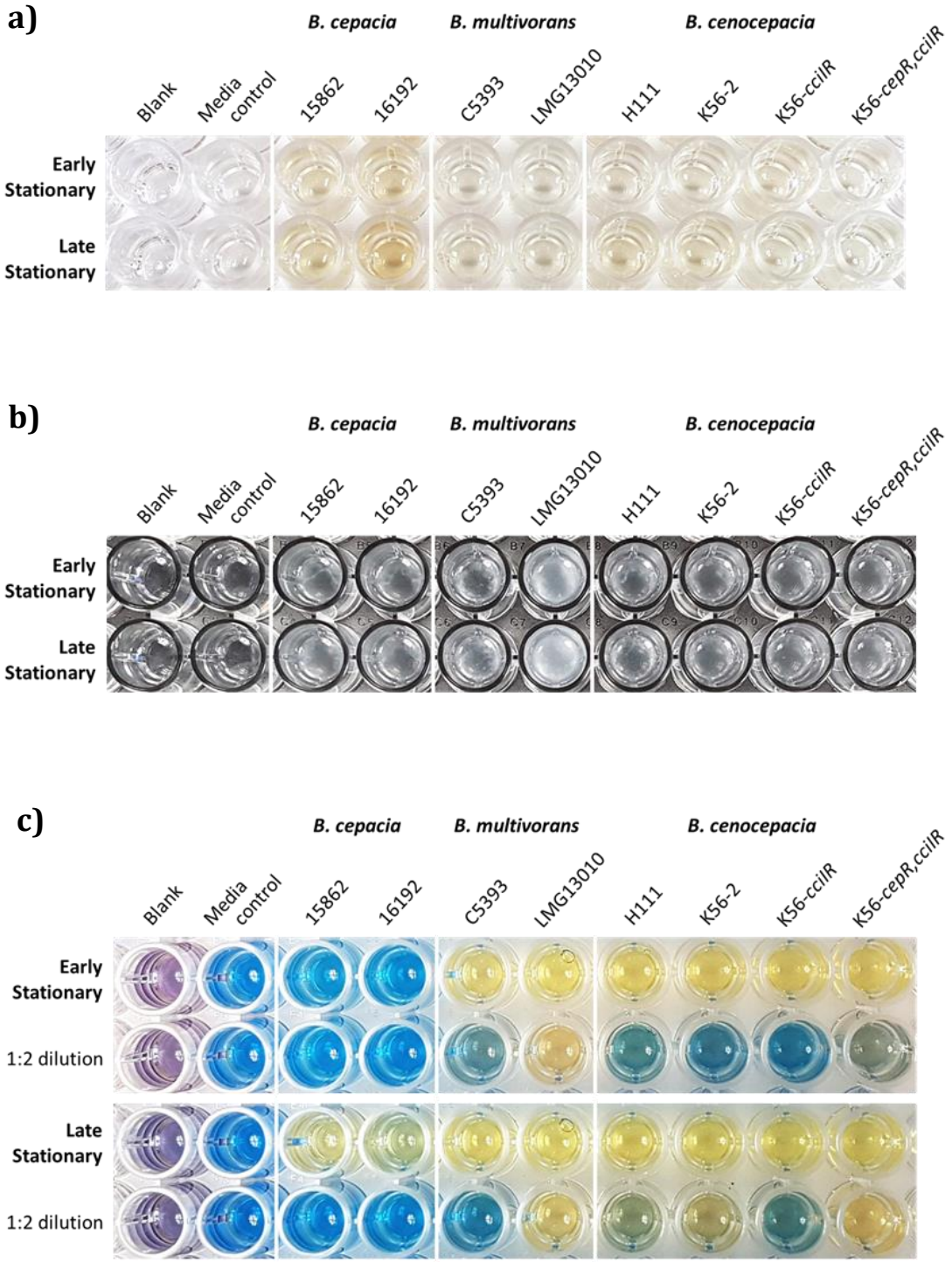
a)
B. cepacia
B. multivorans
B. cenocepacia
Blank
Media control
15862
16192
C5393
LMG13010
H111
K56-2
K56-cciIR
K56-cepR,cciIR
Early Stationary
Late Stationary
b)
B. cepacia
B. multivorans
B. cenocepacia
Blank
Media control
15862
16192
C5393
LMG13010
H111
K56-2
K56-cciIR
K56-cepR,cciIR
Early Stationary
Late Stationary
c)
B. cepacia
B. multivorans
B. cenocepacia
Blank
Media control
15862
16192
C5393
LMG13010
H111
K56-2
K56-cciIR
K56-cepR,cciIR
Early Stationary
1:2 dilution
Late Stationary
1:2 dilution

(2017), with some modifications. Given the sensitivity of this media to changes in pH and the presence of trace elements, the stocks of all required reagents were prepared using plastic scoops and weigh boats and were stored in 50mL falcon tubes following sterilization through 0.2µm filters. For each assay, fresh CAS media was prepared (0.75mL of 2mM CAS, 0.15mL of 10mM ferric chloride hexahydrate, 1.2mL of 10mM hexadecyltrimethylammonium bromide, 5.4mL of UltraPure distilled water (Invitrogen), 2.5mL of 2mM 1,4-piperazinediethanesulfonic acid and 0.01g of sulfosalicylic acid per 10mL of CAS media). The media was mixed by inversion and used within 30 minutes of preparation. The prepared dark red/purple colored CAS media was then aliquoted (75µL) into the wells of a 96-well microplate. Upon the addition of sterile SCFM (75µL), the CAS media shifted to its characteristic blue color, while the addition of experimental samples (75µL) resulted in a range of colors from blue-green-orange-yellow, depending on the amount of siderophore activity present in the sample. When necessary, the cell-free spent media was diluted 3:4 or 1:2 in SCFM prior to addition. The microplate was then allowed to incubate at room temperature for 10 minutes before recording the optical density at 630nm using a Perkin Elmer EnSpire® Multimode plate reader, where a lower OD_{630} reading indicated a higher amount of siderophore activity. The change in OD_{630} compared to the sterile media control was determined for each experimental sample and diluted samples were corrected for when necessary. The results were further standardized to bacterial growth ($\Delta OD_{630}/OD_{600}$). This experiment was carried out two times in triplicate (n=6). An example of the siderophore production by each Bcc strain (untreated controls) at both early and late stationary phase is pictured (Figure 2.1c).

2.5 Biofilm Assessments

2.5.1 Growth conditions

To assess the effects of DKPs on Bcc biofilm formation over time, both the total biofilm biomass as well as the number of viable biofilm cells was quantified following 4, 8, 12 and 24 hours of growth in the presence of DKPs. This involved using two different forms of assessment, the crystal violet (CV) staining method (section 2.5.2) and viable biofilm cell enumeration (section 2.5.3), respectively. In either case, individual cultures of *B. cepacia* (15862 and 16192), *B. multivorans* (C5393 and LMG13010), and *B. cenocepacia* (H111, K56-2, K56-*cciIR*, and K56-*cepR,cciIR*) were prepared and grown in SCFM as outlined in section 2.1.1. These cultures were then normalized to an OD_{600} of 0.005 (~ 2.0 x10^6 CFU/mL) and aliquoted (135µL) into 96-well flat bottom microplates (Nunc, Denmark) along with either PB (15µL) as an untreated control or one of the four DKPs (15µL) to a final concentration of 1, 25 or 100µM. Sterile media control wells were filled with SCFM (150µL), while the outer edge wells were filled with ddH_2O (200µL). Plates were sealed with two layers of parafilm to help avoid desiccation over the duration of the experiment and grown at 37 ° C on a platform orbital shaker (New Brunswick Scientific, C2 Classic Series) set to 120 rpm in humidified conditions.

2.5.2 Crystal violet staining assay

To assess the effects of DKPs on Bcc biofilm biomass production over time, the crystal violet (CV) staining method was used following the procedure by O'Toole (2011), with some modifications. Briefly, four identical 96-well flat bottom microplates containing normalized bacterial culture and various concentrations of DKPs were prepared and grown as outlined above (section 2.5.1). After 4, 8, 12, and 24 hours of incubation, one of the four microplates was removed and subjected to the CV staining procedure. The first step of this procedure involved

the careful removal of the planktonic culture from each of the wells by using a multichannel micropipette. Non-adherent cells were removed by gently washing with 1x phosphate-buffered saline (PBS) (170µL). The microplate was then placed in a biosafety cabinet (Thermo Scientific™ 1300 series A2) to dry prior to staining. After ~1 hour of drying, the plate was removed and 0.1% CV (180µL) was added to each well and allowed to incubate at room temperature for 10 minutes. CV was then removed using a multichannel pipette and the wells were washed twice with ddH_2O (200µL) to remove excess CV stain. The plate was then placed in a fume hood to dry overnight (12-20 hours). To quantify the total amount of biofilm biomass present in each well, 30% acetic acid (150µL) was used to suspend the CV stain and the optical density at 550nm (OD_{550}) was recorded using a Perkin Elmer EnSpire® Multimode plate reader. Percent (%) biofilm biomass was determined for each experimental replicate using the following the equation:

$$\left(\frac{\text{OD}_{550}\text{ of DKP treated well}}{\text{OD}_{550}\text{ of untreated control well}}\right) \text{x}100 = \%\text{ biofilm biomass}$$

This assay was carried out three times in duplicate (n=6). An example of Bcc biofilm biomass (untreated controls) stained with CV after 4, 8, 12 and 24 hours of incubation is pictured (Figure 2.2).

Prior to experimental testing, an equivalency control was carried out to ensure that equivalent growth within each well was obtainable under the defined conditions (Harrison *et al.* 2010). The inner 60 wells of a 96-well microplate were divided into four equivalent quadrants of 15 wells each (Supplementary Figure 2a). Standardized cultures of *B. cepacia* 16192, *B. multivorans* C5393, and *B. cenocepacia* K56-2 as well as sterile SCFM (media control) were each aliquoted (150µL) into one of the four quadrants of the 96-well microplate and

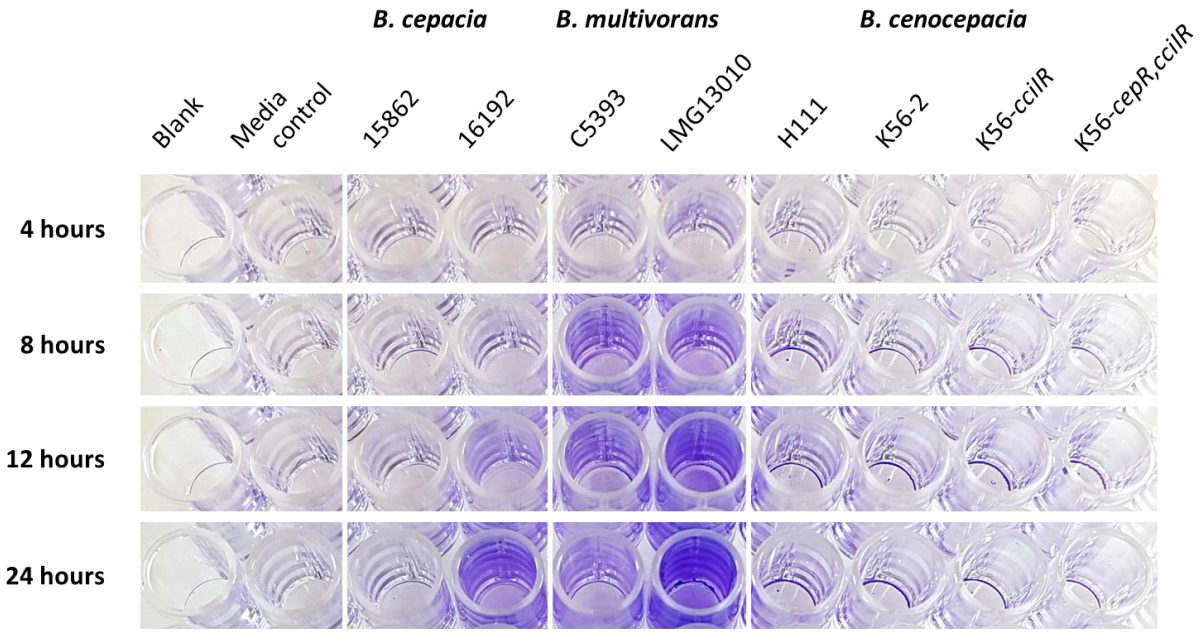

Figure 2.2: Representative images of the crystal violet staining assay

Standardized bacterial cultures of each Bcc strain were grown in 96-well microplates and stained following the CV staining procedure after 4, 8, 12, and 24 hours of incubation (section 2.5.2). All images are representative of two independent experiments performed in triplicate (n=6).

grown at 37 ° C and 120 rpm in humidified conditions as described above. Following 24 hours of incubation, the plate was removed and the CV staining method was carried out. This control was completed two times in order to ensure that equivalent biofilm biomass was obtained across the entire plate prior to experimental treatments with DKPs. Data included as supplementary information (Supplementary Figure 2b).

2.5.3 Viable biofilm cell enumeration

To assess the effect of DKPs on Bcc viable biofilm cell counts, biofilms were cultivated utilizing the Calgary Biofilm Device (CBD) (Innovotech), a device consisting of a 96-well microplate and a lid supporting 96 removable pegs that fit into the wells of the microplate, thus providing a solid surface for biofilms to form (Ceri *et al.* 1999). Viable biofilm cell enumeration was carried out following slightly modified procedures by Ceri *et al.* (2001) and Harrison *et al.* (2010). Briefly, four identical CBDs containing normalized bacterial culture (135µL) along with either PB (15µL) as an untreated control or one of the four DKPs (15µL) to a final concentration of 100µM, were prepared as described (section 2.5.1). After 4, 8, 12, and 24 hours of incubation, one of the four CBDs was removed and the lid was carefully transferred into a new 96-well microplate containing PBS (180µL). The lid was allowed to sit in PBS for ~ 1 minute before being transferred to a new 96-well microplate with wells containing 200µL of recovery media (MHB + 1% (v/v) Tween-20). Biofilm cells were recovered from the pegs by sonicating for 10 minutes in a water bath sonicator (Branson, 2510 MT). Following sonication, the CBD lid was disposed of while 10µL from each recovery well was transferred into new 96-well microplates containing PBS (90µL). Ten-fold serial dilutions were carried out and the serially diluted wells were spotted (5µL) onto MHA plates that were then incubated at 37 ° C for 40-48

hours. The resulting colony forming units (CFU) per peg were calculated and expressed as $\log_{10}$ CFU/peg. This procedure was carried out three times in duplicate (n=6).

Similar to the CV assay, equivalency controls were carried out prior to experimental testing to ensure that equivalent growth on each peg of the CBD lid was obtainable under the defined experimental conditions (Harrison *et al.* 2010). A CBD plate was prepared in the same manner as the CV assay equivalency control (Supplementary Figure 2a) and also grown at 37 ° C and 120 rpm in humidified conditions. Following 24 hours of incubation, the plate was removed and the viable biofilm cells were recovered and counted as described above. This control was completed two times in order to ensure that an equivalent number of viable biofilm cells were obtained across the entire CBD, thus allowing for experimental results to be comparable amongst the various treatments tested. Data included as supplementary information (Supplementary Figure 2c).

2.6 Antibiotic Susceptibility Testing

2.6.1 MBEC of antibiotics to treat Bcc biofilms

The minimum biofilm eradication concentration (MBEC), or the lowest concentration of an antimicrobial required to kill 99.9% (3 $\log_{10}$ reduction) of biofilm-embedded bacteria (Macia *et al.* 2014), was determined for *B. cepacia* 16192, *B. multivorans* C5393, and *B. cenocepacia* K56-2 biofilms treated with ceftazidime (GSK), meropenem (Sigma) or tobramycin (MP Biomedicals). Antibiotic stocks (5,120µg/mL) were prepared in sterile ddH_2O and passed through 0.2µm syringe filters (PES filter; VWR) to sterilize. Stocks were aliquoted into separate microtubes and stored at -20 ° C for long-term storage.

Initial bacterial cultures were first prepared in SCFM as outlined in section 2.1.1 and normalized to an OD_{600} of 0.005 (~ 2.0 x10^6 CFU/mL). Cultures were aliquoted (150µL) into

the inner wells of a CBD (Innovotech) while sterile media control wells were filled with SCFM only (150µL). The outer wells were filled with ddH_2O (200µL) and the plate was sealed with two layers of parafilm to help avoid desiccation. Plates were grown at 37 ˚C on a platform orbital shaker (New Brunswick Scientific, C2 Classic Series) set to 120 rpm in humidified conditions. Following 24 hours of incubation, the CBD lid was carefully removed and placed in a new 96-well microplate containing PBS (180µL) to wash biofilms for ~ 20 seconds. Using sterile bent nose pliers, three pegs of the CBD were removed and viable biofilm cells were recovered and enumerated as previously described (section 2.5.3) in order to determine the mean viable cell count (MVCC) of the pre-treated, established biofilms (Harrison *et al.* 2010). The CBD lid was then placed into a freshly prepared challenge plate, a 96-well microplate containing SCFM (162µL) and either ddH_2O (18µL) as an untreated control or one of the three antibiotics of interest (18µL) to final concentrations ranging in doubling dilutions from 1-512µg/mL. Each treatment well was prepared in duplicate. The challenge plate was incubated for an additional 24 hours at 37 ˚C and 120 rpm before recovering and enumerating the resulting viable biofilm cells as outlined in section 2.5.3. The difference between the pre-treated MVCC and the number of recovered viable biofilm cells following treatment was then determined in order to present the data as a kill-curve. This procedure was carried out three times in duplicate (n=6).

2.6.2 MBEC of antibiotics in combination with DKPs to treat Bcc biofilms

The MBEC for *B. cepacia* 16192, *B. multivorans* C5393, and *B. cenocepacia* K56-2 biofilms treated with ceftazidime (GSK), meropenem (Sigma) or tobramycin (MP Biomedicals) in combination with DKPs (100µM) was determined using the CBD (Innovotech) (Ceri *et al.* 1999). Biofilms were initially cultivated on the peg lid of the CBD and the initial MVCC was

determined after 24 hours of incubation just as described previously (section 2.6.1). The CBD lid was then transferred into a new 96-well microplate containing SCFM (162µL) and either ddH_2O (18µL) as an untreated control or one of the three antibiotics of interest (9µL) to final concentrations ranging in doubling dilutions from 1-512µg/mL. Additionally, one of the four DKPs was also included in the treatment wells (9µL) to a final concentration of 100µM. Each treatment well was prepared in duplicate. The challenge plate was incubated for an additional 24 hours at 37 ˚ C and 120 rpm before recovering and enumerating the resulting viable biofilm cells as outlined in section 2.5.3. The difference between the pre-treated MVCC and the number of recovered viable biofilm cells following treatment was then determined in order to present the data as a kill-curve. This procedure was carried out three times in duplicate (n=6) for each of the antibiotic and DKP combination tested.

2.7 Statistical Analyses

All data were analyzed and graphed using Prism version 5.0 (GraphPad). Unless otherwise stated, significance between experimental treatments and control samples were determined using one-way ANOVA statistics followed by the Dunnett post-hoc test.

Chapter Three: DKPs as Antvirulence Agents

3.1 Introduction

The pathogenicity of species within the *Burkholderia cepacia* complex (Bcc) is characterized by the production of several virulence determinants that play a significant role in their ability to colonize and establish an infection (Sousa *et al.* 2011; Scoffone *et al.* 2017). This includes the production of extracellular virulence factors such as proteases, lipases and siderophores, that together contribute to lung epithelial cell invasion, host immune evasion and bacterial persistence (Visser *et al.* 2004; Mullen *et al.* 2007; Reihill *et al.* 2017; Ganesh *et al.* 2020). Under high cell densities, these determinants are largely regulated by their CepIR quorum sensing (QS) system, where CepR acts as a transcriptional regulator when bound to the C8-HSL or C6-HSL signalling molecules that are produced by the CepI inducer synthase (Lewenza *et al.* 1999; Subsin *et al.* 2007; Suppiger *et al.* 2013). Following the same mechanism, Bcc isolates that carry the cenocepacia pathogenicity island (cci), such as *B. cenocepacia* K56-2, also carry a secondary AHL-mediated QS system, CciIR, that functions with the CepIR system to co-regulate and/or reciprocally regulate many genes required for virulence (Baldwin *et al.* 2004; Malott *et al.* 2005; O'Grady *et al.* 2009).

Although certain virulence determinants are not exclusively regulated by QS, maintaining a functional QS system is highly conserved among Bcc species and is an important regulator of pathogenic traits throughout the entirety of Bcc infection (Wopperer *et al.* 2006; McKeon *et al.* 2011; Subramoni and Sokol, 2012; Scoffone *et al.* 2019). Multiple studies have shown that Bcc strains with mutations in their CepIR and/or CciIR QS components have a decreased virulence phenotype alongside a subsequent decreased ability to maintain an infection in a wide range of hosts (Sokol *et al.* 2003; McKeon *et al.* 2011; Scoffone *et al.* 2016). Targeting QS regulation with

QS inhibitors (QSIs) is therefore regarded as one possible and promising alternative strategy for improving treatment of Bcc infections.

Considered as a novel class of QSIs, 2,5-diketopiperazines (DKPs) are capable of interfering with the production of QS-regulated virulence factors without possessing any antimicrobial activity of their own (Holden *et al.* 1999; Campbell *et al.* 2009; Buroni *et al..* 2018). Recent work in our lab identified DKPs cyclo(-D-ala-val), cyclo(-pro-val), cyclo(-leu-pro) and cyclo(-phe-pro) that alter QS regulation in Bcc species by limiting the expression of both *cepI* and *cepR* of the CepIR QS system (Purighalla, 2011). To further investigate the extent to which these DKPs alter the virulence phenotype of Bcc species, we carried out assays quantifying the changes in QS-regulated virulence factor production. This included measuring both positively regulated factors, including proteases and lipases, as well as one negatively regulated factor, siderophores (Lewenza and Sokol, 2001; Ganesh *et al.* 2020). Based on our current knowledge, we hypothesized that by acting as QSIs, DKPs would alter the virulence phenotype of Bcc species without possessing any antimicrobial activity. More specifically, we predicted that the presence of DKPs would result in a decreased detection of proteases and lipases alongside an increased detection of siderophores without affecting Bcc growth rate or viability.

Of the 24 currently identified species of the Bcc, we examined 6 different clinical isolates from three of the species most commonly isolated from CF patients and other chronic infections (Cystic Fibrosis Canada, 2018). *B. cepacia* (15862 and 16192), *B. multivorans* (C5393 and LMG13010), *B. cenocepacia* (H111 and K56-2), as well as two K56-2 QS mutant variants, K56-*cciIR* and K56-*cepR,cciIR*, were utilized in this study as representative strains for observing the effects of DKPs on the viability (section 3.2.1) and virulence phenotype (section 3.2.3) of

Bcc species. In order to gain insights into the QS altering effects of DKPs over time, the production of extracellular virulence factors was measured at both early stationary phase, when virulence factor production is initially increasing (Lewenza and Sokol, 2001), and at late stationary phase when peak production is typically observed.

3.2 Results

3.2.1 DKPs do not affect the growth rate or viability of Bcc species

One of the defining characteristics of QSIs is the lack of direct antimicrobial activity on the survival of the targeted species, limiting the amount of selective pressure for developing resistance (Slinger *et al.* 2019; Ganesh *et al.* 2020). Although DKPs have not been shown to possess any antimicrobial activity (Purighalla, 2011; Scoffone *et al.* 2016), we wanted to ensure that our DKPs of interest, cyclo(-D-ala-val), cyclo(-pro-val), cyclo(-leu-pro) and cyclo(-phe-pro), did not have any effect on the growth rate or viability of the Bcc isolates used in this study. To test this, all Bcc isolates were grown in the highly defined synthetic cystic fibrosis sputum medium (SCFM) and standard 96-well plates with the addition of either phosphate buffer (PB) as an untreated control or one of the four DKPs to a final concentration of 400μM (section 2.3). By taking optical density readings and colony counts over the span of 24 hours, DKPs did not affect the growth rate or the viability of these Bcc isolates, respectively.

With the addition of DKPs there were slight variations in the optical density (600nm) readings at the later time points of growth for most of the Bcc isolates compared to their PB buffer controls (Figure 3.1). However, none of these variations were calculated as being significantly different. A similar trend was seen for the viability of Bcc species, as the effect of DKPs on viable cell counts did not result in any significant changes from the PB buffer controls at 8, 16, or 24 hours of incubation (Figure 3.2). With these results demonstrating DKPs to lack

Figure 3.1: DKPs do not affect the growth rate of Bcc species

Bacterial strains **(a)** *B. cepacia* 15862, **(b)** *B. cepacia* 16192, **(c)** *B. multivorans* C5393, **(d)** *B. multivorans* LMG13010, **(e)** *B. cenocepacia* H111, **(f)** *B. cenocepacia* K56-2, **(g)** *B. cenocepacia* K56-*cciIR*, **(h)** *B. cenocepacia* K56-*cepR,cciIR* were grown in a 96-well microplate with the addition of either phosphate buffer (PB) as an untreated control or one of the four DKPs to a final concentration of 400μM. The optical density (600nm) was recorded every 2 hours for 24 hours. The procedure was carried out twice in triplicate (n=6). Significance between the PB control and each DKP treatment was determined by one-way ANOVA and the Dunnett post-hoc test where no significance was determined at each time point tested. Bars indicate ± SD.

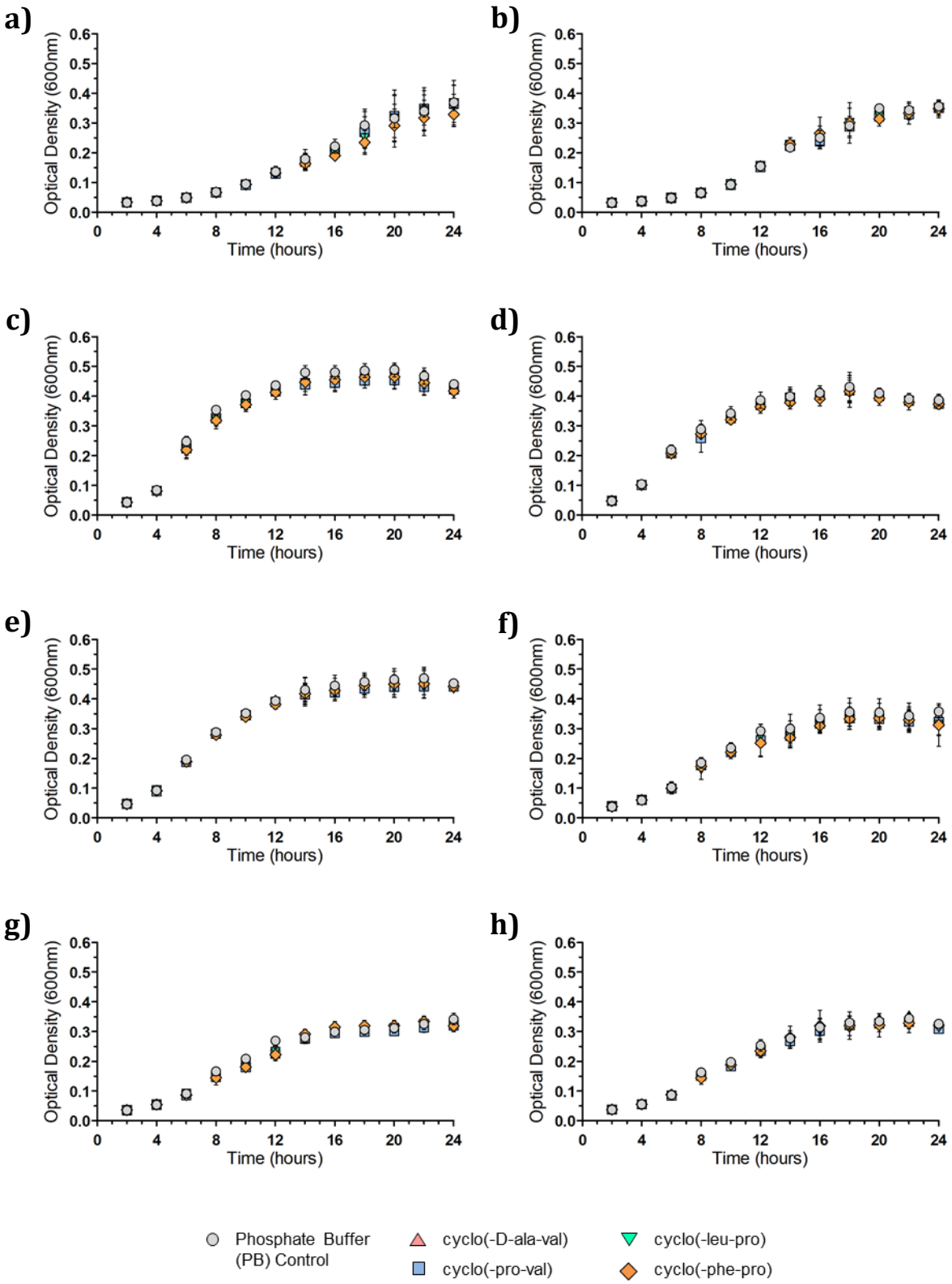
a)
b)
c)
d)
e)
f)
g)
h)
Optical Density (600nm)
Time (hours)
0.0
0.1
0.2
0.3
0.4
0.5
0.6
0
4
8
12
16
20
24
Phosphate Buffer (PB) Control
cyclo(-D-ala-val)
cyclo(-leu-pro)
cyclo(-pro-val)
cyclo(-phe-pro)

Figure 3.2: DKPs do not affect the viable cell count of Bcc species

Bacterial strains **(a)** *B. cepacia* 15862, **(b)** *B. cepacia* 16192, **(c)** *B. multivorans* C5393, **(d)** *B. multivorans* LMG13010, **(e)** *B. cenocepacia* H111, **(f)** *B. cenocepacia* K56-2, **(g)** *B. cenocepacia* K56-*cciIR*, **(h)** *B. cenocepacia* K56-*cepR,cciIR* were grown in a 96-well microplate with the addition of either phosphate buffer (PB) as an untreated control or one of the four DKPs to a final concentration of 400μM. The viable cell count ($\log_{10}$ CFU/mL) was measured every 8 hours for 24 hours. The procedure was carried out twice in triplicate (n=6). Significance between the PB control and each DKP treatment was determined by one-way ANOVA and the Dunnett post-hoc test where no significance was determined at each time point tested. Bars indicate ± SD.

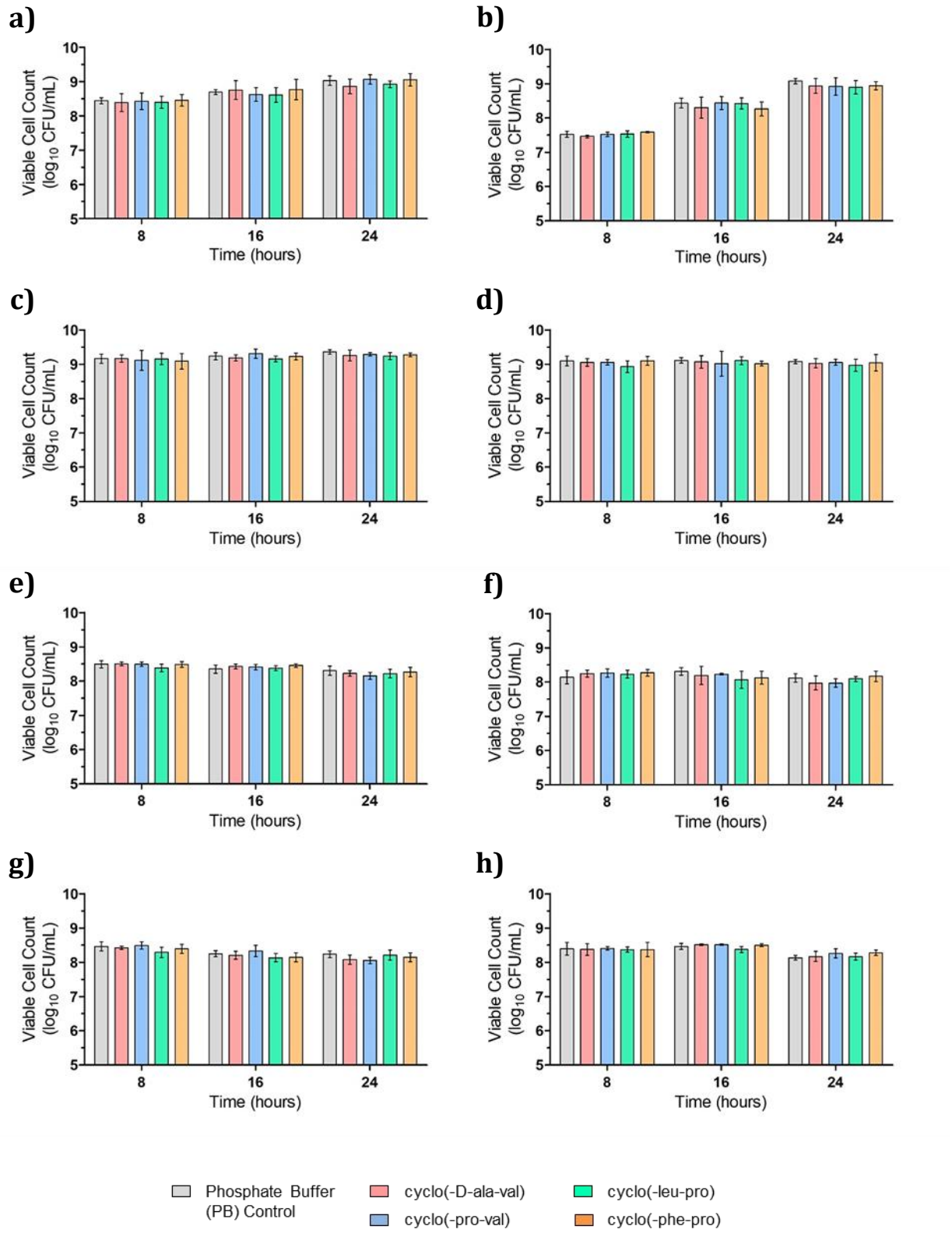
a)
b)
c)
d)
e)
f)
g)
h)
Viable Cell Count (log_{10} CFU/mL)
Time (hours)
Phosphate Buffer (PB) Control
cyclo(-D-ala-val)
cyclo(-pro-val)
cyclo(-leu-pro)
cyclo(-phe-pro)

antimicrobial activity against the Bcc isolates, we then moved ahead with observing the production of proteases, lipases and siderophores by these isolates as well as the extent to which DKPs altered their production.

3.2.2 Extracellular virulence factor production of Bcc species

Prior to the addition of DKPs, Bcc species were first grown without the presence of DKPs in order to assess the untreated production level of extracellular virulence factors and to also ensure that successful detection was possible under the defined experimental conditions. Furthermore, we were interested in observing the production of these factors in Bcc species over time, specifically, the production of proteases, lipases and siderophores during both early and late stationary phase. To determine appropriate time points for observation, growth assessments were done on each of the isolates as outlined in section 2.4.1. Early stationary phase was determined to occur around 12 hours for *B. multivorans* isolates and 14 hours for *B. cepacia* and *B. cenocepacia* isolates when grown as 3mL cultures in SCFM (Supplementary Figure 1). While late stationary phase was deemed to occur six hours later, being 18 hours for *B. multivorans* and 20 hours for *B. cepacia* and *B. cenocepacia*. By isolating cell-free spent media at these time points, multiple analyses were conducted in parallel to determine the extracellular virulence factor production of each Bcc isolate.

Following collection of cell-free spent media, the use of the chromogenic protease substrate azocaesin allowed for positive detection of proteases secreted by Bcc species (Figure 3.3a). The production of proteases was similar between isolates of the same species, where both *B. cepacia* isolates, 15862 and 16192, had the greatest amount of protease production compared to all other Bcc isolates with average productions of 0.070 and 0.064 at early stationary phase and 0.081 and 0.085 at late stationary phase, respectively. In contrast to this,

Figure 3.3: Extracellular virulence factor production of Bcc species at early and late stationary phases of bacterial growth

(a) protease production, **(b)** lipase production, and **(c)** siderophore production was quantified at both early stationary (*solid bars*) and late stationary (*striped bars*) phase for each of the Bcc isolates when grown in the presence of phosphate buffer (PB), utilized to represent the untreated control in this study. Cell-free spent media was collected after 12 and 18 hours of incubation for *B. multivorans* isolates and after 14 and 20 hours of incubation for *B. cepacia* and *B. cenocepacia* isolates grown as 3mL cultures in SCFM. Various microplate-based methods were utilized to measure the extracellular virulence factor production spectrophotometrically (section 2.4). Each procedure was carried out twice in triplicate and significance between K56-2 and each of the two QS mutant strains was determined by an unpaired t-test; ns (no significance), * ($p \leq 0.05$), ** ($p \leq 0.01$), *** ($p \leq 0.001$). Bars indicate ± SD.

a)

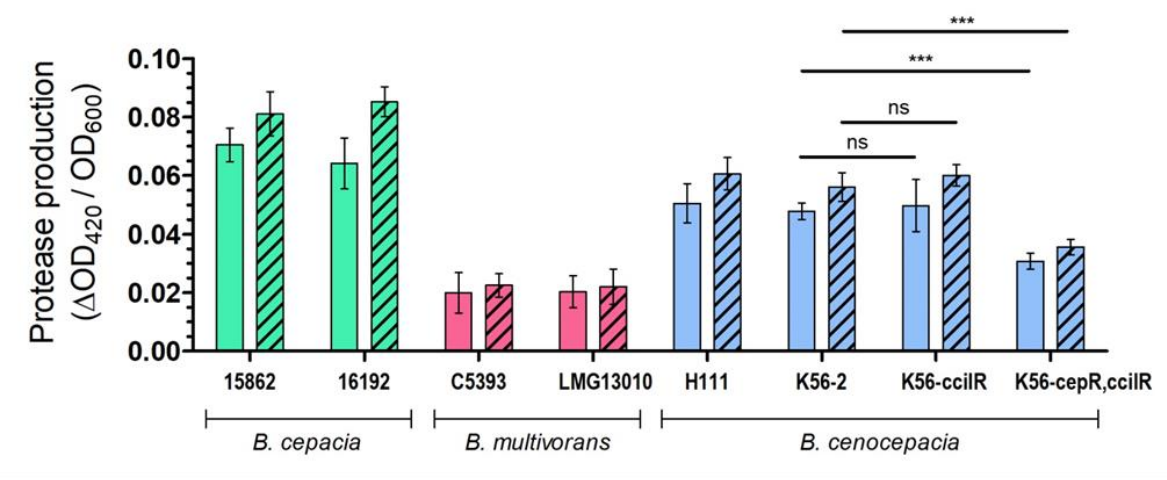
Protease production
(ΔOD420 / OD600)
0.10
0.08
0.06
0.04
0.02
0.00
***
***
ns
ns
15862
16192
C5393
LMG13010
H111
K56-2
K56-ccilR
K56-cepR,ccilR
B. cepacia
B. multivorans
B. cenocepacia

b)

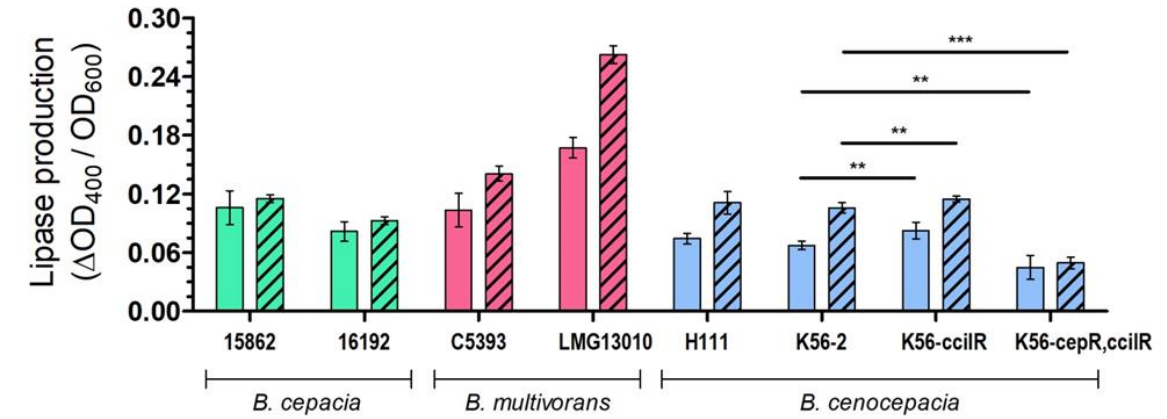
Lipase production
(ΔOD400 / OD600)
0.30
0.24
0.18
0.12
0.06
0.00
***
**
**
**
15862
16192
C5393
LMG13010
H111
K56-2
K56-ccilR
K56-cepR,ccilR
B. cepacia
B. multivorans
B. cenocepacia

c)

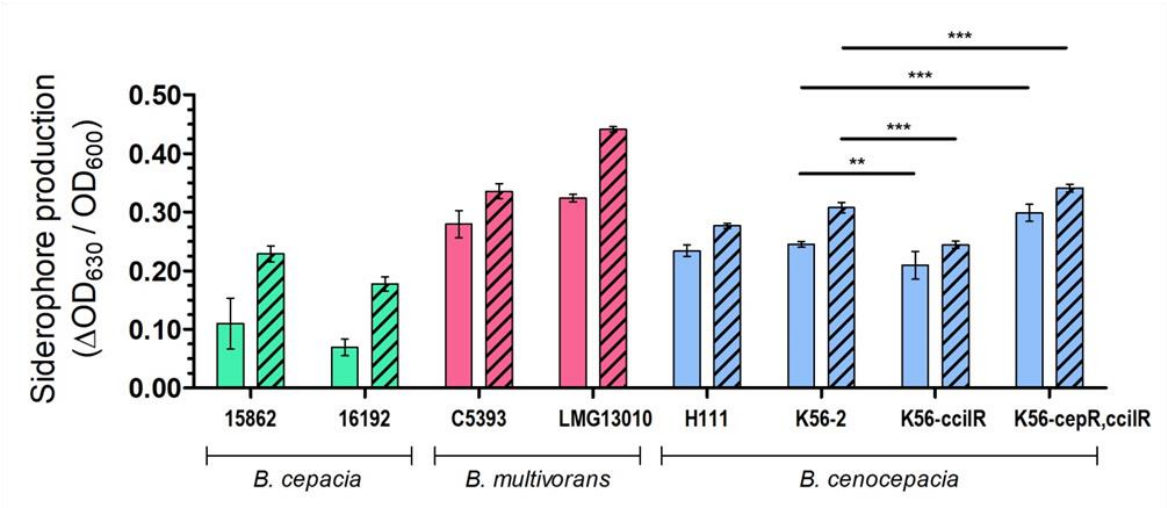
Siderophore production
(ΔOD630 / OD600)
0.50
0.40
0.30
0.20
0.10
0.00
***
***
***
**
15862
16192
C5393
LMG13010
H111
K56-2
K56-ccilR
K56-cepR,ccilR
B. cepacia
B. multivorans
B. cenocepacia

both of the *B. multivorans* isolates, C5393 and LMG13010, had minimal protease detection with no significant increase in production over time as the average $\Delta OD_{420}/OD_{600}$ at early and late stationary phase for both isolates was 0.020 and 0.022, respectively. The *B. cenocepacia* isolate H111 had an intermediate level of protease production over time with an average value of 0.050 at early stationary phase and 0.060 at late stationary phase, while the production of proteases by isolate K56-2 was highly dependent on the presence of mutations in QS genes (Figure 3.3a). Protease production in strain K56-*cciIR* was slightly higher than the parental strain K56-2, but not significantly higher. Whereas the production in the double QS mutant, K56-*cepR,cciIR,* was significantly lower than K56-2, showing protease levels that were ~33% less at both early and late stationary phase.

By utilizing Tween-20 as a polyoxyethylene substrate for the measurement of lipases, the precipitate formed as a result of lipase activity was quantified at an optical density of 400nm, showing a somewhat opposing pattern compared to what was seen in the detection of proteases (Figure 3.3b). Unlike the large amount of proteases produced by the *B. cepacia* isolates, both 15862 and 16192 produced a relatively low amount of lipases that did not significantly increase over time. Also, notably, the *B. multivorans* isolates C5393 and LMG1301, which had the lowest amount of proteases detected, produced the greatest amount of lipases with $\Delta OD_{400}/OD_{600}$ readings that were on average ~20% and ~130% higher than all other isolates at late stationary phase, respectively. Similar to the results of protease production, the lipase production of *B. cenocepacia* K56-2 was also significantly different from the two QS mutant variants (Figure 3.3b). Isolate K56-2 had an average lipase production of 0.067 at early stationary phase, whereas K56-*cciIR* had a significantly higher value of 0.083 and K56-*cepR,cciIR* produced ~40% less with an average $\Delta OD_{400}/OD_{600}$ of 0.045. This trend was also

seen at the later time point; however the difference was even greater between K56-2 and K56-*cepR,cciIR* as the double mutant produced less than 50% than that of the parental strain.

The total production of extracellular siderophores was detected using the colorimetric and highly sensitive chrome azurol S (CAS) assay, where a relatively high amount of siderophore activity was detected in all of the Bcc isolates in this study (Figure 3.3c). Unlike what was seen in the production of the other extracellular virulence factors, the production of siderophores was highly growth-phase dependent as a significantly greater amount of siderophore activity was seen at the later stationary phase for all of the Bcc isolates. Of the 8 isolates examined, both of the *B. cepacia* isolates had the greatest increase from early to late stationary phase as the $\Delta OD_{630}/OD_{600}$ doubled in isolate 15862 and tripled in isolate 16192. Similar to lipase production, *B. multivorans* isolates C5393 and LMG13010 had the greatest detection of siderophores with values of 0.336 and 0.441 at late stationary phase, respectively. Both of the *B. cenocepacia* isolates, H111 and K56-2, had similar levels of siderophore production over time, while the production levels of the two QS mutant variants were significantly different from the parental strain (Figure 3.3c). In an opposing manner to the results seen for the production of lipases, K56-*cciIR* had a significantly lower detection of siderophores compared to K56-2 while a significantly higher detection was observed for K56-*cepR,cciIR* at both early and late stationary phase.

With successful detection of each of the extracellular virulence factors under investigation, changes in the production of proteases, lipases, and siderophores as a result of exposure to DKPs cyclo(-D-ala-val), cyclo(-pro-val), cyclo(-leu-pro) and cyclo(-phe-pro) was then determined with the results reported below.

3.2.3 DKPs alter extracellular virulence factor production of Bcc species

3.2.3.1 Protease production

With the addition of DKPs our original hypothesis was supported as a lower amount of protease activity was detected over time for each of the Bcc species (Table 3.1 & 3.2). With an increasing concentration of DKPs there was a subsequently larger decrease in the $\Delta OD_{420}/OD_{600}$ readings compared to the PB buffer controls (0μM DKP) for most of the isolates tested. As bacterial growth progressed from early to late stationary phase, the inhibitory effects of DKPs showed a similar pattern of significance at both time points. Looking specifically at *B. cepacia*, although all four DKPs of interest decreased the production of proteases, their effects differed between the two isolates. Both cyclo(-D-ala-val) and cyclo(-phe-pro) resulted in the greatest decrease of 30% in isolate 15862, while cyclo(-pro-val) and cyclo(-phe-pro) were the most inhibitory towards 16192 with a 35% decrease (Table 3.1). Interestingly, this was not seen in the later time point as the presence of cyclo(-leu-pro) resulted in the greatest decrease of ~30% in both *B. cepacia* isolates (Table 3.2).

Both of the *B. multivorans* strains produced a relatively minimal amount of proteases over time as detected using the substrate azocaesin (Table 3.1 & 3.2). Seen at both early and late stationary phases, DKPs were not effective towards *B. multivorans* LMG13010 as none of the four molecules resulted in a significant change from the PB buffer control $\Delta OD_{420}/OD_{600}$ values of 0.020 and 0.022, respectively. Isolate C5393 was also not greatly affected as only cyclo(-leu-pro) and cyclo(-phe-pro) decreased protease production by ~25% at early stationary phase (Table 3.1), while cyclo(-pro-val) was the only DKP to result such a decrease at late stationary phase (Table 3.2). In contrast to this, all 4 DKPs resulted in significant decreases in each of the *B. cenocepacia* isolates over time, except for the double QS mutant,

Table 3.1: DKPs decrease Bcc protease production at early stationary phase

Bcc isolates were grown as 3mL cultures in synthetic cystic fibrosis sputum medium (SCFM) with the addition of either phosphate buffer (PB) as an untreated control (0μM DKP) or one of the four DKPs to a final concentration of 25, 100 or 400μM. Cell-free spent media was collected after 12 hours of incubation for *B. multivorans* isolates and 14 hours for *B. cepacia* and *B. cenocepacia* isolates. Spent media samples were incubated with azocasein for 2 hours as described (section 2.4.2) and the $\Delta OD_{420}/OD_{600}$ was determined spectrophotometrically. This procedure was carried out twice in triplicate and significance (sig.) was determined by one-way ANOVA and the Dunnett post-hoc test (ns = no significance; * = $p<0.05$; ** = $p<0.01$; *** = $p<0.001$). SD = ± standard deviation.

strain	DKP [µM]	Cyclo(-D-ala-val)			Cyclo(-pro-val)			Cyclo(-leu-pro)			Cyclo(-phe-pro)		
		$\Delta OD_{420}/OD_{600}$	SD	Sig.	**$\Delta OD_{420}/OD_{600}$**	SD	Sig.	**$\Delta OD_{420}/OD_{600}$**	SD	Sig.	**$\Delta OD_{420}/OD_{600}$**	SD	Sig.
***B. cepacia* (15862)**	0	**0.070**	0.006		**0.070**	0.006		**0.070**	0.006		**0.070**	0.006	
	25	**0.059**	0.004	*	**0.064**	0.004	ns	**0.064**	0.003	ns	**0.059**	0.003	ns
	100	**0.069**	0.012	ns	**0.060**	0.010	ns	**0.063**	0.011	ns	**0.060**	0.004	ns
	400	**0.050**	0.008	***	**0.059**	0.001	*	**0.056**	0.006	**	**0.050**	0.004	***
***B. cepacia* (16192)**	0	**0.064**	0.009		**0.064**	0.009		**0.064**	0.009		**0.064**	0.009	
	25	**0.056**	0.004	ns	**0.055**	0.008	ns	**0.057**	0.004	ns	**0.057**	0.002	ns
	100	**0.057**	0.002	ns	**0.047**	0.007	***	**0.054**	0.005	*	**0.051**	0.003	**
	400	**0.051**	0.008	**	**0.042**	0.006	***	**0.052**	0.005	**	**0.044**	0.006	***
***B. multivorans* (C5393)**	0	**0.020**	0.007		**0.020**	0.007		**0.020**	0.007		**0.020**	0.007	
	25	**0.023**	0.002	ns	**0.021**	0.004	ns	**0.017**	0.001	ns	**0.016**	0.002	ns
	100	**0.018**	0.001	ns	**0.017**	0.003	ns	**0.018**	0.001	ns	**0.016**	0.003	ns
	400	**0.017**	0.003	ns	**0.016**	0.002	ns	**0.015**	0.001	*	**0.015**	0.002	*
***B. multivorans* (LMG13010)**	0	**0.020**	0.005		**0.020**	0.005		**0.020**	0.005		**0.020**	0.005	
	25	**0.017**	0.003	ns	**0.020**	0.004	ns	**0.019**	0.003	ns	**0.018**	0.003	ns
	100	**0.017**	0.004	ns	**0.016**	0.003	ns	**0.020**	0.001	ns	**0.016**	0.004	ns
	400	**0.015**	0.004	ns	**0.018**	0.001	ns	**0.016**	0.005	ns	**0.018**	0.003	ns
***B. cenocepacia* (H111)**	0	**0.050**	0.007		**0.050**	0.007		**0.050**	0.007		**0.050**	0.007	
	25	**0.047**	0.007	ns	**0.048**	0.005	ns	**0.050**	0.005	ns	**0.044**	0.004	ns
	100	**0.045**	0.002	ns	**0.047**	0.008	ns	**0.049**	0.004	ns	**0.039**	0.002	**
	400	**0.040**	0.006	**	**0.042**	0.005	*	**0.041**	0.002	*	**0.037**	0.003	***
***B. cenocepacia* (K56-2)**	0	**0.048**	0.003		**0.048**	0.003		**0.048**	0.003		**0.048**	0.003	
	25	**0.045**	0.004	ns	**0.044**	0.005	ns	**0.046**	0.002	ns	**0.040**	0.002	**
	100	**0.045**	0.003	ns	**0.045**	0.003	ns	**0.040**	0.002	***	**0.044**	0.004	ns
	400	**0.041**	0.004	**	**0.038**	0.003	***	**0.040**	0.002	**	**0.039**	0.003	***
***B. cenocepacia* (K56-*ciiR*)**	0	**0.050**	0.009		**0.050**	0.009		**0.050**	0.009		**0.050**	0.009	
	25	**0.049**	0.005	ns	**0.050**	0.006	ns	**0.045**	0.004	ns	**0.044**	0.008	ns
	100	**0.043**	0.006	ns	**0.043**	0.006	ns	**0.036**	0.006	**	**0.041**	0.005	ns
	400	**0.033**	0.005	***	**0.034**	0.006	***	**0.035**	0.007	**	**0.035**	0.004	***
***B. cenocepacia* (K56-*cepR,ciiR*)**	0	**0.031**	0.003		**0.031**	0.003		**0.031**	0.003		**0.031**	0.003	
	25	**0.034**	0.003	ns	**0.030**	0.005	ns	**0.029**	0.005	ns	**0.027**	0.002	ns
	100	**0.034**	0.004	ns	**0.030**	0.003	ns	**0.026**	0.003	ns	**0.025**	0.002	ns
	400	**0.025**	0.002	ns	**0.025**	0.002	ns	**0.026**	0.005	ns	**0.023**	0.003	**

Table 3.2: DKPs decrease Bcc protease production at late stationary phase

Bcc isolates were grown as 3mL cultures in synthetic cystic fibrosis sputum medium (SCFM) with the addition of either phosphate buffer (PB) as an untreated control (0μM DKP) or one of the four DKPs to a final concentration of 25, 100 or 400μM. Cell-free spent media was collected after 18 hours of incubation for *B. multivorans* isolates and 20 hours for *B. cepacia* and *B. cenocepacia* isolates. Spent media samples were incubated with azocasein for 2 hours as described (section 2.4.2) and the $\Delta OD_{420}/OD_{600}$ was determined spectrophotometrically. This procedure was carried out twice in triplicate and significance (sig.) was determined by one-way ANOVA and the Dunnett post-hoc test (ns = no significance; * = $p<0.05$; ** = $p<0.01$; *** = $p<0.001$). SD = ± standard deviation.

strain	DKP [µM]	Cyclo(-D-ala-val)			Cyclo(-pro-val)			Cyclo(-leu-pro)			Cyclo(-phe-pro)		
		$\Delta OD_{420}/OD_{600}$	SD	Sig.	**$\Delta OD_{420}/OD_{600}$**	SD	Sig.	**$\Delta OD_{420}/OD_{600}$**	SD	Sig.	**$\Delta OD_{420}/OD_{600}$**	SD	Sig.
***B. cepacia* (15862)**	0	**0.081**	0.007		**0.081**	0.007		**0.081**	0.007		**0.081**	0.007	
	25	**0.082**	0.003	ns	**0.072**	0.007	ns	**0.069**	0.008	ns	**0.079**	0.013	ns
	100	**0.078**	0.010	ns	**0.066**	0.011	*	**0.069**	0.010	ns	**0.070**	0.003	ns
	400	**0.065**	0.004	**	**0.064**	0.007	**	**0.059**	0.008	***	**0.065**	0.002	**
***B. cepacia* (16192)**	0	**0.085**	0.005		**0.085**	0.005		**0.085**	0.005		**0.085**	0.005	
	25	**0.075**	0.009	ns	**0.084**	0.005	ns	**0.075**	0.009	ns	**0.083**	0.013	ns
	100	**0.081**	0.008	ns	**0.078**	0.002	ns	**0.069**	0.006	**	**0.074**	0.005	ns
	400	**0.075**	0.007	ns	**0.072**	0.005	*	**0.058**	0.004	***	**0.064**	0.006	***
***B. multivorans* (C5393)**	0	**0.023**	0.004		**0.023**	0.004		**0.023**	0.004		**0.023**	0.004	
	25	**0.025**	0.004	ns	**0.022**	0.004	ns	**0.023**	0.004	ns	**0.023**	0.004	ns
	100	**0.025**	0.008	ns	**0.021**	0.005	ns	**0.021**	0.005	ns	**0.017**	0.002	ns
	400	**0.019**	0.006	ns	**0.015**	0.001	*	**0.018**	0.002	ns	**0.017**	0.002	ns
***B. multivorans* (LMG13010)**	0	**0.022**	0.006		**0.022**	0.006		**0.022**	0.006		**0.022**	0.006	
	25	**0.024**	0.006	ns	**0.022**	0.006	ns	**0.025**	0.005	ns	**0.022**	0.003	ns
	100	**0.015**	0.007	ns	**0.026**	0.005	ns	**0.025**	0.006	ns	**0.019**	0.003	ns
	400	**0.016**	0.004	ns	**0.020**	0.005	ns	**0.020**	0.005	ns	**0.016**	0.006	ns
***B. cenocepacia* (H111)**	0	**0.061**	0.006		**0.061**	0.006		**0.061**	0.006		**0.061**	0.006	
	25	**0.065**	0.008	ns	**0.054**	0.002	ns	**0.056**	0.004	ns	**0.059**	0.008	ns
	100	**0.059**	0.005	ns	**0.054**	0.004	ns	**0.054**	0.002	ns	**0.052**	0.003	*
	400	**0.050**	0.003	**	**0.053**	0.002	*	**0.052**	0.002	**	**0.050**	0.002	***
***B. cenocepacia* (K56-2)**	0	**0.056**	0.005		**0.056**	0.005		**0.056**	0.005		**0.056**	0.005	
	25	**0.051**	0.006	ns	**0.049**	0.005	ns	**0.051**	0.007	ns	**0.050**	0.004	ns
	100	**0.049**	0.005	ns	**0.048**	0.008	ns	**0.047**	0.004	*	**0.049**	0.001	ns
	400	**0.040**	0.008	***	**0.045**	0.005	**	**0.045**	0.003	**	**0.040**	0.005	***
***B. cenocepacia* (K56-*ciiR*)**	0	**0.060**	0.004		**0.060**	0.004		**0.060**	0.004		**0.060**	0.004	
	25	**0.062**	0.001	ns	**0.057**	0.005	ns	**0.059**	0.004	ns	**0.057**	0.005	ns
	100	**0.057**	0.004	ns	**0.055**	0.002	ns	**0.051**	0.001	***	**0.051**	0.001	***
	400	**0.048**	0.002	***	**0.049**	0.002	***	**0.050**	0.003	***	**0.049**	0.006	***
***B. cenocepacia* (K56-*cepR,ciiR*)**	0	**0.036**	0.003		**0.036**	0.003		**0.036**	0.003		**0.036**	0.003	
	25	**0.034**	0.002	ns	**0.037**	0.001	ns	**0.033**	0.003	ns	**0.031**	0.004	ns
	100	**0.036**	0.002	ns	**0.037**	0.002	ns	**0.031**	0.002	ns	**0.031**	0.005	ns
	400	**0.034**	0.002	ns	**0.033**	0.005	ns	**0.031**	0.002	ns	**0.030**	0.002	*

K56-*cepR,cciIR,* which only experienced a decrease while in the presence of cyclo(-phe-pro) (Table 3.1 & 3.2). Both cyclo(-leu-pro) and cyclo(-phe-pro) proved to be the most inhibitory towards protease production in these isolates as the other two DKPs, cyclo(-D-ala-val) and cyclo(-pro-val), only resulted in a significant decrease when added at a concentration of 400μM. It is also interesting to note that at this concentration of DKPs, protease production in K56-*cciIR* decreased to levels that were similar to the untreated control of the double mutant, K56-*cepR,cciIR,* at early stationary phase (Table 3.1).

3.2.3.2 Lipase production

In a similar manner to protease production, lipases are also positively regulated by QS (Lewenza *et al.* 1999; O'Grady *et al.* 2009), therefore our hypothesis was the same with the prediction that the addition of DKPs would result in a decreased level of lipase detection in Bcc species. Our data supported this hypothesis as the presence of DKPs was inhibitory towards lipase production of the Bcc isolates used in this study (Table 3.3 & 3.4). In general, a greater difference was observed at late stationary phase compared to the earlier time point, showing an increase in inhibition over time. At early stationary phase, cyclo(-leu-pro) was the most effective as all of the Bcc isolates, except for K56-*cepR,cciIR,* experienced a significant decrease in lipase production (Table 3.3). While at late stationary phase cyclo(-phe-pro) was the most inhibitory as even the smallest concentration tested of 25μM resulted in significant decreases in many of the Bcc isolates (Table 3.4).

The changes in lipase production over time in the *B. cepacia* isolates were observed to be highly dependent on the DKP molecule that was present (Table 3.3 & 3.4). Neither cyclo(-D-ala-val) or cyclo(-pro-val) significantly decreased production in 15862 or 16192 until the late stationary phase where a ~20% decrease was observed. Whereas cyclo(-phe-pro) inhibited

Table 3.3: DKPs decrease Bcc lipase production at early stationary phase

Bcc isolates were grown as 3mL cultures in synthetic cystic fibrosis sputum medium (SCFM) with the addition of either phosphate buffer (PB) as an untreated control (0μM DKP) or one of the four DKPs to a final concentration of 25, 100 or 400μM. Cell-free spent media was collected after 12 hours of incubation for *B. multivorans* isolates and 14 hours for *B. cepacia* and *B. cenocepacia* isolates. Spent media samples were incubated with Tween-20 for 2 hours as described (section 2.4.3) and the $\Delta OD_{400}/OD_{600}$ was determined spectrophotometrically. This procedure was carried out twice in triplicate and significance (sig.) was determined by one-way ANOVA and the Dunnett post-hoc test (ns = no significance; * = $p<0.05$; ** = $p<0.01$; *** = $p<0.001$). SD = ± standard deviation.

strain	DKP [µM]	Cyclo(-D-ala-val)			Cyclo(-pro-val)			Cyclo(-leu-pro)			Cyclo(-phe-pro)		
		$\Delta OD_{400}/OD_{600}$	SD	Sig.	**$\Delta OD_{400}/OD_{600}$**	SD	Sig.	**$\Delta OD_{400}/OD_{600}$**	SD	Sig.	**$\Delta OD_{400}/OD_{600}$**	SD	Sig.
***B. cepacia* (15862)**	0	**0.106**	0.017		**0.106**	0.017		**0.106**	0.017		**0.106**	0.017	
	25	**0.092**	0.009	ns	**0.095**	0.009	ns	**0.101**	0.016	ns	**0.082**	0.010	*
	100	**0.099**	0.022	ns	**0.095**	0.019	ns	**0.098**	0.019	ns	**0.082**	0.007	*
	400	**0.084**	0.009	ns	**0.097**	0.015	ns	**0.073**	0.004	**	**0.059**	0.013	***
***B. cepacia* (16192)**	0	**0.082**	0.010		**0.082**	0.010		**0.082**	0.010		**0.082**	0.010	
	25	**0.076**	0.007	ns	**0.092**	0.012	ns	**0.070**	0.007	ns	**0.066**	0.004	*
	100	**0.080**	0.006	ns	**0.076**	0.004	ns	**0.067**	0.006	*	**0.063**	0.012	**
	400	**0.080**	0.012	ns	**0.070**	0.010	ns	**0.069**	0.008	ns	**0.061**	0.004	***
***B. multivorans* (C5393)**	0	**0.104**	0.017		**0.104**	0.017		**0.104**	0.017		**0.104**	0.017	
	25	**0.099**	0.010	ns	**0.102**	0.009	ns	**0.106**	0.011	ns	**0.103**	0.007	ns
	100	**0.104**	0.007	ns	**0.097**	0.003	ns	**0.082**	0.014	*	**0.096**	0.003	ns
	400	**0.095**	0.003	ns	**0.097**	0.005	ns	**0.092**	0.008	ns	**0.093**	0.008	ns
***B. multivorans* (LMG13010)**	0	**0.167**	0.011		**0.167**	0.011		**0.167**	0.011		**0.167**	0.011	
	25	**0.170**	0.022	ns	**0.183**	0.021	ns	**0.149**	0.023	ns	**0.162**	0.011	ns
	100	**0.164**	0.032	ns	**0.153**	0.013	ns	**0.127**	0.040	*	**0.151**	0.011	ns
	400	**0.161**	0.022	ns	**0.141**	0.016	ns	**0.117**	0.020	**	**0.145**	0.024	ns
***B. cenocepacia* (H111)**	0	**0.074**	0.005		**0.074**	0.005		**0.074**	0.005		**0.074**	0.005	
	25	**0.070**	0.003	ns	**0.064**	0.006	ns	**0.068**	0.004	ns	**0.065**	0.008	ns
	100	**0.068**	0.009	ns	**0.066**	0.003	ns	**0.061**	0.007	*	**0.066**	0.005	ns
	400	**0.057**	0.011	**	**0.057**	0.013	**	**0.061**	0.006	*	**0.059**	0.006	*
***B. cenocepacia* (K56-2)**	0	**0.067**	0.004		**0.067**	0.004		**0.067**	0.004		**0.067**	0.004	
	25	**0.056**	0.011	ns	**0.053**	0.009	ns	**0.052**	0.014	*	**0.055**	0.006	ns
	100	**0.059**	0.007	ns	**0.054**	0.010	ns	**0.051**	0.016	*	**0.060**	0.004	ns
	400	**0.051**	0.005	*	**0.052**	0.008	*	**0.052**	0.003	*	**0.054**	0.002	ns
***B. cenocepacia* (K56-*ciiR*)**	0	**0.082**	0.008		**0.082**	0.008		**0.082**	0.008		**0.082**	0.008	
	25	**0.080**	0.005	ns	**0.088**	0.006	ns	**0.075**	0.007	ns	**0.078**	0.007	ns
	100	**0.077**	0.009	ns	**0.076**	0.009	ns	**0.072**	0.006	ns	**0.072**	0.003	*
	400	**0.069**	0.005	**	**0.067**	0.007	**	**0.071**	0.003	**	**0.063**	0.005	**
***B. cenocepacia* (K56-*cepR,ciiR*)**	0	**0.045**	0.012		**0.045**	0.012		**0.045**	0.012		**0.045**	0.012	
	25	**0.051**	0.012	ns	**0.045**	0.009	ns	**0.036**	0.004	ns	**0.041**	0.006	ns
	100	**0.050**	0.011	ns	**0.046**	0.011	ns	**0.036**	0.006	ns	**0.034**	0.003	ns
	400	**0.039**	0.004	ns	**0.035**	0.004	ns	**0.041**	0.006	ns	**0.035**	0.005	ns

Table 3.4: DKPs decrease Bcc lipase production at late stationary phase

Bcc isolates were grown as 3mL cultures in synthetic cystic fibrosis sputum medium (SCFM) with the addition of either phosphate buffer (PB) as an untreated control (0μM DKP) or one of the four DKPs to a final concentration of 25, 100 or 400μM. Cell-free spent media was collected after 18 hours of incubation for *B. multivorans* isolates and 20 hours for *B. cepacia* and *B. cenocepacia* isolates. Spent media samples were incubated with Tween-20 for 2 hours as described (section 2.4.3) and the $\Delta OD_{400}/OD_{600}$ was determined spectrophotometrically. This procedure was carried out twice in triplicate and significance (sig.) was determined by one-way ANOVA and the Dunnett post-hoc test (ns = no significance; * = $p<0.05$; ** = $p<0.01$; *** = $p<0.001$). SD = ± standard deviation.

strain	DKP [μM]	Cyclo(-D-ala-val)			Cyclo(-pro-val)			Cyclo(-leu-pro)			Cyclo(-phe-pro)		
		$\Delta OD_{400}/OD_{600}$	SD	Sig.	**$\Delta OD_{400}/OD_{600}$**	SD	Sig.	**$\Delta OD_{400}/OD_{600}$**	SD	Sig.	**$\Delta OD_{400}/OD_{600}$**	SD	Sig.
***B. cepacia* (15862)**	0	**0.115**	0.004		**0.115**	0.004		**0.115**	0.004		**0.115**	0.004	
	25	**0.111**	0.012	ns	**0.095**	0.013	ns	**0.091**	0.015	*	**0.098**	0.015	ns
	100	**0.095**	0.011	ns	**0.098**	0.008	ns	**0.085**	0.018	**	**0.091**	0.005	**
	400	**0.097**	0.014	ns	**0.095**	0.012	*	**0.080**	0.017	***	**0.085**	0.010	***
***B. cepacia* (16192)**	0	**0.093**	0.004		**0.093**	0.004		**0.093**	0.004		**0.093**	0.004	
	25	**0.077**	0.012	ns	**0.088**	0.009	ns	**0.078**	0.005	ns	**0.072**	0.016	**
	100	**0.076**	0.008	*	**0.073**	0.010	**	**0.071**	0.011	**	**0.072**	0.007	**
	400	**0.077**	0.008	ns	**0.071**	0.010	**	**0.073**	0.010	*	**0.067**	0.010	***
***B. multivorans* (C5393)**	0	**0.141**	0.008		**0.141**	0.008		**0.141**	0.008		**0.141**	0.008	
	25	**0.137**	0.007	ns	**0.129**	0.020	ns	**0.135**	0.005	ns	**0.128**	0.010	ns
	100	**0.134**	0.010	ns	**0.119**	0.011	*	**0.122**	0.007	*	**0.109**	0.010	***
	400	**0.111**	0.007	***	**0.111**	0.020	**	**0.123**	0.008	ns	**0.109**	0.010	***
***B. multivorans* (LMG13010)**	0	**0.263**	0.009		**0.263**	0.009		**0.263**	0.009		**0.263**	0.009	
	25	**0.247**	0.007	ns	**0.243**	0.016	ns	**0.243**	0.011	ns	**0.243**	0.010	ns
	100	**0.259**	0.024	ns	**0.241**	0.024	ns	**0.231**	0.006	**	**0.241**	0.014	*
	400	**0.232**	0.010	*	**0.240**	0.009	*	**0.237**	0.012	*	**0.224**	0.013	***
***B. cenocepacia* (H111)**	0	**0.111**	0.011		**0.111**	0.011		**0.111**	0.011		**0.111**	0.011	
	25	**0.096**	0.011	ns	**0.096**	0.015	ns	**0.111**	0.003	ns	**0.091**	0.005	**
	100	**0.115**	0.007	ns	**0.105**	0.008	ns	**0.093**	0.006	*	**0.087**	0.008	***
	400	**0.098**	0.009	ns	**0.098**	0.012	ns	**0.083**	0.014	***	**0.082**	0.010	***
***B. cenocepacia* (K56-2)**	0	**0.106**	0.005		**0.106**	0.005		**0.106**	0.005		**0.106**	0.005	
	25	**0.098**	0.007	ns	**0.095**	0.007	ns	**0.095**	0.004	ns	**0.090**	0.005	**
	100	**0.101**	0.012	ns	**0.095**	0.011	ns	**0.092**	0.006	**	**0.089**	0.006	**
	400	**0.100**	0.010	ns	**0.094**	0.009	ns	**0.092**	0.004	*	**0.090**	0.007	**
***B. cenocepacia* (K56-*ciiR*)**	0	**0.115**	0.003		**0.115**	0.003		**0.115**	0.003		**0.115**	0.003	
	25	**0.108**	0.008	ns	**0.111**	0.006	ns	**0.111**	0.004	ns	**0.107**	0.008	ns
	100	**0.112**	0.006	ns	**0.109**	0.008	ns	**0.105**	0.005	ns	**0.103**	0.008	*
	400	**0.103**	0.007	*	**0.104**	0.006	*	**0.105**	0.005	ns	**0.106**	0.004	ns
***B. cenocepacia* (K56-*cepR,ciiR*)**	0	**0.050**	0.006		**0.050**	0.006		**0.050**	0.006		**0.050**	0.006	
	25	**0.048**	0.005	ns	**0.048**	0.004	ns	**0.043**	0.003	ns	**0.043**	0.004	ns
	100	**0.045**	0.004	ns	**0.051**	0.003	ns	**0.042**	0.005	*	**0.041**	0.004	*
	400	**0.043**	0.003	ns	**0.047**	0.004	ns	**0.040**	0.006	**	**0.041**	0.006	*

production at all of the concentrations tested, with the 400μM concentration resulting in decreases of ~ 40% in 15862 and ~25% in 16192 at both early and late stationary phase. In contrast to this, the effects of DKPs on the lipase production in *B. multivorans* were more dependent on the growth phase as there was a much greater amount of inhibition seen at late stationary phase. At the earlier time point, only cyclo(-leu-pro) resulted in significant changes in each of the isolates (Table 3.3), whereas six hours later, all four DKPs decreased the $\Delta OD_{400}/OD_{600}$ by ~20% in isolate C5393 and ~15% in isolate LMG13010 (Table 3.4). *B. cenocepacia* was the only Bcc species to be affected by cyclo(-D-ala-val) and cyclo(-pro-val) at early stationary phase as they each resulted in a ~25% decrease in isolates H111 and K56-2 as well as a ~15% decrease in K56-*cciIR* (Table 3.3). Interestingly, this inhibitory effect was lost over time as the lipase production in H111 and K56-2 was no longer significantly different from the PB buffer control in late stationary phase (Table 3.4). The double QS mutant variant which had the lowest production of lipases among all of the Bcc isolates tested was the least affected by DKPs as the only change was seen at late stationary phase while in the presence of cyclo(-leu-pro) and cyclo(-phe-pro).

3.2.3.3 Siderophore production

As opposed to the regulation of proteases and lipases, the main siderophore produced by Bcc species, ornibactin, is negatively regulated by QS (Lewenza and Sokol, 2001; O'Grady *et al.* 2009). Based on this, our original hypothesis was to observe an increased detection of siderophores while in the presence of DKPs as compared to the PB buffer controls. The results of the CAS assays conducted in this study supported this prediction as higher $\Delta OD_{630}/OD_{600}$ values were recorded for all of the Bcc isolates (Table 3.5 & 3.6). Siderophore production was the most affected extracellular virulence factor tested as all of the isolates had an increased

Table 3.5: DKPs increase Bcc siderophore production at early stationary phase

Bcc isolates were grown as 3mL cultures in synthetic cystic fibrosis sputum medium (SCFM) with the addition of either phosphate buffer (PB) as an untreated control (0μM DKP) or one of the four DKPs to a final concentration of 25, 100 or 400μM. Cell-free spent media was collected after 12 hours of incubation for *B. multivorans* isolates and 14 hours for *B. cepacia* and *B. cenocepacia* isolates. Siderophores present in spent media samples were detected using the chrome azurol S (CAS) assay as described (section 2.4.4) and the $\Delta OD_{630}/OD_{600}$ was determined spectrophotometrically. This procedure was carried out twice in triplicate and significance (sig.) was determined by one-way ANOVA and the Dunnett post-hoc test (ns = no significance; * = $p<0.05$; ** = $p<0.01$; *** = $p<0.001$). SD = ± standard deviation.

strain	DKP [μM]	Cyclo(-D-ala-val)			Cyclo(-pro-val)			Cyclo(-leu-pro)			Cyclo(-phe-pro)		
		$\Delta OD_{630}/OD_{600}$	SD	Sig.	**$\Delta OD_{630}/OD_{600}$**	SD	Sig.	**$\Delta OD_{630}/OD_{600}$**	SD	Sig.	**$\Delta OD_{630}/OD_{600}$**	SD	Sig.
***B. cepacia* (15862)**	0	**0.110**	0.043		**0.110**	0.043		**0.110**	0.043		**0.110**	0.043	
	25	**0.097**	0.008	ns	**0.114**	0.016	ns	**0.072**	0.026	ns	**0.104**	0.004	ns
	100	**0.115**	0.035	ns	**0.176**	0.020	***	**0.101**	0.036	ns	**0.129**	0.009	ns
	400	**0.120**	0.023	ns	**0.165**	0.029	**	**0.078**	0.037	ns	**0.140**	0.006	ns
***B. cepacia* (16192)**	0	**0.069**	0.014		**0.069**	0.014		**0.069**	0.014		**0.069**	0.014	
	25	**0.045**	0.019	ns	**0.062**	0.009	ns	**0.085**	0.013	ns	**0.083**	0.015	ns
	100	**0.069**	0.024	ns	**0.068**	0.013	ns	**0.085**	0.017	ns	**0.087**	0.013	ns
	400	**0.074**	0.007	ns	**0.096**	0.026	*	**0.107**	0.008	***	**0.111**	0.013	***
***B. multivorans* (C5393)**	0	**0.280**	0.023		**0.280**	0.023		**0.280**	0.023		**0.280**	0.023	
	25	**0.283**	0.006	ns	**0.283**	0.004	ns	**0.298**	0.035	ns	**0.272**	0.024	ns
	100	**0.300**	0.020	ns	**0.289**	0.019	ns	**0.302**	0.039	ns	**0.266**	0.014	ns
	400	**0.287**	0.024	ns	**0.320**	0.018	*	**0.308**	0.014	ns	**0.313**	0.006	ns
***B. multivorans* (LMG13010)**	0	**0.324**	0.007		**0.324**	0.007		**0.324**	0.007		**0.324**	0.007	
	25	**0.329**	0.020	ns	**0.334**	0.018	ns	**0.338**	0.013	ns	**0.323**	0.003	ns
	100	**0.330**	0.002	ns	**0.319**	0.011	ns	**0.329**	0.007	ns	**0.333**	0.004	ns
	400	**0.318**	0.006	ns	**0.337**	0.006	ns	**0.337**	0.007	ns	**0.339**	0.007	*
***B. cenocepacia* (H111)**	0	**0.234**	0.010		**0.234**	0.010		**0.234**	0.010		**0.234**	0.010	
	25	**0.249**	0.012	ns	**0.244**	0.024	ns	**0.256**	0.011	ns	**0.239**	0.009	ns
	100	**0.251**	0.009	ns	**0.249**	0.011	ns	**0.260**	0.006	*	**0.258**	0.016	*
	400	**0.253**	0.013	ns	**0.251**	0.021	ns	**0.266**	0.011	***	**0.272**	0.007	***
***B. cenocepacia* (K56-2)**	0	**0.245**	0.005		**0.245**	0.005		**0.245**	0.005		**0.245**	0.005	
	25	**0.239**	0.009	ns	**0.239**	0.010	ns	**0.244**	0.006	ns	**0.232**	0.006	ns
	100	**0.243**	0.006	ns	**0.248**	0.010	ns	**0.253**	0.019	ns	**0.257**	0.011	ns
	400	**0.244**	0.014	ns	**0.245**	0.006	ns	**0.283**	0.010	***	**0.291**	0.005	***
***B. cenocepacia* (K56-*ciiR*)**	0	**0.209**	0.024		**0.209**	0.024		**0.209**	0.024		**0.209**	0.024	
	25	**0.213**	0.013	ns	**0.257**	0.024	***	**0.234**	0.013	ns	**0.236**	0.016	ns
	100	**0.213**	0.023	ns	**0.249**	0.021	**	**0.235**	0.019	ns	**0.231**	0.010	ns
	400	**0.228**	0.027	ns	**0.230**	0.012	ns	**0.250**	0.015	**	**0.240**	0.009	*
***B. cenocepacia* (K56-*cepR,ciiR*)**	0	**0.297**	0.015		**0.297**	0.015		**0.297**	0.015		**0.297**	0.015	
	25	**0.316**	0.009	ns	**0.288**	0.015	ns	**0.298**	0.006	ns	**0.287**	0.009	ns
	100	**0.330**	0.013	**	**0.316**	0.004	ns	**0.285**	0.020	ns	**0.278**	0.021	ns
	400	**0.306**	0.023	ns	**0.289**	0.012	ns	**0.316**	0.019	ns	**0.306**	0.015	ns

Table 3.6: DKPs increase Bcc siderophore production at late stationary phase

Bcc isolates were grown as 3mL cultures in synthetic cystic fibrosis sputum medium (SCFM) with the addition of either phosphate buffer (PB) as an untreated control (0μM DKP) or one of the four DKPs to a final concentration of 25, 100 or 400μM. Cell-free spent media was collected after 18 hours of incubation for *B. multivorans* isolates and 20 hours for *B. cepacia* and *B. cenocepacia* isolates. Siderophores present in spent media samples were detected using the chrome azurol S (CAS) assay as described (section 2.4.4) and the $\Delta OD_{630}/OD_{600}$ was determined spectrophotometrically. This procedure was carried out twice in triplicate and significance (sig.) was determined by one-way ANOVA and the Dunnett post-hoc test (ns = no significance; * = $p<0.05$; ** = $p<0.01$; *** = $p<0.001$). SD = ± standard deviation.

strain	DKP [µM]	Cyclo(-D-ala-val)			Cyclo(-pro-val)			Cyclo(-leu-pro)			Cyclo(-phe-pro)		
		OD_{630}/ OD_{600}	SD	Sig.	**ΔOD_{630}/ OD_{600}**	SD	Sig.	**ΔOD_{630}/ OD_{600}**	SD	Sig.	**ΔOD_{630}/ OD_{600}**	SD	Sig.
***B. cepacia* (15862)**	0	**0.229**	0.013		**0.229**	0.013		**0.229**	0.013		**0.229**	0.013	
	25	**0.219**	0.014	ns	**0.256**	0.020	ns	**0.244**	0.017	ns	**0.236**	0.005	ns
	100	**0.249**	0.015	ns	**0.287**	0.033	***	**0.250**	0.032	ns	**0.261**	0.016	*
	400	**0.245**	0.020	ns	**0.298**	0.020	***	**0.288**	0.010	***	**0.300**	0.010	***
***B. cepacia* (16192)**	0	**0.178**	0.012		**0.178**	0.012		**0.178**	0.012		**0.178**	0.012	
	25	**0.164**	0.016	ns	**0.180**	0.014	ns	**0.168**	0.005	ns	**0.166**	0.005	ns
	100	**0.200**	0.007	*	**0.186**	0.003	ns	**0.182**	0.004	ns	**0.179**	0.017	ns
	400	**0.209**	0.031	**	**0.206**	0.002	**	**0.205**	0.008	**	**0.208**	0.018	**
***B. multivorans* (C5393)**	0	**0.336**	0.013		**0.336**	0.013		**0.336**	0.013		**0.336**	0.013	
	25	**0.333**	0.009	ns	**0.338**	0.020	ns	**0.319**	0.012	ns	**0.321**	0.005	ns
	100	**0.370**	0.009	**	**0.316**	0.008	ns	**0.341**	0.019	ns	**0.318**	0.013	ns
	400	**0.351**	0.010	ns	**0.371**	0.004	**	**0.374**	0.026	**	**0.384**	0.031	***
***B. multivorans* (LMG13010)**	0	**0.441**	0.004		**0.441**	0.004		**0.441**	0.004		**0.441**	0.004	
	25	**0.469**	0.010	ns	**0.502**	0.019	***	**0.481**	0.017	*	**0.461**	0.046	ns
	100	**0.522**	0.031	***	**0.488**	0.040	**	**0.472**	0.018	ns	**0.467**	0.004	ns
	400	**0.478**	0.011	ns	**0.490**	0.018	**	**0.528**	0.009	***	**0.471**	0.005	*
***B. cenocepacia* (H111)**	0	**0.273**	0.011		**0.273**	0.011		**0.273**	0.011		**0.273**	0.011	
	25	**0.269**	0.011	ns	**0.292**	0.018	ns	**0.296**	0.022	ns	**0.281**	0.013	ns
	100	**0.303**	0.013	**	**0.306**	0.013	**	**0.299**	0.018	*	**0.289**	0.011	ns
	400	**0.271**	0.006	ns	**0.302**	0.013	**	**0.309**	0.010	***	**0.291**	0.022	ns
***B. cenocepacia* (K56-2)**	0	**0.308**	0.009		**0.308**	0.009		**0.308**	0.009		**0.308**	0.009	
	25	**0.313**	0.007	ns	**0.303**	0.006	ns	**0.322**	0.003	ns	**0.322**	0.003	ns
	100	**0.332**	0.012	***	**0.315**	0.003	ns	**0.320**	0.017	ns	**0.334**	0.007	***
	400	**0.326**	0.015	*	**0.328**	0.014	**	**0.344**	0.006	***	**0.346**	0.013	***
***B. cenocepacia* (K56-*ciiR*)**	0	**0.244**	0.006		**0.244**	0.006		**0.244**	0.006		**0.244**	0.006	
	25	**0.238**	0.004	ns	**0.250**	0.004	ns	**0.251**	0.013	ns	**0.256**	0.013	ns
	100	**0.246**	0.007	ns	**0.256**	0.003	ns	**0.256**	0.016	ns	**0.253**	0.008	ns
	400	**0.247**	0.012	ns	**0.260**	0.005	ns	**0.269**	0.008	***	**0.265**	0.016	**
***B. cenocepacia* (K56-*cepR,ciiR*)**	0	**0.344**	0.009		**0.344**	0.009		**0.344**	0.009		**0.344**	0.009	
	25	**0.358**	0.014	ns	**0.335**	0.005	ns	**0.355**	0.004	ns	**0.342**	0.003	ns
	100	**0.373**	0.018	***	**0.356**	0.015	ns	**0.349**	0.006	ns	**0.341**	0.007	ns
	400	**0.352**	0.008	ns	**0.357**	0.004	ns	**0.362**	0.007	*	**0.360**	0.008	*

production while in the presence of at least one of the DKPs. It was also the virulence factor to be the most growth-phase dependent as there was a much larger number of significant changes seen in late stationary phase (Table 3.6).

Of the two *B. cepacia* isolates, 16192 was more affected by the presence of DKPs at early stationary phase as siderophore production increased by ~50% with the addition of cyclo(-pro-val), cyclo(-leu-pro) or cyclo(-phe-pro) (Table 3.5). At the later time point, however, these DKPs only resulted in an increase of ~15%, while isolate 15862 was affected to a larger degree resulting in a ~30% increase compared to the PB buffer control average $\Delta OD_{630}/OD_{600}$ value of 0.229 (Table 3.6). Apart from the double QS mutant, the siderophore production in *B. multivorans* was the least affected by DKPs at early stationary phase with only a couple treatments resulting in an increase in siderophore production. A change in production was much larger at late stationary phase, however, as all 4 DKPs increased the $\Delta OD_{630}/OD_{600}$ of both C5393 and LMG13010. This trend was highly similar in the case of the *B. cenocepacia* isolates H111 and K56-2, where all 4 DKPs altered production significantly at the later time point while only cyclo(-leu-pro) and cyclo(-phe-pro) caused an increase in siderophore production during early stationary phase. It is also interesting to note that at both phases of growth the addition of these two DKPs to cultures of K56-2 resulted in $\Delta OD_{630}/OD_{600}$ values that were no different from the untreated control values of the double QS mutant, K56-*cepR,cciIR* (Table 3.5 & 3.6).

3.3 Summary

One possible alternative strategy that is currently being investigated for improving the treatment of Bcc infections is the use of QSIs as a means of limiting their virulence factor production and pathogenicity (Scoffone *et al.* 2017; Shaw and Wuest, 2020). Based on previous work in our lab conducted by Purighalla (2011), we were interested in further characterizing

the effects of DKPs cyclo(-D-ala-val), cyclo(-pro-val), cyclo(-leu-pro) and cyclo(-phe-pro) on the QS-mediated virulence phenotype of Bcc species, more specifically, their effect on the production of extracellular virulence factors. Based on our current knowledge, we hypothesized that by acting as QSIs, DKPs would alter the production of proteases, lipases, and siderophores of Bcc species without possessing any antimicrobial activity. Through the use of viability tests and multiple virulence factor assays, our data supported this hypothesis as DKPs did not affect the growth rate or viable cell count of Bcc species (section 3.2.1) while significantly altering their production of extracellular virulence factors (section 3.2.3).

With the addition of DKPs, both of the positively regulated factors, proteases and lipases, had significantly decreased production compared to the PB buffer controls, while the negatively regulated factor, siderophores, were significantly increased. The extent of these effects proved to be highly dependent on the DKP molecule present, the concentration of the DKP, as well as the growth phase of the Bcc isolate. In general, DKPs cyclo(-leu-pro) and cylo(-phe-pro) and the concentrations of 100μM and 400μM were the most effective at altering extracellular virulence factor production of the Bcc isolates tested. Furthermore, the inhibitory effects of DKPs increased over time as the differences observed were often greater in late stationary phase compared to early stationary phase. Taken together, these data supported our hypothesis as the presence of DKPs altered the virulence phenotype of the different Bcc isolates over time without any affect towards their growth and viability.

Chapter Four: DKPs as Antibiofilm Agents

4.1 Introduction

Of the various virulence factor determinants that *Burkholderia cepacia* complex (Bcc) species employ, the production of biofilm is largely involved in the ability of these species to survive in a wide range of environmental conditions and to colonize and persist as a chronic infection (Koo *et al.* 2017; Ferreira *et al.* 2019). Bcc biofilm formation is a tightly regulated, multistep process that includes dynamic intra- and extracellular signalling to orchestrate the activation of a number of regulatory systems (Ferreira *et al.* 2011; Sharma *et al.* 2019). Of the various regulatory systems involved in this lifestyle switch from planktonic to biofilm growth, quorum sensing (QS) plays a vital role in regulating the production of biofilm-associated factors such as the many different adhesins and extracellular polymeric substances (EPS) that Bcc species possess (McClean and Callaghan, 2009; Fazli *et al.* 2014; Abraham, 2016). Together, these factors along with extracellular DNA, amyloidogenic proteins and lipids collectively comprise the extracellular matrix (ECM), accounting for the majority of the biofilm's biomass and providing the microbial community with a protective barrier (Cunha *et al.* 2004; Messiaen *et al.* 2014; Sharma *et al.* 2019). Identifying molecules that are capable of affecting the structural integrity of the ECM by interfering with QS regulation could therefore hold clinical significance in the development of alternative treatment options for Bcc infections.

Although QS is not exclusively responsible for biofilm formation in Bcc species, it is a regulatory system that is considered to be highly important as mutations in its components have been shown to cause significant structural alterations during biofilm formation, particularly at the later stages of growth and maturation (Huber *et al.* 2001; Tomlin *et al.* 2005; Brackman *et al.* 2009). Given its importance in Bcc biofilm formation, QS inhibitors (QSIs), such

as DKPs, have been highly studied recently in their ability to function as antibiofilm agents (Brackman and Coenye 2015; Scoffone *et al.* 2016; Buroni *et al.* 2018). With all four DKPs of interest affecting the production of QS-regulated extracellular virulence factors (Chapter 3), we were interested in observing any possible inhibitory effects that DKPs could also have towards biofilm formation of Bcc species. Based on our current findings and recently published work, it was originally hypothesized that by acting as QSIs, DKPs would limit the formation of Bcc biofilms, resulting in a decrease in the overall biofilm biomass and biofilm viability.

To address this hypothesis, Bcc isolates were grown in the presence of each of the four DKPs, cyclo(-D-ala-val), cyclo(-pro-val), cyclo(-leu-pro) and cyclo(-phe-pro), and the resulting biofilm biomass (section 4.2.1) as well as the viable biofilm cell count (section 4.2.2) were both determined. Furthermore, we were interested in observing the effects of DKPs on the various stages of biofilm formation, namely: initial bacterial adhesion, early biofilm development, biofilm maturation, and late-stage dispersal (Koo *et al.* 2017; Jiang *et al.* 2020). To do this, four identical replicates of each experimental condition were prepared and grown in parallel for different lengths of time: 4 hours, 8 hours, 12 hours, and 24 hours. If DKPs possess any antibiofilm properties towards species of the Bcc, we would expect their presence to limit the production of biofilm biomass with a subsequent reduction in viable biofilm cell count with respect to the untreated PB buffer controls.

4.2 Results

4.2.1 Bcc biofilm biomass production over time

Prior to assessing the effects of DKPs on Bcc biofilm biomass, biofilm formation was first examined without their presence in order to gauge the wildtype production of each bacterial strain and to also ensure that biofilms were cultivable under the defined experimental

conditions. As outlined in section 2.5.2, Bcc biofilms were cultivated using the highly defined synthetic cystic fibrosis sputum medium (SCFM) (Palmer *et al.* 2007) and standard 96-well microtiter plates. The use of the crystal violet (CV) staining method (O'Toole, 2011), showed each of the Bcc species under investigation to produce an increasing amount of biofilm biomass over time to varying degrees (Figure 4.1). The early stages of biofilm development at 4, 8, and 12 hours of incubation were similar for most of the Bcc strains as the average OD_{550} readings for the *B. cepacia* and *B. cenocepacia* isolates were all within 0.2-0.4 at these time points. The two *B. multivorans* strains, however, produced on average 2-4 times more biofilm biomass at these time points in comparison to the other Bcc isolates.

At the later stages of biofilm development, a greater degree of variability was seen between the different Bcc isolates tested (Figure 4.1). Similar to the early time points, after 24 hours the two *B. multivorans* isolates, LMG13010 and C5393, produced the largest amount of biomass with average OD_{550} readings of 1.46 and 0.96, respectively. Interestingly, the two *B. cepacia* isolates had very large differences in their OD_{550} readings as isolate 16192 generated 3.5 times the amount of biofilm biomass compared to isolate 15862. As expected, the two *B. cenocepacia* QS mutants, K56-*cciIR* and K56-*cepR,cciIR*, had the least amount of biofilm biomass production at 24 hours with average OD_{550} readings of 0.32 and 0.25, respectively. These values were significantly lower than the OD_{500} value of 0.96 that was seen for the parental strain, K56-2, while isolate H111 had an intermediate value of 0.71. With these results showing successful biofilm biomass detection and OD_{550} values similar to previously published work (Tomlin *et al.* 2005), the effects of DKPs on Bcc biofilm biomass was then determined using the same defined experimental conditions.

Figure 4.1: Bcc biofilm biomass production over time

Bcc biofilms were cultivated in SCFM and standard 96-well plates. The crystal violet (CV) staining method was used to measure biofilm biomass after 4, 8, 12, and 24 hours of incubation. This procedure was conducted two times in triplicate (n=6) and significance between K56-2 and each of the two QS mutant strains was determined by an unpaired t-test; ns (no significance), * ($p \leq 0.05$), ** ($p \leq 0.01$), *** ($p \leq 0.001$). Bars indicate ± SD.

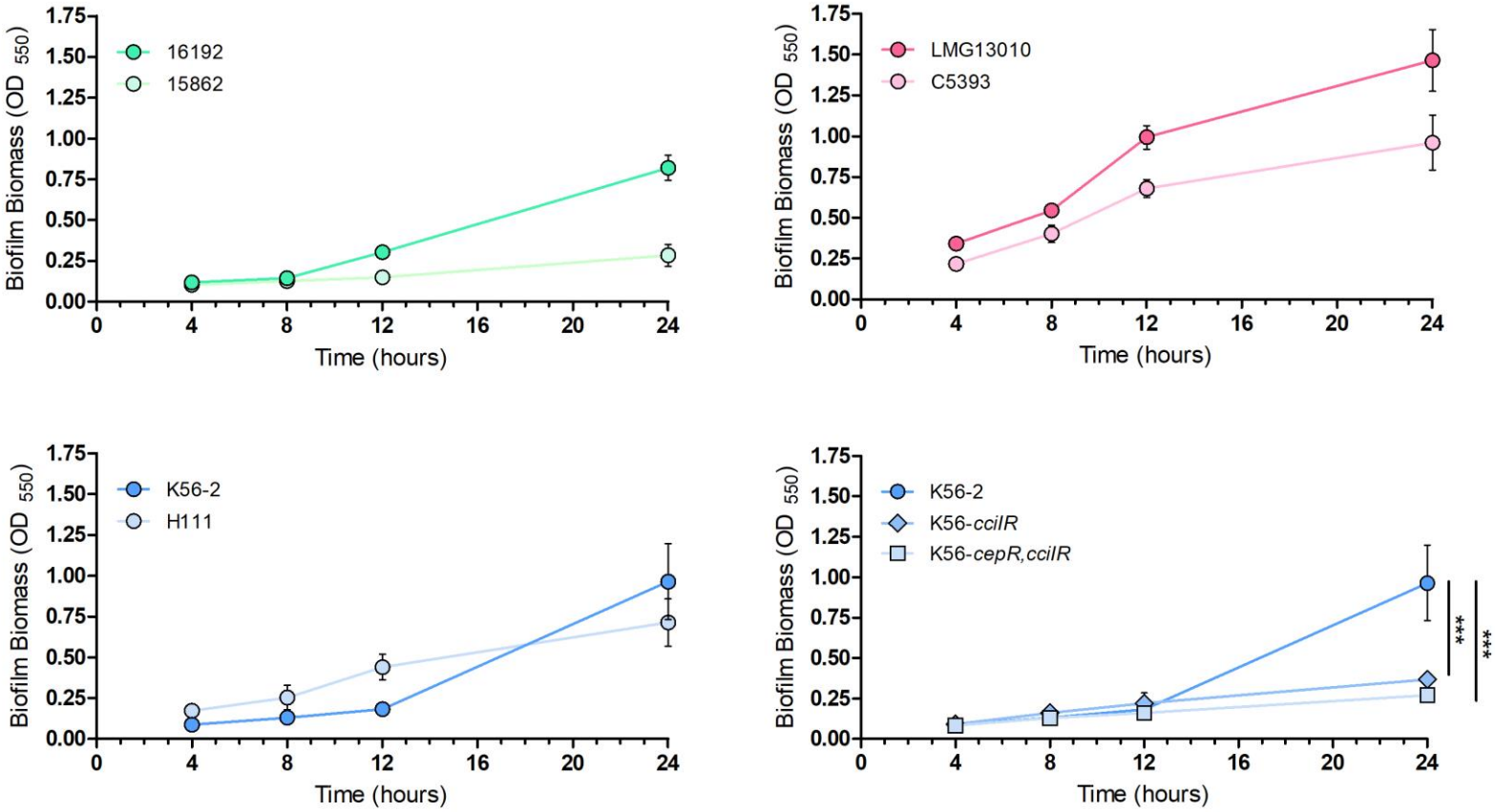
Biofilm Biomass (OD 550)
Time (hours)
16192
15862
LMG13010
C5393
K56-2
H111
K56-2
K56-cciIR
K56-cepR,cciIR
***
***

4.2.2 DKPs limit Bcc biofilm biomass production

To assess the effects of DKPs cyclo(-D-ala-val), cyclo(-pro-val), cyclo(-leu-pro) and cyclo(-phe-pro) on the production of Bcc biofilm biomass, initial bacterial cultures included the addition of either phosphate buffer (PB) as an untreated control or one of the four DKPs to final concentrations of 1, 25, or 100μM. Given the large number of experimental conditions under investigation and the high amount of variation between experimental replicates, the OD_{550} data collected from each replicate was converted to a percent value with respect to its PB buffer control (section 2.5.2) and presented in a table format (Sathyanarayanan *et al.* 2013; Gaglione *et al.* 2020). With the PB buffer control (0μM DKP) for each replicate effectively considered as 100% biofilm biomass production, the antibiofilm effects of DKPs were more readily visualized and quantified.

Looking first at the effects of DKPs on initial bacterial adhesion (4 hours); the presence of DKPs resulted in varying effects on Bcc biofilm biomass production as determined using the CV staining method (O'Toole, 2011) (Table 4.1). Although the majority of the conditions tested did not result in a significant change in biofilm biomass at this time point, most of the Bcc isolates had a decreasing percent of biofilm biomass with an increasing concentration of DKPs as compared to the PB buffer controls (0μM DKP). Both of the *B. cepacia* isolates, 15862 and 16192, were the most affected by the presence of DKPs as the 100μM concentrations resulted in biofilm biomass values that were 10-15% and 15-30% lower, respectively (Table 4.1). While to a lesser extent, *B. multivorans* (C5393 and LMG13010) and *B. cenocepacia* (H111 and K56-2) biofilms were inhibited by 10-20% when formed in the presence of 100μM of DKPs, with cyclo(-leu-pro) as the most inhibitory DKP towards biofilm biomass production in these Bcc isolates. The two QS mutant strains, K56-*cciIR* and K56-*cepR,cciIR,* had no significant difference

Table 4.1: DKPs limit Bcc biofilm biomass production after 4 hours of incubation

Bcc biofilms were cultivated in SCFM and standard 96-well plates with the addition of either phosphate buffer (PB) as an untreated control (0μM DKP) or one of the four DKPs to a final concentration of 1, 25 or 100μM. After 4 hours of incubation, the crystal violet (CV) staining method was used to measure the biofilm biomass of each experimental replicate and, with respect to the biofilm biomass of the PB buffer control (0μM DKP), the percent (%) biofilm biomass was determined. Percentages are the mean of three independent experiments performed in duplicate (n=6) and significance (sig.) was determined by one-way ANOVA and the Dunnett post-hoc test (ns = no significance; * = $p<0.05$; ** = $p<0.01$; *** = $p<0.001$). SD = ± standard deviation.

strain	DKP [µM]	Cyclo(-D-ala-val) % Biofilm Biomass	SD	Sig.	Cyclo(-pro-val) % Biofilm Biomass	SD	Sig.	Cyclo(-leu-pro) % Biofilm Biomass	SD	Sig.	Cyclo(-phe-pro) % Biofilm Biomass	SD	Sig.
***B. cepacia* (15862)**	0	**100**	0		**100**	0		**100**	0		**100**	0	
	1	**95.4**	4.9	ns	**95.4**	7.2	ns	**90.6**	3.7	ns	**90.6**	9.1	ns
	25	**94.6**	8.3	ns	**93.4**	8.0	ns	**92.7**	11.8	ns	**87.0**	12.2	ns
	100	**89.9**	6.1	*	**91.0**	11.2	ns	**88.1**	9.8	ns	**84.2**	13.6	ns
***B. cepacia* (16192)**	0	**100**	0		**100**	0		**100**	0		**100**	0	
	1	**93.6**	15.8	ns	**97.9**	11.4	ns	**86.4**	10.8	ns	**84.7**	6.0	ns
	25	**85.6**	17.1	ns	**97.4**	9.9	ns	**78.2**	15.6	*	**79.4**	11.0	**
	100	**76.5**	12.3	*	**86.1**	12.2	ns	**72.8**	14.7	**	**76.9**	13.9	**
***B. multivorans* (C5393)**	0	**100**	0		**100**	0		**100**	0		**100**	0	
	1	**92.9**	8.8	ns	**91.8**	10.5	ns	**87.6**	8.1	ns	**82.9**	16.3	ns
	25	**93.0**	10.9	ns	**91.2**	9.0	ns	**83.3**	11.5	*	**81.2**	17.8	ns
	100	**88.6**	9.7	ns	**85.7**	9.7	*	**82.5**	13.5	*	**80.1**	18.8	ns
***B. multivorans* (LMG13010)**	0	**100**	0		**100**	0		**100**	0		**100**	0	
	1	**91.5**	11.1	ns	**97.1**	6.6	ns	**90.6**	5.6	ns	**89.3**	8.1	ns
	25	**91.8**	9.4	ns	**91.3**	8.9	ns	**88.1**	9.3	*	**85.8**	11.9	ns
	100	**84.6**	11.0	*	**90.0**	10.7	ns	**89.5**	10.3	ns	**90.0**	10.4	ns
***B. cenocepacia* (H111)**	0	**100**	0		**100**	0		**100**	0		**100**	0	
	1	**99.5**	5.9	ns	**93.1**	7.3	ns	**90.0**	6.8	ns	**90.6**	8.9	ns
	25	**92.6**	11.7	ns	**89.2**	10.1	ns	**84.3**	8.4	*	**92.6**	11.4	ns
	100	**95.6**	12.4	ns	**89.7**	12.8	ns	**80.9**	11.0	**	**79.8**	12.6	*
***B. cenocepacia* (K56-2)**	0	**100**	0		**100**	0		**100**	0		**100**	0	
	1	**104.7**	8.9	ns	**94.6**	7.4	ns	**84.8**	10.7	*	**92.5**	5.8	ns
	25	**96.9**	6.6	ns	**95.0**	7.0	ns	**81.0**	11.0	**	**91.3**	9.8	ns
	100	**96.1**	7.6	ns	**90.6**	9.8	ns	**81.1**	10.1	**	**87.9**	5.9	*
***B. cenocepacia* (K56-*cciIR*)**	0	**100**	0		**100**	0		**100**	0		**100**	0	
	1	**92.9**	7.5	ns	**91.1**	8.1	ns	**97.5**	7.4	ns	**95.2**	4.7	ns
	25	**92.9**	7.0	ns	**96.6**	8.3	ns	**97.4**	4.9	ns	**95.7**	8.9	ns
	100	**91.2**	10.7	ns	**94.0**	9.2	ns	**98.9**	12.7	ns	**95.3**	11.1	ns
***B. cenocepacia* (K56-*cepR,cciIR*)**	0	**100**	0		**100**	0		**100**	0		**100**	0	
	1	**94.2**	8.5	ns	**101.0**	10.6	ns	**96.4**	7.9	ns	**92.4**	7.0	ns
	25	**101.7**	8.4	ns	**101.1**	11.2	ns	**99.4**	9.8	ns	**99.6**	8.3	ns
	100	**96.5**	11.4	ns	**104.9**	10.3	ns	**94.4**	10.3	ns	**98.1**	10.5	ns

in percent biofilm biomass at this time point.

After 8 hours of incubation, a similar trend was observed as Bcc biofilms grown in the presence of DKPs resulted in a lesser amount of biofilm biomass compared to the PB buffer controls (0μM DKP) (Table 4.2). Just as before, the highest concentration tested of 100μM was the most inhibitory, with cyclo(-leu-pro) and cyclo(-phe-pro) resulting in the greatest significant decreases. Unlike the results seen at the 4-hour time point, however, the *B. cepacia* isolates only had a maximum decrease of 5-15% at 8 hours in comparison to the PB buffer controls. The *B. multivorans* isolates had a similar decrease of 10-20%, while interestingly, the percent decrease in biofilm biomass production for the *B. cenocepacia* isolates, H111 and K56-2, showed to be highly dependent on the DKP molecule (Table 4.2). When grown in the presence of cyclo(-D-ala-val) or cyclo(-pro-val) there was only a decrease of 5-15%, whereas with the addition of cyclo(-leu-pro) or cyclo(-phe-pro) there was a much more significant 25-30% inhibition of biofilm biomass production. In contrast to this, the two K56-2 strains with mutations in their QS systems, K56-*cciIR* and K56-*cepR,cciIR*, were not affected when grown in the presence of DKPs as the percent biofilm biomass did not significantly change in comparison to the PB buffer controls.

The inhibitory effects of DKPs increased greatly over time as several experimental conditions at the 12-hour time point resulted in a significantly lower percent biofilm biomass in all of the Bcc isolates tested (Table 4.3). Similar to what was seen at the 4- and 8-hour time points, cyclo(-D-ala-val) was the least inhibitory as the biofilm biomass of most of the strains did not decrease more than 10% compared to their PB buffer controls. The other three DKP molecules, however, resulted in much greater decreases, inhibiting the biofilm biomass production of the two *B. cepacia* strains by 15-25%. Although the *B. multivorans* strains only

Table 4.2: DKPs limit Bcc biofilm biomass production after 8 hours of incubation

Bcc biofilms were cultivated in SCFM and standard 96-well plates with the addition of either phosphate buffer (PB) as an untreated control (0μM DKP) or one of the four DKPs to a final concentration of 1, 25 or 100μM. After 8 hours of incubation, the crystal violet (CV) staining method was used to measure the biofilm biomass of each experimental replicate and, with respect to the biofilm biomass of the PB buffer control (0μM DKP), the percent (%) biofilm biomass was determined. Percentages are the mean of three independent experiments performed in duplicate (n=6) and significance (sig.) was determined by one-way ANOVA and the Dunnett post-hoc test (ns = no significance; * = $p<0.05$; ** = $p<0.01$; *** = $p<0.001$). SD = ± standard deviation.

strain	DKP [µM]	Cyclo(-D-ala-val) % Biofilm Biomass	SD	Sig.	Cyclo(-pro-val) % Biofilm Biomass	SD	Sig.	Cyclo(-leu-pro) % Biofilm Biomass	SD	Sig.	Cyclo(-phe-pro) % Biofilm Biomass	SD	Sig.
***B. cepacia* (15862)**	0	**100**	0		**100**	0		**100**	0		**100**	0	
	1	**96.6**	9.2	ns	**97.4**	12.7	ns	**91.6**	12.8	ns	**89.9**	12.2	ns
	25	**95.8**	8.7	ns	**91.7**	9.6	ns	**90.4**	15.2	ns	**90.3**	14.7	ns
	100	**95.1**	11.9	ns	**90.9**	12.1	ns	**88.9**	15.1	ns	**89.8**	16.1	ns
***B. cepacia* (16192)**	0	**100**	0		**100**	0		**100**	0		**100**	0	
	1	**93.3**	11.5	ns	**101.7**	7.6	ns	**91.4**	11.3	ns	**86.2**	7.2	ns
	25	**96.3**	10.3	ns	**99.3**	9.7	ns	**83.8**	12.2	ns	**85.6**	8.4	*
	100	**91.3**	8.4	ns	**92.9**	10.2	ns	**85.4**	11.9	ns	**83.5**	9.4	**
***B. multivorans* (C5393)**	0	**100**	0		**100**	0		**100**	0		**100**	0	
	1	**93.0**	10.8	ns	**101.0**	5.5	ns	**91.4**	8.3	ns	**94.8**	3.8	ns
	25	**93.4**	12.1	ns	**92.3**	5.7	ns	**87.3**	10.1	*	**87.3**	10.6	*
	100	**89.8**	9.2	ns	**93.0**	8.0	ns	**90.7**	6.2	ns	**87.2**	10.4	*
***B. multivorans* (LMG13010)**	0	**100**	0		**100**	0		**100**	0		**100**	0	
	1	**94.4**	9.1	ns	**96.7**	10.7	ns	**89.0**	5.7	*	**90.0**	6.8	ns
	25	**93.7**	10.5	ns	**86.7**	12.8	ns	**85.5**	7.7	**	**83.4**	11.7	*
	100	**91.8**	14.2	ns	**78.9**	9.1	**	**86.1**	8.7	**	**83.3**	13.7	*
***B. cenocepacia* (H111)**	0	**100**	0		**100**	0		**100**	0		**100**	0	
	1	**93.2**	13.0	ns	**90.8**	6.9	ns	**81.7**	7.9	***	**85.9**	12.2	*
	25	**87.2**	14.3	ns	**89.2**	10.4	ns	**72.6**	6.8	***	**75.6**	7.8	***
	100	**95.3**	10.8	ns	**86.8**	7.7	*	**70.8**	8.8	***	**75.3**	12.3	***
***B. cenocepacia* (K56-2)**	0	**100**	0		**100**	0		**100**	0		**100**	0	
	1	**101.4**	8.7	ns	**87.3**	10.1	ns	**83.8**	8.8	ns	**83.5**	7.6	*
	25	**99.4**	10.5	ns	**87.2**	11.4	ns	**80.3**	13.9	*	**82.1**	11.2	*
	100	**93.3**	12.5	ns	**87.2**	9.7	ns	**73.7**	14.3	**	**77.2**	13.8	**
***B. cenocepacia* (K56-*ccilR*)**	0	**100**	0		**100**	0		**100**	0		**100**	0	
	1	**87.9**	6.2	ns	**91.4**	9.6	ns	**91.4**	9.6	ns	**96.9**	12.3	ns
	25	**97.2**	11.6	ns	**92.9**	12.5	ns	**92.9**	12.5	ns	**96.8**	9.0	ns
	100	**100.5**	11.8	ns	**97.3**	8.0	ns	**97.3**	8.0	ns	**98.1**	12.2	ns
***B. cenocepacia* (K56-*cepR,ccilR*)**	0	**100**	0		**100**	0		**100**	0		**100**	0	
	1	**97.4**	12.2	ns	**98.4**	10.7	ns	**93.3**	10.9	ns	**104.7**	6.9	ns
	25	**95.2**	10.3	ns	**98.0**	12.8	ns	**97.5**	10.4	ns	**103.6**	11.6	ns
	100	**95.2**	13.0	ns	**97.6**	12.9	ns	**100.8**	11.4	ns	**104.6**	12.4	ns

Table 4.3: DKPs limit Bcc biofilm biomass production after 12 hours of incubation

Bcc biofilms were cultivated in SCFM and standard 96-well plates with the addition of either phosphate buffer (PB) as an untreated control (0μM DKP) or one of the four DKPs to a final concentration of 1, 25 or 100μM. After 12 hours of incubation, the crystal violet (CV) staining method was used to measure the biofilm biomass of each experimental replicate and, with respect to the biofilm biomass of the PB buffer control (0μM DKP), the percent (%) biofilm biomass was determined. Percentages are the mean of three independent experiments performed in duplicate (n=6) and significance (sig.) was determined by one-way ANOVA and the Dunnett post-hoc test (ns = no significance; * = $p<0.05$; ** = $p<0.01$; *** = $p<0.001$). SD = ± standard deviation.

strain	DKP [µM]	Cyclo(-D-ala-val) % Biofilm Biomass	SD	Sig.	Cyclo(-pro-val) % Biofilm Biomass	SD	Sig.	Cyclo(-leu-pro) % Biofilm Biomass	SD	Sig.	Cyclo(-phe-pro) % Biofilm Biomass	SD	Sig.
***B. cepacia* (15862)**	0	**100**	0		**100**	0		**100**	0		**100**	0	
	1	**94.4**	9.9	ns	**93.6**	10.4	ns	**91.8**	8.5	ns	**84.2**	12.3	ns
	25	**91.2**	6.1	ns	**88.2**	10.3	ns	**89.6**	5.9	ns	**82.1**	10.6	ns
	100	**90.4**	8.8	ns	**85.0**	10.5	*	**83.4**	11.6	**	**76.9**	10.6	*
***B. cepacia* (16192)**	0	**100**	0		**100**	0		**100**	0		**100**	0	
	1	**98.1**	10.2	ns	**89.2**	11.8	ns	**79.1**	11.1	*	**80.8**	10.1	*
	25	**92.8**	10.1	ns	**79.6**	12.2	**	**74.8**	12.8	*	**76.3**	10.8	**
	100	**94.8**	10.1	ns	**75.8**	7.1	**	**74.3**	15.8	**	**73.9**	11.7	**
***B. multivorans* (C5393)**	0	**100**	0		**100**	0		**100**	0		**100**	0	
	1	**98.0**	7.1	ns	**96.2**	8.1	ns	**91.9**	4.6	*	**91.6**	5.2	*
	25	**96.9**	6.0	ns	**90.1**	6.4	*	**84.3**	4.7	***	**92.8**	4.7	**
	100	**92.8**	5.8	ns	**90.9**	6.2	*	**84.1**	6.2	***	**90.2**	5.4	**
***B. multivorans* (LMG13010)**	0	**100**	0		**100**	0		**100**	0		**100**	0	
	1	**91.5**	5.4	ns	**96.6**	4.5	ns	**92.2**	2.7	**	**90.0**	6.6	*
	25	**98.9**	6.3	ns	**96.2**	2.8	ns	**91.9**	4.7	***	**88.0**	7.6	**
	100	**88.9**	5.5	**	**91.2**	7.1	**	**88.1**	3.5	***	**85.3**	5.2	***
***B. cenocepacia* (H111)**	0	**100**	0		**100**	0		**100**	0		**100**	0	
	1	**91.6**	8.7	ns	**95.1**	7.6	ns	**85.1**	13.1	ns	**88.4**	9.3	ns
	25	**91.9**	7.1	ns	**97.4**	7.2	ns	**77**	11.8	**	**88.2**	9.5	ns
	100	**93.6**	6.5	ns	**84.4**	13.7	*	**76.3**	9.4	**	**82.3**	11.7	*
***B. cenocepacia* (K56-2)**	0	**100**	0		**100**	0		**100**	0		**100**	0	
	1	**97.2**	3.3	ns	**81.6**	12.2	*	**85.9**	6.9	**	**86.5**	6.7	ns
	25	**90.8**	10.5	ns	**74.4**	12.7	**	**80.1**	7.0	***	**78.6**	11.5	**
	100	**86.7**	9.5	*	**74.9**	12.5	**	**75.0**	5.9	***	**74.0**	11.2	***
***B. cenocepacia* (K56-*ciiR*)**	0	**100**	0		**100**	0		**100**	0		**100**	0	
	1	**87.8**	11.3	ns	**95.8**	10.7	ns	**95.3**	10.5	ns	**94.6**	8.1	ns
	25	**93.8**	13.1	ns	**90.1**	13.6	ns	**90.0**	5.4	*	**88.7**	11.5	ns
	100	**99.0**	14.9	ns	**99.2**	12.2	ns	**89.2**	3.5	*	**82.8**	7.4	**
***B. cenocepacia* (K56-*cepR,ciiR*)**	0	**100**	0		**100**	0		**100**	0		**100**	0	
	1	**105.1**	12.8	ns	**94.0**	11.6	ns	**101.8**	11.9	ns	**94.9**	10.8	ns
	25	**91.5**	11.9	ns	**96.6**	16.6	ns	**92.8**	10.9	ns	**90.0**	9.9	ns
	100	**92.5**	14.8	ns	**104.3**	15.7	ns	**92.7**	12.9	ns	**84.5**	8.1	*

had a 10-15% decrease compared to the PB buffer controls, this amount was considered to be quite large considering their untreated OD_{550} readings were the highest amongst all of the Bcc species tested at 0.68 and 0.99, respectively (Figure 4.1). Unlike the earlier stages of biofilm development, the mutant *B. cenocepacia* strains were somewhat inhibited after 12 hours of incubation as the higher concentrations of both cyclo(-leu-pro) and cyclo(-phe-pro) resulted in significant reductions of 10-15% (Table 4.3).

An even greater amount of inhibition was seen after 24 hours of incubation where many of the treatments resulted in a significant decrease in percent biofilm biomass of the different Bcc isolates tested (Table 4.4). Even the smallest concentration of 1μM resulted in significant decreases, particularly in the formation of the *B. multivorans* biofilms where a 10-20% decrease compared to the untreated PB buffer control was recorded. Just as seen at other time points, both of the *B. cepacia* isolates experienced a large amount of inhibition, especially with the addition of cyclo(-pro-val) where the greatest decrease of ~40% was seen in isolate 16192. In contrast to this, the greatest amount of inhibition towards *B. cenocepacia* H111 biofilm biomass production was seen with the addition of cyclo(-leu-pro) and cyclo(-phe-pro) rather than cyclo(-pro-val) which did not result in any significant changes (Table 4.4). Similar to what occurred at other time points, the two QS mutant isolates, K56-*cciIR* and K56-*cepR,cciIR*, were the least inhibited. However, incubation with cyclo(-leu-pro) and cyclo(-phe-pro) still resulted in a slight decrease of 10-15% in biofilm biomass production just as seen at 12 hours.

Overall, the inhibitory effects of DKPs were greater at the later stages of biofilm development as the production of Bcc biofilm biomass was the most affected at the later time points of observation compared to the earlier time points. The level of inhibition by DKPs also differed depending on the Bcc species, the DKP molecule, and the DKP concentration tested.

Table 4.4: DKPs limit Bcc biofilm biomass production after 24 hours of incubation

Bcc biofilms were cultivated in SCFM and standard 96-well plates with the addition of either phosphate buffer (PB) as an untreated control (0μM DKP) or one of the four DKPs to a final concentration of 1, 25 or 100μM. After 24 hours of incubation, the crystal violet (CV) staining method was used to measure the biofilm biomass of each experimental replicate and, with respect to the biofilm biomass of the PB buffer control (0μM DKP), the percent (%) biofilm biomass was determined. Percentages are the mean of three independent experiments performed in duplicate (n=6) and significance (sig.) was determined by one-way ANOVA and the Dunnett post-hoc test (ns = no significance; * = $p<0.05$; ** = $p<0.01$; *** = $p<0.001$). SD = ± standard deviation.

strain	DKP [µM]	Cyclo(-D-ala-val) % Biofilm Biomass	SD	Sig.	Cyclo(-pro-val) % Biofilm Biomass	SD	Sig.	Cyclo(-leu-pro) % Biofilm Biomass	SD	Sig.	Cyclo(-phe-pro) % Biofilm Biomass	SD	Sig.
***B. cepacia* (15862)**	0	**100**	0		**100**	0		**100**	0		**100**	0	
	1	**89.3**	15.5	ns	**84.9**	13.8	ns	**91.5**	9.5	ns	**95.2**	7.2	ns
	25	**85.2**	19.2	ns	**84.8**	17.5	ns	**88.2**	10.6	*	**91.3**	11.8	ns
	100	**79.1**	14.2	ns	**73.7**	12.6	*	**80.8**	5.4	*	**77.5**	11.9	**
***B. cepacia* (16192)**	0	**100**	0		**100**	0		**100**	0		**100**	0	
	1	**89.7**	14.1	ns	**76.4**	15.9	*	**89.6**	9.4	ns	**83.8**	9.0	**
	25	**83.4**	12.2	ns	**67.4**	13.4	**	**80.7**	11.4	**	**81.1**	7.5	***
	100	**79.3**	15.7	*	**61.9**	13.4	***	**74.9**	10.1	***	**76.5**	9.3	***
***B. multivorans* (C5393)**	0	**100**	0		**100**	0		**100**	0		**100**	0	
	1	**83.9**	7.9	***	**99.0**	5.9	ns	**91.9**	7.1	*	**91.9**	5.9	ns
	25	**78.6**	6.2	***	**93.2**	5.7	ns	**87.8**	5.1	***	**90.0**	8.3	*
	100	**82.1**	7.4	***	**83.2**	5.5	***	**83.7**	4.0	***	**86.1**	5.5	**
***B. multivorans* (LMG13010)**	0	**100**	0		**100**	0		**100**	0		**100**	0	
	1	**88.7**	6.1	***	**90.7**	5.1	**	**90.2**	6.9	**	**87.8**	5.7	***
	25	**90.0**	5.0	**	**90.0**	4.9	**	**87.4**	4.9	***	**85.2**	4.9	***
	100	**85.1**	4.4	***	**86.3**	4.6	***	**84.6**	4.2	***	**80.7**	5.0	***
***B. cenocepacia* (H111)**	0	**100**	0		**100**	0		**100**	0		**100**	0	
	1	**94.5**	15.4	ns	**90.5**	7.0	ns	**77.8**	9.4	**	**79.6**	14.7	*
	25	**95.5**	10.6	ns	**95.3**	6.2	ns	**70.5**	13.6	***	**69.6**	14.8	**
	100	**86.6**	7.0	ns	**93.4**	9.0	ns	**66.8**	11.8	***	**67.6**	12.9	**
***B. cenocepacia* (K56-2)**	0	**100**	0		**100**	0		**100**	0		**100**	0	
	1	**89.4**	10.1	ns	**86.9**	10.5	ns	**88.4**	8.1	*	**93.7**	4.4	ns
	25	**82.4**	8.4	**	**80.4**	14.4	*	**88.0**	4.5	*	**87.9**	7.5	**
	100	**75.2**	10.4	***	**79.2**	10.2	*	**78.7**	10.3	***	**81.8**	4.8	***
***B. cenocepacia* (K56-*ccilR*)**	0	**100**	0		**100**	0		**100**	0		**100**	0	
	1	**96.4**	11.3	ns	**97.9**	11.6	ns	**88.8**	11.8	ns	**90.2**	6.9	*
	25	**95.4**	11.2	ns	**88.7**	7.8	ns	**91.5**	5.5	ns	**90.1**	7.0	*
	100	**88.3**	5.8	ns	**88.8**	8.9	ns	**87.1**	8.1	*	**90.6**	4.2	*
***B. cenocepacia* (K56-*cepR,ccilR*)**	0	**100**	0		**100**	0		**100**	0		**100**	0	
	1	**87.4**	8.4	ns	**98.3**	7.4	ns	**97.1**	9.8	ns	**98.5**	11.9	ns
	25	**91.4**	13.8	ns	**102.2**	6.3	ns	**98.6**	10.6	ns	**94.5**	11.2	ns
	100	**97.1**	11.3	ns	**96.9**	9.6	ns	**89.1**	4.1	*	**86.0**	5.0	*

Of the different DKPs under investigation, cyclo(-leu-pro) and cyclo(-phe-pro) were the most effective at limiting the production of biofilm biomass and the highest concentration of these molecules (100μM) was the most inhibitory towards each of the Bcc isolates.

4.2.3 Bcc viable biofilm cell count over time

To further examine the antibiofilm effects of DKPs cyclo(-D-ala-val), cyclo(-pro-val), cyclo(-leu-pro) and cyclo(-phe-pro) on Bcc biofilm development, the changes in biofilm viability were also measured over time. However, just as in the previous section, biofilm viability was first measured without the addition of DKPs in order to gauge the wildtype biofilm formation and ensure that biofilms were cultivable within the experimental conditions. As outlined in section 2.5.3, Bcc biofilms were grown using synthetic cystic fibrosis sputum medium (SCFM) (Palmer *et al.* 2007) and the Calgary Biofilm Device (CBD) (Ceri *et al.* 1999; Harrison *et al.* 2010). Through the use of sonication to recover viable biofilm cells grown on the CBD pegs, the results of this assay not only showed successful biofilm cultivation, but they also showed an unexpected pattern when compared to the CV staining data.

All of the Bcc isolates had a very similar pattern of growth to each other, where the greatest increase in $\log_{10}$ CFU/peg occurred between the hours of 4-12, followed by a much smaller increase from 12 to 24 hours (Figure 4.2). The *B. cepacia* isolates showed a similar trend to the biofilm biomass data collected, where isolate 16192 had a larger viable biofilm cell count of 5.77 ($\log_{10}$ CFU/peg) as compared to isolate 15862 which had a mean $\log_{10}$ value of 4.90 after 24 hours of growth. Also as expected based on the high level of biofilm biomass, the two *B. multivorans* isolates, C5393 and LMG13010, had the greatest number of viable biofilm cells with average $\log_{10}$ CFU/peg values of 6.89 and 7.03 after 24 hours, respectively. Unexpectedly, however, the two QS mutants, K56-*cciIR* and K56-*cepR,cciIR,* had mean counts of

Figure 4.2: Bcc viable biofilm cell count over time

Bcc biofilms were cultivated in SCFM and the CBD. The number of recovered viable biofilm cells was determined after 4, 8, 12, and 24 hours of incubation and presented as $\log_{10}$ CFU per peg. This procedure was conducted two times in triplicate (n=6). Significance between K56-2 and each of the two QS mutant strains was determined by an unpaired t-test where no significance was calculated. Bars indicate ± SD.

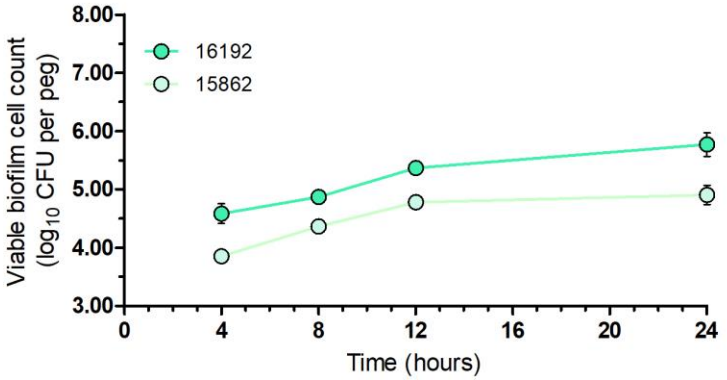
16192
15862
Viable biofilm cell count
(log10 CFU per peg)
Time (hours)

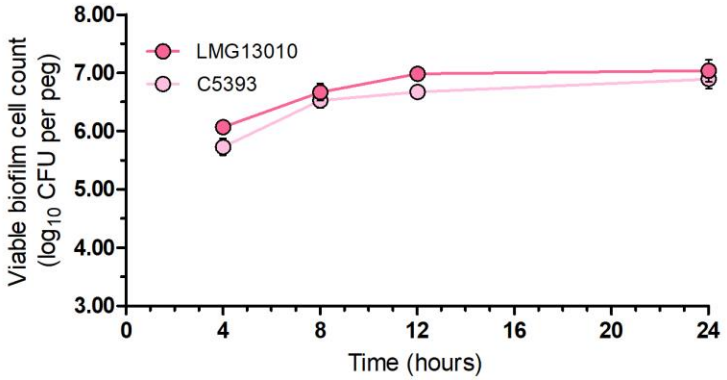
LMG13010
C5393
Viable biofilm cell count
(log10 CFU per peg)
Time (hours)

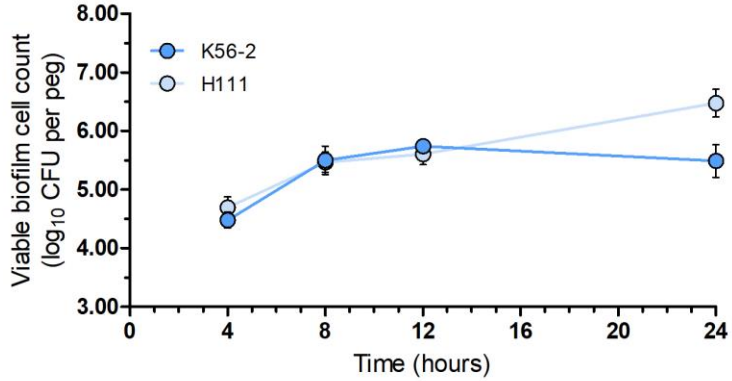
K56-2
H111
Viable biofilm cell count
(log10 CFU per peg)
Time (hours)

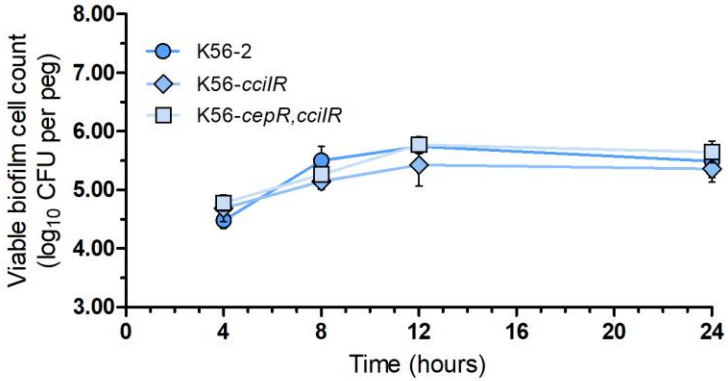
K56-2
K56-cciIR
K56-cepR,cciIR
Viable biofilm cell count
(log10 CFU per peg)
Time (hours)

5.36 and 5.64, which were no different than the parental strain, K56-2, which had an average $\log_{10}$ CFU/peg value of 5.48. This was not the case in terms of biofilm biomass, where the two mutant strains had on average 3-4 times less biomass after 24 hours of incubation (Figure 4.1).

4.2.4 DKPs do not affect the viability of Bcc species

To then asses the effects of DKPs on biofilm viability, Bcc biofilms were grown in SCFM and the CBD in the same manner, however, with the addition of either phosphate buffer (PB) as an untreated control or one of the four DKPs of interest to a final concentration of 100μM. Given that this concentration of DKPs resulted in the greatest amount of inhibition towards the production of Bcc biofilm biomass (section 4.2.2), we were the most interested in observing its effects on the Bcc viable biofilm cell count at each stage of biofilm formation. Our original hypothesis stated that by acting as QSIs, DKPs would limit the amount of Bcc biofilm biomass and biofilm viability over time. Although this was supported by the biofilm biomass data collected in the previous section, this was not the case in terms of biofilm viability.

With the addition of DKPs, the viable biofilm cell counts for each of the Bcc species were not significantly affected at any stages of biofilm development tested (Table 4.5). Only two isolates, *B. cepacia* 15862 and *B. cenocepacia* K56-2 had minor, yet significant, decreases in $\log_{10}$ CFU/peg values. After 24 hours of incubation, the presence of cyclo(-D-ala-val) or cyclo(-phe-pro) resulted $\log_{10}$ decreases of 0.27 and 0.24 in *B. cepacia* 15862 viable biofilm cell count as compared to the PB buffer control, respectively. Whereas a 0.29 and 0.31 $\log_{10}$ decrease in *B. cenocepacia* K56-2 viable cell counts occurred after 12 hours with the addition of cyclo(-pro-val) and cyclo(-phe-pro), respectively. All other experimental conditions that were tested did not result in any significant changes in the viable biofilm cell counts of the Bcc isolates over time (Table 4.5).

Table 4.5: DKPs do not affect Bcc viable biofilm cell counts over time

Bcc biofilms were cultivated in SCFM and the CBD with the addition of either phosphate buffer (PB) as an untreated control (0µM DKP) or one of the four DKPs to a final concentration of 100µM. The number of recovered viable biofilm cells was determined after 4, 8, 12, and 24 hours of incubation and presented as $\log_{10}$ CFU/peg. This procedure was conducted three times in duplicate (n=6) and significance (sig.) was determined by one-way ANOVA and the Dunnett post-hoc test (ns = no significance; * = $p<0.05$; ** = $p<0.01$; *** = $p<0.001$). SD = ± standard deviation.

Strain	Time (h)	PB Control (0µM DKP)		Cyclo(-D-ala-val)			Cyclo(-pro-val)			Cyclo(-leu-pro)			Cyclo(-phe-pro)		
		Log_{10} CFU/peg	SD	**Log_{10} CFU/peg**	SD	Sig.	**Log_{10} CFU/peg**	SD	Sig.	**Log_{10} CFU/peg**	SD	Sig.	**Log_{10} CFU/peg**	SD	Sig.
***B. cepacia* (15862)**	4	**3.85**	0.115	**3.80**	0.085	ns	**3.77**	0.137	ns	**3.83**	0.176	ns	**3.71**	0.154	ns
	8	**4.37**	0.116	**4.39**	0.120	ns	**4.35**	0.125	ns	**4.34**	0.138	ns	**4.39**	0.199	ns
	12	**4.88**	0.079	**4.90**	0.270	ns	**4.98**	0.059	ns	**5.01**	0.099	ns	**4.93**	0.185	ns
	24	**4.90**	0.164	**4.63**	0.228	*	**4.75**	0.135	ns	**4.92**	0.139	ns	**4.66**	0.103	*
***B. cepacia* (16192)**	4	**4.58**	0.170	**4.46**	0.129	ns	**4.55**	0.111	ns	**4.49**	0.134	ns	**4.52**	0.141	ns
	8	**4.87**	0.101	**4.80**	0.181	ns	**4.83**	0.135	ns	**4.87**	0.076	ns	**4.83**	0.110	ns
	12	**5.38**	0.109	**5.44**	0.065	ns	**5.26**	0.154	ns	**5.44**	0.131	ns	**5.35**	0.252	ns
	24	**5.80**	0.201	**5.76**	0.062	ns	**5.89**	0.088	ns	**5.74**	0.174	ns	**5.78**	0.125	ns
***B. multivorans* (C5393)**	4	**5.73**	0.144	**5.73**	0.145	ns	**5.70**	0.078	ns	**5.62**	0.103	ns	**5.74**	0.052	ns
	8	**6.53**	0.129	**6.55**	0.212	ns	**6.53**	0.164	ns	**6.68**	0.075	ns	**6.58**	0.212	ns
	12	**6.67**	0.120	**6.63**	0.181	ns	**6.69**	0.087	ns	**6.59**	0.169	ns	**6.60**	0.122	ns
	24	**6.89**	0.167	**6.94**	0.063	ns	**6.57**	0.129	ns	**6.75**	0.166	ns	**6.82**	0.101	ns
***B. multivorans* (LMG13010)**	4	**6.07**	0.079	**6.07**	0.091	ns	**6.05**	0.145	ns	**6.40**	0.086	ns	**6.12**	0.084	ns
	8	**6.67**	0.146	**6.61**	0.229	ns	**6.44**	0.199	ns	**6.68**	0.186	ns	**6.71**	0.074	ns
	12	**6.98**	0.079	**7.07**	0.106	ns	**7.01**	0.116	ns	**7.03**	0.107	ns	**6.95**	0.195	ns
	24	**7.03**	0.189	**7.01**	0.120	ns	**6.98**	0.253	ns	**6.96**	0.268	ns	**7.10**	0.189	ns

Strain	Time (h)	PB Control (0µM DKP)		Cyclo(-D-ala-val)			Cyclo(-pro-val)			Cyclo(-leu-pro)			Cyclo(-phe-pro)		
		Log_{10} CFU/peg	SD	**Log_{10} CFU/peg**	SD	Sig.	**Log_{10} CFU/peg**	SD	Sig.	**Log_{10} CFU/peg**	SD	Sig.	**Log_{10} CFU/peg**	SD	Sig.
***B. cenocepacia* (H111)**	4	**4.70**	0.176	**4.75**	0.123	ns	**4.75**	0.150	ns	**4.71**	0.117	ns	**4.86**	0.096	ns
	8	**5.48**	0.172	**5.47**	0.194	ns	**5.44**	0.158	ns	**5.41**	0.253	ns	**5.55**	0.164	ns
	12	**5.60**	0.182	**5.51**	0.231	ns	**5.62**	0.251	ns	**5.66**	0.266	ns	**5.61**	0.369	ns
	24	**6.47**	0.236	**6.46**	0.106	ns	**6.32**	0.215	ns	**6.31**	0.301	ns	**6.48**	0.273	ns
***B. cenocepacia* (K56-2)**	4	**4.48**	0.131	**4.60**	0.105	ns	**4.54**	0.142	ns	**4.40**	0.142	ns	**4.42**	0.236	ns
	8	**5.58**	0.222	**5.44**	0.186	ns	**5.50**	0.167	ns	**5.45**	0.257	ns	**5.54**	0.236	ns
	12	**5.74**	0.096	**5.48**	0.301	ns	**5.45**	0.148	*	**5.66**	0.121	ns	**5.43**	0.224	*
	24	**5.49**	0.230	**5.43**	0.210	ns	**5.26**	0.218	ns	**5.30**	0.210	ns	**5.43**	0.145	ns
***B. cenocepacia* (K56-*cciIR*)**	4	**4.69**	0.223	**4.59**	0.131	ns	**4.72**	0.265	ns	**4.71**	0.172	ns	**4.70**	0.080	ns
	8	**5.06**	0.118	**4.92**	0.209	ns	**4.96**	0.158	ns	**5.01**	0.144	ns	**5.09**	0.079	ns
	12	**5.42**	0.362	**5.49**	0.134	ns	**5.49**	0.141	ns	**5.53**	0.065	ns	**5.64**	0.136	ns
	24	**5.36**	0.225	**5.14**	0.283	ns	**5.22**	0.207	ns	**5.21**	0.223	ns	**5.37**	0.211	ns
***B. cenocepacia* (K56-*cepR,cciIR*)**	4	**4.77**	0.135	**4.67**	0.090	ns	**4.73**	0.144	ns	**4.86**	0.131	ns	**4.83**	0.042	ns
	8	**5.26**	0.095	**5.12**	0.102	ns	**5.16**	0.073	ns	**5.18**	0.109	ns	**5.14**	0.134	ns
	12	**5.77**	0.136	**5.79**	0.087	ns	**5.70**	0.166	ns	**5.69**	0.214	ns	**5.70**	0.214	ns
	24	**5.64**	0.188	**5.61**	0.135	ns	**5.52**	0.132	ns	**5.74**	0.128	ns	**5.61**	0.217	ns

4.3 Summary

The adaptive lifestyle switch from planktonic to biofilm growth is a highly beneficial strategy that many bacterial species, including those within the Bcc, employ as a means of surviving in unfavorable conditions (Ferreira *et al.* 2019; Ganesh *et al.* 2020). The process of forming the protective ECM, which makes up the majority of the biofilm's biomass, is complex in nature and has been previously shown to be significantly affected by the interference of QS regulation (Tomlin *et al.* 2005; Scoffone *et al.* 2016). With DKPs cyclo(-D-ala-val), cyclo(-pro-val), cyclo(-leu-pro) and cyclo(-phe-pro) affecting the production of QS-regulated extracellular virulence factors in Bcc species (Chapter 3), we were interested in addressing the hypothesis that by the same mechanism of functioning as QSIs, DKPs would also interfere with the formation of biofilm. We originally predicted the presence of DKPs to result in a decreased production of biofilm biomass with a subsequent decrease in viable biofilm cells. However, the experimental data collected in this study only partially supported this hypothesis.

By utilizing the crystal violet (CV) staining method to quantify biofilm biomass, the addition of DKPs, especially cyclo(-leu-pro) and cyclo(-phe-pro), resulted in significantly decreased biomass production over time with the later stages of development being the most affected (section 4.2.2). Interestingly, when grown under the same conditions, the viable biofilm cell count of most of the Bcc isolates was not significantly affected at any stage of biofilm formation tested (section 4.2.4). With the loss of fully functional QS regulation, isolates K56-*cciIR* and K56-*cepR,cciIR* had minimal biomass production compared to the wildtype parental strain K56-2, however, no differences were observed in viable biofilm cell counts. Together these data demonstrated the presence of DKPs to only exhibit antibiofilm properties in regard to the

production of biofilm biomass and not towards biofilm viability of the different Bcc isolates under investigation.

Chapter Five: DKPs as Antibiotic Potentiators

5.1 Introduction

The biofilm extracellular matrix (ECM) of *Burkholderia cepacia* complex (Bcc) species plays an important role in their ability to adapt to various ecological niches and persist chronically in the context of pathogenic interactions (Flemming and Wingender, 2010; Ferreira *et al.* 2011). Not only does the ECM provide protection against unfavorable environmental conditions, such as limited nutrients and resources, changes in pH and osmolarity, or mechanical and shear forces (Sharma *et al.* 2019), but it also acts as a physical barrier from the antimicrobial activity of host immune cells and antibiotics (Messiaen *et al.* 2014; Ernst *et al.* 2018). Treating pre-existing Bcc biofilm infections is therefore a challenging process that often times requires the use of complex combination treatment methods (Peeters *et al.* 2009; Garcia *et al.* 2018). In order to successfully penetrate the protective ECM barrier and cause a significant reduction in biofilm viability, conventional treatment methods include the use of multiple different types of antibiotics in relatively high concentrations over an extended period of time (Koo *et al.* 2017; Jiang *et al.* 2020). Despite the ability of these methods to control Bcc biofilm infections, the increasing emergence of antibiotic resistant strains has led to the need for identifying alternative therapeutic strategies.

One current and widely studied alternative strategy for combating Bcc biofilm infections involves investigating the use of antibiotics in combination with antibiotic potentiators, or small molecules that are defined by their ability to potentiate antibiotic activity with little to no antimicrobial activity on their own (Wright, 2016; Scoffone *et al.* 2017; Tyers and Wright, 2019).These can include molecules that alter host biology or, more commonly, molecules that interfere with bacterial metabolism and resistance mechanisms, resulting in increased

antimicrobial susceptibility. By not directly affecting the viability of bacterial cells, the lack of selective pressure deems antibiotic potentiators as 'evolution proof' or 'resistance breaker' molecules, making their use an ideal strategy for recovering antibiotic efficacy (Allen *et al.* 2014; Brown, 2015; Tyers and Wright, 2019).

Based on the results of Chapters 3 and 4, DKPs do not possess antimicrobial properties on their own as the viability of Bcc species was not affected when grown as planktonic cultures or as biofilms, respectively. However, all four DKPs of interest decreased the total amount of biofilm biomass over time, suggesting possible inhibition of ECM production during biofilm formation. Given the protective nature of the ECM to biofilm viability, it was hypothesized that DKPs would act as antibiotic potentiators by interfering with ECM production of Bcc species and thus increasing their susceptibility to antibiotic treatment.

To test our hypothesis, three different, commonly administered antibiotics, ceftazidime, meropenem and tobramycin, were chosen to treat preformed *B. cepacia* 16192, *B. multivorans* C5393 and *B. cenocepacia* K56-2 biofilms (Abbott *et al.* 2016; Sfeir, 2018; Garcia *et al.* 2018). The minimum biofilm eradication concentration (MBEC), which is defined as the lowest concentration of an antimicrobial required to eradicate 99.9% of biofilm-embedded bacteria (3 $\log_{10}$ reduction) (Rudilla *et al.* 2018; Thieme *et al.* 2019), was determined for treatments of antibiotics alone (section 5.2.1) and antibiotics in combination with each of the four DKPs, cyclo(-D-ala-val), cyclo(-pro-val), cyclo(-leu-pro) and cyclo(-phe-pro) (section 5.2.2). If DKPs possess any antibiotic potentiating activity, we would expect the combination treatments to result in an increased reduction in biofilm viability and a reduced MBEC value compared to treatments with antibiotics alone.

5.2 Results

5.2.1 Bcc biofilms have a high level of tolerance to antibiotics

Prior to the addition of DKPs, Bcc biofilms were first treated with each of the antibiotics alone using a wide range of concentrations. This was done in order to determine the MBEC value for each of the antibiotics used, as well as to identify a suitable concentration range that would then be used in the combination treatment assays. To do this, biofilms were cultivated utilizing synthetic cystic fibrosis sputum medium (SCFM) (Palmer *et al.* 2007) and the Calgary Biofilm Device (CBD) (Ceri *et al.* 1999; Harrison *et al.* 2010) as outlined in section 2.6.1. After 24 hours of incubation, the established biofilms were subjected to treatment with ceftazidime, meropenem or tobramycin. To determine the MBEC values, a high concentration range of 1 – 512 μg/mL was needed to treat the biofilms given the multitude of resistance mechanisms that Bcc species possess (Peeters *et al.* 2009; Tseng *et al.* 2014). Following treatment, viable biofilm cells were enumerated and graphed as log-kill curves, showing all three isolates, *B. cepacia* 16192, *B. multivorans* C5393 and *B. cenocepacia* K56-2, to have a high level of tolerance to each of the antibiotics when grown as biofilms (Figure 5.1).

Taking a closer look at each of the Bcc species, *B. cepacia* 16192 had a steady reduction in biofilm viability with increasing concentrations of antibiotics (Figure 5.1a). As expected, the MBEC value for each of the antibiotics was very high with a 3 $\log_{10}$ reduction in viable biofilm cells occurring at the higher concentrations of ≤256μg/mL for meropenem and ≤512μg/mL for ceftazidime and tobramycin. Based on the log-kill curves, the testable concentrations used for the combination treatments were determined to be 8-64μg/mL for ceftazidime and meropenem. *B. cepacia* 16192 was less susceptible to tobramycin and therefore a slightly higher range of 16-128μg/mL was chosen.

Figure 5.1: Antibiotic treatment of Bcc biofilms, *in vitro*

(a) *B. cepacia* 16192, **(b)** *B. multivorans* C5393, and **(c)** *B. cenocepacia* K56-2 biofilms were cultivated using SCFM and the CBD. After 24 hours of incubation, biofilms were treated for an additional 24 hours with ceftazidime, meropenem, or tobramycin in concentrations ranging from 1-512 μg/mL. Resulting viable biofilm cells presented as log-kill values in comparison to the pre-treatment mean viable cell count (MVCC) of each Bcc species. For clarity, the MVCC is shown as a black dashed line, while the MBEC is represented by a grey dashed line. This procedure was carried out three times in duplicate (n=6) with error bars representing ± SD.

a)

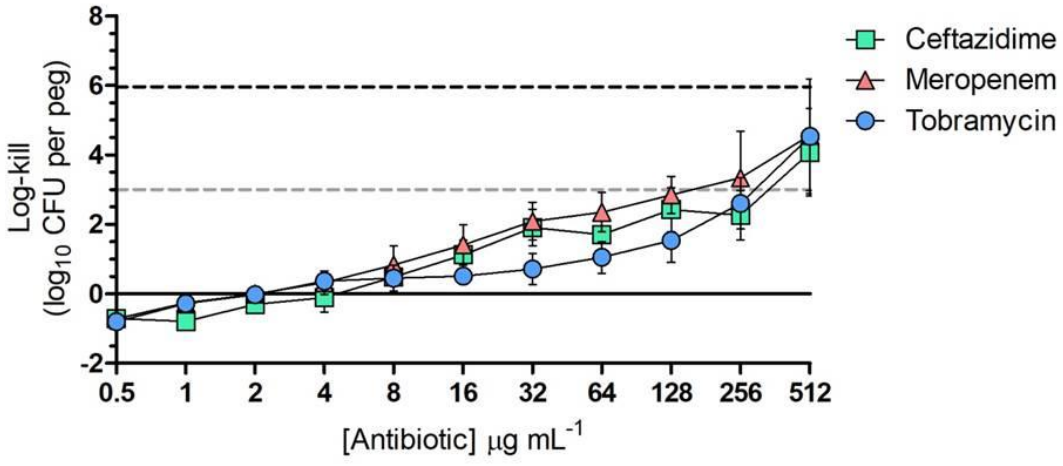
Log-kill
(log_{10} CFU per peg)
8
6
4
2
0
-2
0.5
1
2
4
8
16
32
64
128
256
512
[Antibiotic] μg mL^{-1}
Ceftazidime
Meropenem
Tobramycin

b)

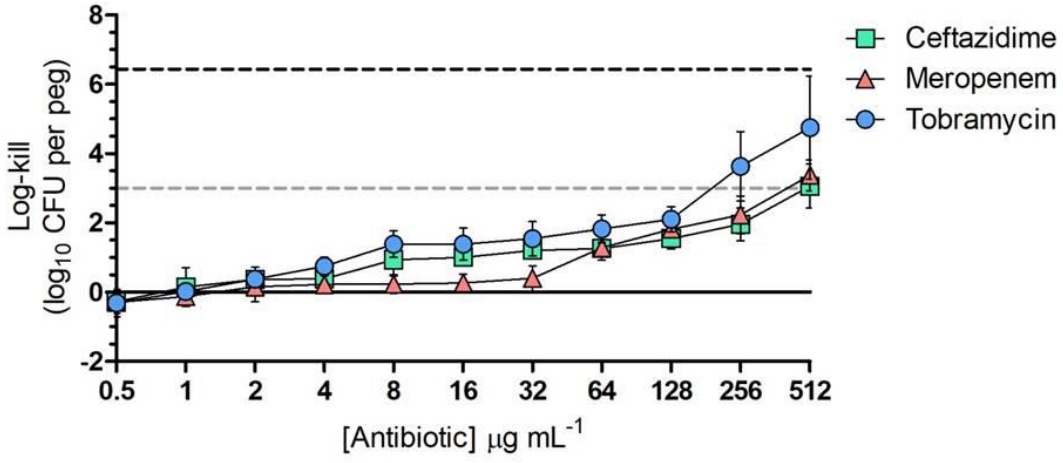
Log-kill
(log_{10} CFU per peg)
8
6
4
2
0
-2
0.5
1
2
4
8
16
32
64
128
256
512
[Antibiotic] μg mL^{-1}
Ceftazidime
Meropenem
Tobramycin

c)

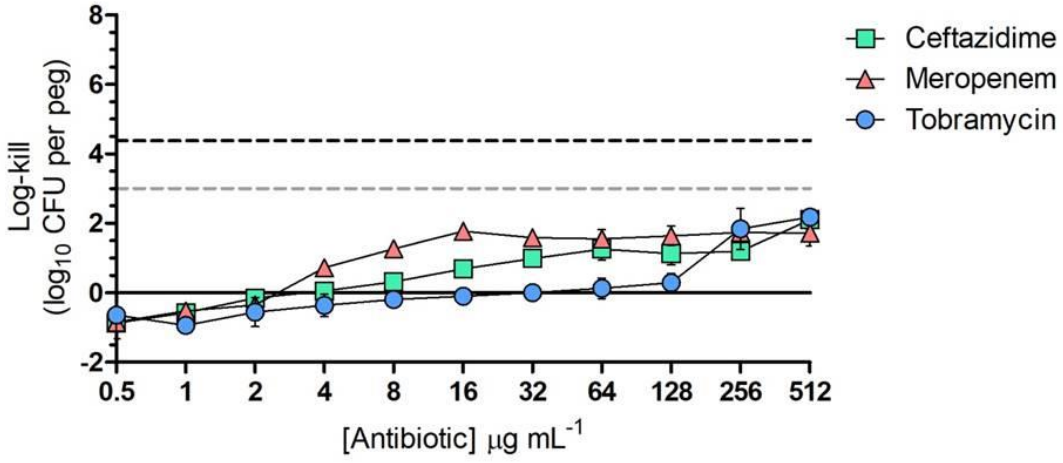
Log-kill
(log_{10} CFU per peg)
8
6
4
2
0
-2
0.5
1
2
4
8
16
32
64
128
256
512
[Antibiotic] μg mL^{-1}
Ceftazidime
Meropenem
Tobramycin

Unlike the log-kill pattern seen for *B. cepacia* 16192, the amount of *B. multivorans* C5393 biofilm reduction was fairly constant throughout most of the concentrations of antibiotics tested (Figure 5.1b). Rather than a steady increase, the log-kill increased by ~1.0 $\log_{10}$ from 0-8μg/mL and then remained relatively constant from 8-32μg/mL when treated with ceftazidime or tobramycin. In the case of meropenem, *B. multivorans* C5393 was the least susceptible to it as the log-kill did not exceed a value of 0.4 $\log_{10}$ from 0-32μg/mL. At the higher concentrations, however, all antibiotics resulted in an increase in biofilm reduction, with an MBEC value of ≤256 for tobramycin and ≤512μg/mL for ceftazidime and meropenem. Ultimately, the concentration range of 16-128μg/mL was chosen to be used for each of the antibiotics in the combination treatment assays.

Of the three Bcc species tested, *B. cenocepacia* K56-2 showed to have the greatest amount of resistance to antibiotic treatment when grown as a biofilm, *in vitro* (Figure 5.1c). The use of meropenem and ceftazidime resulted in similar log-kill patterns, where both treatments resulted in a steady increase in log-kill with increasing antibiotic concentration until reaching plateaus around 16μg/mL and 64μg/mL, respectively. The concentration range of 8-64μg/mL was therefore chosen for the combination treatment assays using meropenem and ceftazidime in order to see if the addition of DKPs could enhance their antimicrobial activity. *B. cenocepacia* K56-2 was the least susceptible to tobramycin treatment as biofilm viability did not result in any reduction until reaching a high concentration of 64μg/mL. The antibiotic range chosen for this antibiotic was therefore higher compared to the other two at a range of 64-512μg/mL. None of the antibiotics reached a log-kill of 3 within the range of antibiotics tested, therefore the MBEC values were all considered to be >512μg/mL.

5.2.2 DKPs potentiate antibiotic activity in the treatment of Bcc biofilms

To test our hypothesis that DKPs possess antibiotic potentiating activity, Bcc biofilms were cultivated using SCFM and the CBD as previously described and were treated using the antibiotic concentration ranges that were determined in the previous section. In combination with antibiotics, treatments also included the addition of either phosphate buffer (PB) as an untreated control or one of the four DKPs, cyclo(-D-ala-val), cyclo(-pro-val), cyclo(-leu-pro) and cyclo(-phe-pro) (section 2.6.2). Given that the 100μM concentration of DKPs showed the greatest level of inhibition towards biofilm formation (Chapter 4), it was chosen as the ideal concentration for investigating their ability to potentiate the activities of ceftazidime, meropenem and tobramycin.

5.2.2.1 Ceftazidime

In the treatment of Bcc biofilms, DKPs potentiated the activity of ceftazidime with the greatest effect on the biofilm viability of *B. cepacia* 16192 (Figure 5.2). In comparison to the PB buffer control, the addition of DKPs significantly increased the log-kill of *B. cepacia* 16192 biofilms at all of the antibiotic concentrations tested (Figure 5.2a). In the previous section it was determined that the MBEC for treatment with ceftazidime alone was ≤512μg/mL. However, with the addition of DKPs, a 99.9% reduction in biofilm viability was seen at an antibiotic concentration as low as 64μg/mL, a decrease of three doubling dilutions.

In a similar manner, the combination treatment of *B. multivorans* C5393 and *B. cenocepacia* K56-2 biofilms resulted in significantly higher log-kill numbers compared to their PB buffer controls, although to a lesser extent than what was observed for *B. cepacia* 16192. The original MBEC of ≤512μg/mL for the treatment of *B. multivorans* C5393 biofilms was decreased by two doubling dilutions to a concentration of 128μg/mL with the addition of DKPs

Figure 5.2: DKPs potentiate the activity of ceftazidime in the treatment of Bcc biofilms

(a) *B. cepacia* 16192, **(b)** *B. multivorans* C5393, and **(c)** *B. cenocepacia* K56-2 biofilms were cultivated using SCFM and the CBD as previously described. After 24 hours of incubation, biofilms were treated with doubling concentrations of ceftazidime in combination with either phosphate buffer (PB) as an untreated control or one of the four DKPs to a final concentration of 100μM. Resulting viable biofilm cell counts presented as log-kill values in comparison to the pre-treatment mean viable cell count (MVCC). For clarity, the MVCC is shown as a black dashed line, while the MBEC is represented by a grey dashed line. This procedure was carried out three times in duplicate (n=6). Significance was determined by one-way ANOVA and Dunnett post-hoc test compared to control treatment; ◊ ($p \leq 0.05$), ⧫ ($p \leq 0.01$), ♦ ($p \leq 0.001$). Bars represent ± SD.

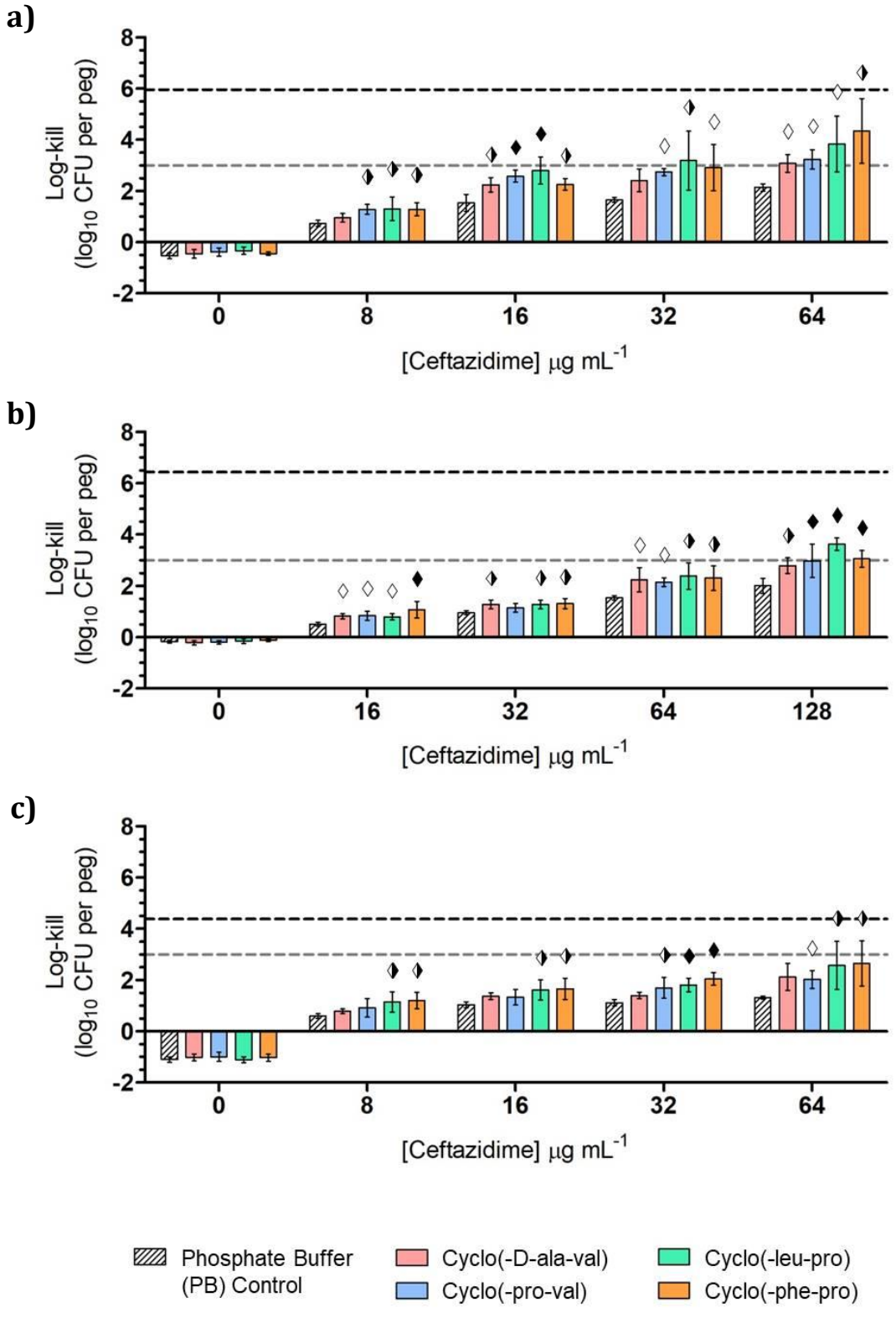
a)
b)
c)
Log-kill
(log10 CFU per peg)
[Ceftazidime] μg mL-1
0
8
16
32
64
128
Phosphate Buffer
(PB) Control
Cyclo(-D-ala-val)
Cyclo(-pro-val)
Cyclo(-leu-pro)
Cyclo(-phe-pro)

(Figure 5.2b). In the case of *B. cenocepacia* K56-2 biofilms, however, none of the treatments reached an average 3 $\log_{10}$ reduction within the antibiotic range tested and therefore a possible change in the MBEC was considered to be undetermined (Figure 5.2c). Overall, in can be reported that the greatest amount of biofilm reduction for these two species occurred at the higher concentrations of antibiotics, where a ~1.0 $\log_{10}$ increase in log-kill was seen for the combination treatments compared to the PB buffer controls. It is also important to note that cyclo(-leu-pro) and cyclo(-phe-pro) had the greatest potentiating activity at most of the concentrations tested.

5.2.2.2 Meropenem

Similar to the results seen for ceftazidime, treatment of Bcc biofilms with a combination of meropenem and DKPs resulted in a significant increase in the log-kill of viable biofilm cells compared to PB buffer controls (Figure 5.3). Just as before, *B. cepacia* 16192 was the most affected Bcc species as the addition of DKPs cyclo(-pro-val), cyclo(-leu-pro) or cyclo(-phe-pro) all caused a 99.9% decrease in biofilm viability at a meropenem concentration of 64μg/mL (Figure 5.3a). These three DKPs were also the most effective at potentiating the activity of meropenem at each of the concentrations tested, with log-kill values being 0.5-1.0 $\log_{10}$ greater than their respective PB buffer controls. Unlike the combination treatments with ceftazidime, cyclo(-D-ala-val) had minimal to no effect on the killing activity of meropenem. Interestingly, this was also the case for the other two Bcc species as the addition of cyclo(-D-ala-val) did not result in an average log-kill greater than 3 $\log_{10}$ for any of the meropenem concentrations tested (Figure 5.3).

In the treatment of *B. multivorans* C5393 and *B. cenocepacia* K56-2 biofilms, the addition of DKPs to the lower concentrations of meropenem resulted in a small, yet significant, increases

Figure 5.3: DKPs potentiate the activity of meropenem in the treatment of Bcc biofilms **(a)** *B. cepacia* 16192, **(b)** *B. multivorans* C5393, and **(c)** *B. cenocepacia* K56-2 biofilms were cultivated using SCFM and the CBD as previously described. After 24 hours of incubation, biofilms were treated with doubling concentrations of meropenem in combination with either phosphate buffer (PB) as an untreated control or one of the four DKPs to a final concentration of 100μM. Resulting viable biofilm cell counts presented as log-kill values in comparison to the pre-treatment mean viable cell count (MVCC). For clarity, the MVCC is shown as a black dashed line, while the MBEC is represented by a grey dashed line. This procedure was carried out three times in duplicate (n=6). Significance was determined by one-way ANOVA and Dunnett post-hoc test compared to control treatment; ◊ ($p \leq 0.05$), ⧫ ($p \leq 0.01$), ♦ ($p \leq 0.001$). Bars represent ± SD.

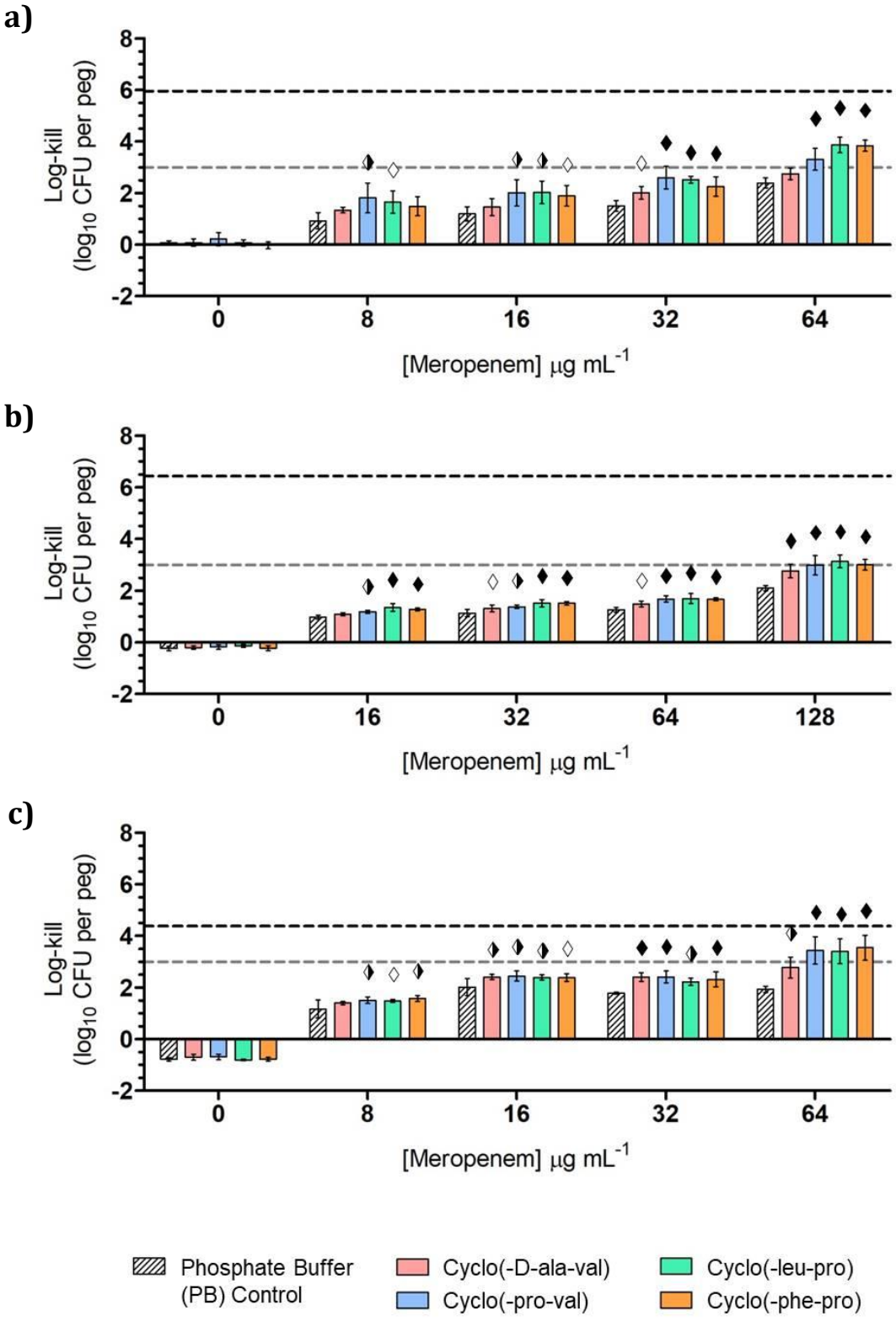
a)
b)
c)
Log-kill
(log_{10} CFU per peg)
8
6
4
2
0
-2
0
8
16
32
64
128
[Meropenem] μg mL^{-1}
Phosphate Buffer
(PB) Control
Cyclo(-D-ala-val)
Cyclo(-pro-val)
Cyclo(-leu-pro)
Cyclo(-phe-pro)

in the log-kill. At the higher meropenem concentrations, however, there was an even greater effect seen with the addition of DKPs as the reduction in biofilm viability was ~1.0-1.5 $\log_{10}$ larger in comparison to PB buffer controls (Figure 5.3b & c). In the case of *B. multivorans* C5393, when treated with meropenem alone the MBEC was determined to be ≤512μg/mL, however, when in combination with cyclo(-pro-val), cyclo(-leu-pro) or cyclo(-phe-pro), a 3 $\log_{10}$ reduction was seen at 128μg/mL, indicating a decrease in the MBEC of at least two doubling dilutions (Figure 5.3b). Similarly in the treatment of *B. cenocepacia* K56-2 biofilms, the original MBEC of >512μg/mL was also lowered with the addition of these DKPs to a meropenem concentration of 64μg/mL, a decrease of three doubling dilutions (Figure 5.3c). Overall, these trends are highly similar to those that were seen for ceftazidime as DKPs in combination with the higher antibiotic concentrations tested resulted in the greatest increase in log-kill of Bcc biofilms (Figure 5.3).

5.2.2.3 Tobramycin

Of the three antibiotics used in this study, DKPs had the greatest potentiating activity in combination with tobramycin for the treatment of Bcc biofilms (Figure 5.4). All three Bcc species had very large MBEC values when treated with tobramycin alone as determined in the previous section (section 5.2.1). However, with the addition of DKPs, significantly greater log-kill numbers, and even points of complete eradication, were seen for all species at the higher tobramycin concentrations tested. *B. cepacia* 16192 and *B. multivorans* C5393 were the most affected by the combination treatments and had almost identical log-kill patterns (Figure 5.4a & b). The addition of cyclo(-leu-pro) and cyclo(-phe-pro) were the most effective DKPs, with log-kill values 2-2.5 times greater than the PB buffer control at multiple tobramycin concentrations tested. Compared to their original MBEC values of ≤512μg/mL and ≤256μg/mL,

Figure 5.4: DKPs potentiate the activity of tobramycin in the treatment of Bcc biofilms

(a) *B. cepacia* 16192, **(b)** *B. multivorans* C5393, and **(c)** *B. cenocepacia* K56-2 biofilms were cultivated using SCFM and the CBD as previously described. After 24 hours of incubation, biofilms were treated with doubling concentrations of tobramycin in combination with either phosphate buffer (PB) as an untreated control or one of the four DKPs to a final concentration of 100μM. Resulting viable biofilm cell counts presented as log-kill values in comparison to the pre-treatment mean viable cell count (MVCC). For clarity, the MVCC is shown as a black dashed line, while the MBEC is represented by a grey dashed line. This procedure was carried out three times in duplicate (n=6). Significance was determined by one-way ANOVA and Dunnett post-hoc test compared to control treatment; ◊ ($p \leq 0.05$), ⧫ ($p \leq 0.01$), ♦ ($p \leq 0.001$). Bars represent ± SD.

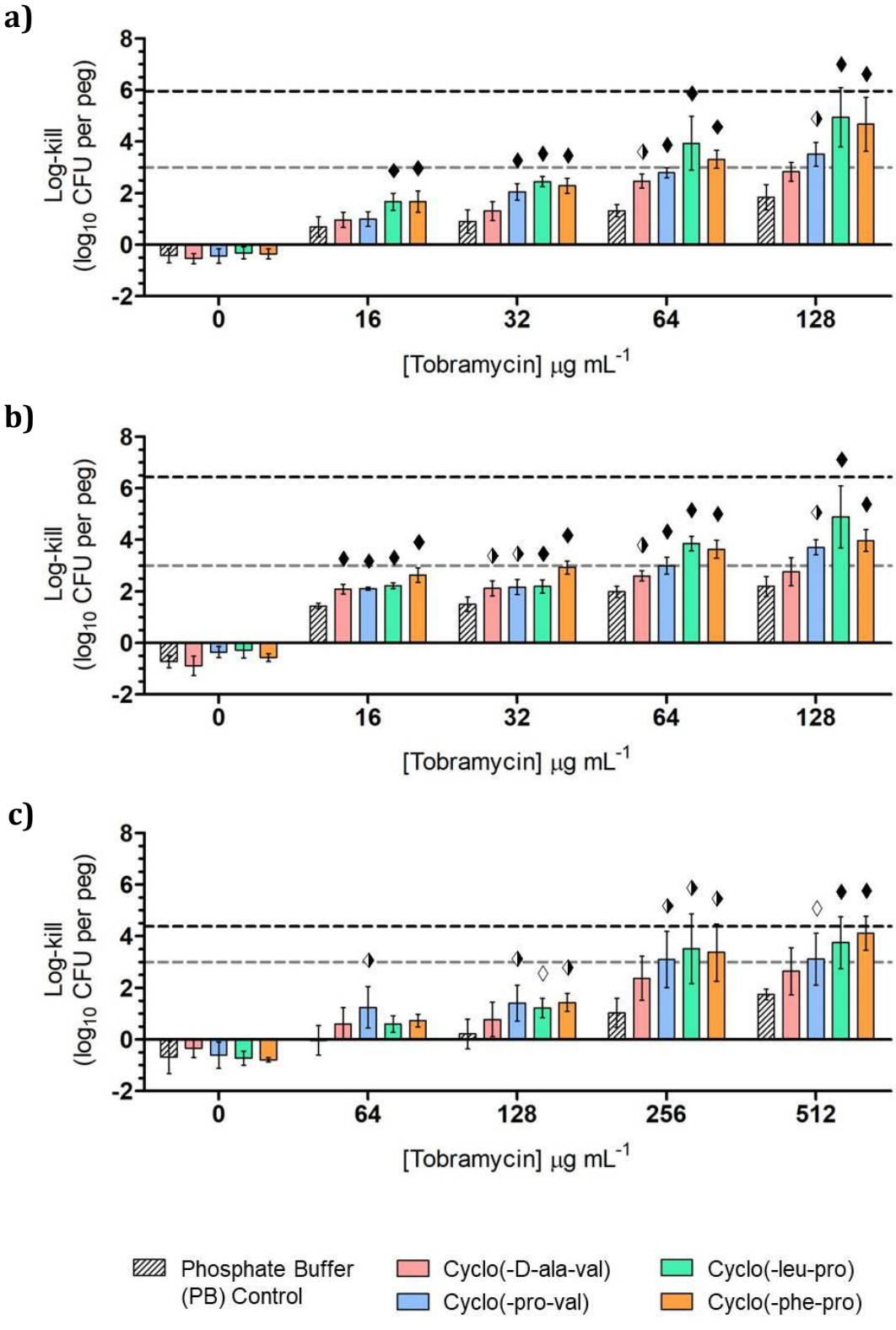
a)
b)
c)
Log-kill
(log10 CFU per peg)
8
6
4
2
0
-2
0
16
32
64
128
[Tobramycin] μg mL-1
0
64
128
256
512
[Tobramycin] μg mL-1
Phosphate Buffer
(PB) Control
Cyclo(-D-ala-val)
Cyclo(-pro-val)
Cyclo(-leu-pro)
Cyclo(-phe-pro)

a 3 $\log_{10}$ reduction in *B. cepacia* 16192 and *B. multivorans* C5393 viable biofilm cells was seen at 64μg/mL with the addition of cyclo(-leu-pro) or cyclo(-phe-pro). Interestingly, treatment with 128μg/mL of tobramycin in combination with either of these two DKPs resulted in complete eradication in 1-3 out of 6 experimental replicates (Figure 5.4a & b).

The combination treatments were less effective at reducing biofilm viability of *B. cenocepacia* (K56-2) compared to the other two Bcc species. At the lower concentrations of tobramycin tested, the addition of DKPs had varying effects with only minimally significant increases in log-kill numbers compared to the PB buffer controls (Figure 5.4c). Only at the higher concentrations of 256 and 512μg/mL was an increase in the log-kill observed, where 3-4 out of 6 experimental replicates resulted in complete eradication of biofilm viable cells. The MBEC of >512μg/mL therefore decreased down to ≤256μg/mL with the addition of cyclo(-pro-val), cyclo(-leu-pro), or cyclo(-phe-pro). Just as seen in the previous combination treatments, cyclo(-D-ala-val) had minimal to no significant effect on the killing activity of tobramycin and did not result in an average log-kill greater than 3 $\log_{10}$ for any of the Bcc isolates tested (Figure 5.4).

5.3 Summary

With the need for identifying alternative therapeutic options for the treatment of chronic and recurring Bcc infections, the use of antibiotic potentiators has become a highly researched strategy for increasing antibiotic efficacy. Previously, our data demonstrated DKPs cyclo(-D-ala-val), cyclo(-pro-val), cyclo(-leu-pro) and cyclo(-phe-pro) to all have an effect on the production of biofilm biomass without affecting biofilm cell viability, suggesting possible inhibition of ECM formation (Chapter 4). Given the protective nature of the ECM to biofilm viability, it was hypothesized that DKPs would act as antibiotic potentiators by interfering with

the production of ECM and thus potentiating the antimicrobial activity of antibiotics in the treatment of Bcc biofilms.

With the use of SCFM and the CBD to cultivate and treat *B. cepacia* 16192, *B. multivorans* C5393 and *B. cenocepacia* K56-2 biofilms *in vitro*, our data showed DKPs to possess potentiating activity towards the commonly administered antibiotics, ceftazidime, meropenem and tobramycin. When used on their own, relatively high concentrations of these antibiotics were needed in order to reduce biofilm viability by a $\log_{10}$ of 3, resulting in high MBEC values ranging from ≤256μg/mL to >512μg/mL (section 5.2.1). With the addition of DKPs, however, a significantly greater amount of biofilm reduction was observed compared to the phosphate buffer controls (section 5.2.2). Specifically, DKPs cyclo(-pro-val), cyclo(-leu-pro) and cyclo(-phe-pro) were highly effective at potentiating each of the antibiotics, particularly tobramycin, as the concentration of antibiotics needed to eradicate 99.9% of viable biofilm cells was two to three doubling dilutions lower compared to antibiotics on their own. Together, these data support our hypothesis that DKPs possess the ability to potentiate antibiotic treatments of Bcc biofilms, *in vitro*.

Chapter Six: Discussion

2,5-Diketopiperazines (DKPs) are a highly diverse and abundant group of biologically active cyclic dipeptides that carry a number of important chemical and medicinal properties (Ressurreicao *et al.* 2011; Ortiz and Sansinenea, 2017). Consisting of a semi-rigid, heterocyclic six-membered-ring core and highly variable substituent groups, the unique physiochemical nature of DKPs has allowed for their use in a wide range of therapeutic applications (Corey, 1938; Borthwick, 2012). Quite notably, DKPs have been shown to possess clinically significant functions such as anti-viral (Maeda *et al.* 2004), anti-fungal (Houston *et al.* 2002), anti-inflammatory (Shimazaki *et al.* 1991), and even anti-cancer activities (Nicholson *et al.* 2006; Ding *et al.* 2020). However, with the increasing need for improving treatments of multi-drug resistant bacterial infections, the sub-class of DKPs that possess antivirulence and antibiofilm activity by functioning as quorum sensing inhibitors (QSIs) has over recent years become an area of high interest in research (Holden *et al.* 1999; Campbell *et al.* 2009; Scoffone *et al.* 2017).

Considered as an important group of human pathogens, species within the *Burkholderia cepacia* complex (Bcc) are one such group of bacterial pathogens that require attention towards improving treatment options due to their high level of resistance to many antibiotics used in clinical practice (Mahenthiralingam *et al.* 2005; Tseng *et al.* 2014; Rhodes and Schweizer, 2016). Infection with Bcc species has been shown to lead to detrimental clinical outcomes, particularly in regard to patients with cystic fibrosis (CF) where long-term colonization and recurrent infections can lead to a more rapid decline in lung function (Isles *et al.* 1984; Courtney *et al.* 2004; Coutinho *et al.* 2011). Therefore, researchers have looked into a number of alternative therapeutic approaches, including the use of natural products that possess antimicrobial activity, molecules that are already in use to treat other diseases, as well

as QSIs, like DKPs, as a means of decreasing the pathogenicity of Bcc species (Fraser-Pitt *et al.* 2016; Scoffone *et al.* 2017; Ernst *et al.* 2018).

Targeting quorum sensing (QS) regulation is regarded as an ideal method for improving treatment of Bcc infections given its significance in influencing the pathogenicity of these species (Subramoni and Sokol, 2012; Scoffone *et al.* 2019). Not only is the CepIR QS system conserved among species of the Bcc (Wopperer *et al.* 2006; Subramoni and Sokol, 2012), but its function is also known to be highly maintained throughout all stages of infection and important for acute and chronic colonization (Sokol *et al.* 2003; Chambers *et al.* 2005; McKeon *et al.* 2011). Therefore, identifying QSIs, such as DKPs, that are capable of actively targeting and interfering with QS regulation in Bcc species pose as potential candidates for further investigation.

Previous work conducted by Purighalla (2011), identified four DKP molecules as having antagonistic effects towards species of the Bcc. DKPs cyclo(-D-ala-val), cyclo(-pro-val), cyclo(-leu-pro) and cyclo(-phe-pro) were all shown to non-competitively inhibit the expression of both *cepI* and *cepR* genes of the CepIR QS systems as demonstrated using *lux*-reporter assays. Recently, the first proposed mechanism of action behind the QSI properties of DKPs was put forth by Buroni and colleagues (2018), who screened a panel of larger, synthesized DKP molecules and showed their inhibition to occur through interaction with the CepI synthase, thus limiting production of the autoinducer molecules necessary for QS regulation. With this new evidence and knowing the significant role that QS systems play in the production of virulence factor determinants and the formation of biofilm in Bcc species, we were interested in further characterizing the inhibitory properties of these four DKPs.

This thesis focused on investigating the ability of DKPs to function as QSIs by observing their effects on the pathogenic phenotype of various Bcc species. With the aim of gaining insights into their potential role in alternative therapeutics, we were interested in determining the extent to which DKPs cyclo(-D-ala-val), cyclo(-pro-val), cyclo(-leu-pro) and cyclo(-phe-pro) could act as antivirulence agents, as antibiofilm agents, and as antibiotic potentiators in the treatment of Bcc biofilms, *in vitro*. Based on recently published data and previous findings in our lab, our hypothesis was that by interfering with QS regulation, DKPs would alter the production of extracellular virulence factors and the formation of biofilm with a subsequent increase in susceptibility to antibiotic treatment when grown as biofilms. Other notable QSIs, such as baicalin hydrate (BH) and furanone derivatives have already been reported to significantly affect the pathogenicity of Bcc species, particularly *B. multivorans* and *B. cenocepacia* (Brackman *et al.* 2011; Brackman *et al.* 2012). Therefore, demonstrating DKPs to also possess antivirulence and antibiofilm activities could contribute to this field of study, unveiling potential for the improvement of Bcc infection treatments.

6.1 DKPs alter the virulence phenotype of Bcc species

In the first part of this study, we examined the ability of cyclo(-D-ala-val), cyclo(-pro-val), cyclo(-leu-pro) and cyclo(-phe-pro) to act as antivirulence agents against species of the Bcc. We did this by quantifying the production of different QS-regulated extracellular virulence factors while exposed to each of the four DKPs (Chapter 3). Bcc species are known to rely heavily on QS regulation for the coordinated expression of hundreds of genes, many of which are related to their virulence traits (Subsin *et al.* 2007; O'Grady *et al.* 2009). Indeed, multiple studies have shown that genetic mutations in the CepIR QS system, as well as in the secondary CciIR QS system of *B. cenocepacia* K56-2, alters the production of extracellular virulence factors (Sokol

et al. 2003; Castonguay-Vanier *et al.* 2010; McKeon *et al.* 2011). Furthermore, the results of these studies also demonstrated Bcc QS mutants to lack the ability to maintain an infection *in vivo,* highlighting the potential for QSIs to hold clinically significant functions.

One of the defining characteristics of QSIs is their lack of direct antimicrobial activity on the targeted species, limiting the selective pressure for developing antibiotic resistance (Sokol *et al.* 2007; Brackman *et al.* 2009). Growth assessments performed in this study showed DKPs to not possess any direct antimicrobial activity towards any of the Bcc isolates, thus confirming their lack of selective pressure towards the development of resistance. From here we then moved forward with conducting several high-throughput virulence factor assays quantifying the production of extracellular virulence factors. The results collected from these experiments supported our hypothesis, indicating DKPs to significantly affect QS regulation in Bcc species as demonstrated by the decreased production of proteases and lipases along with an increased detection of siderophores. By examining the production of these factors under a number of different experimental parameters, our data showed the effect of DKPs on QS regulation to be dependent on several conditions including the DKP molecule and its concentration, the Bcc species under investigation, as well as the growth phase of the isolate.

The production of the two zinc-dependent metalloproteases, ZmpA and ZmpB, which make up the majority of total proteases in Bcc species, is known to be a highly conserved QS-regulated phenotype (Sokol *et al.* 2003; Wopperer *et al.* 2006; Reihill *et al.* 2017). In this study, the addition of DKPs cyclo(-D-ala-val), cyclo(-pro-val), cyclo(-leu-pro) or cyclo(-phe-pro) each resulted in a significant decrease in the production of these proteases as detected using the azocasein assay. As compared to the untreated phosphate buffer control, a 20-30% reduction was seen for most of the Bcc isolates tested with a few surprising and notable observations.

Unlike what was seen for the other virulence factors tested, the reduction of proteases proved to be very concentration-dependent, with the highest DKP concentration of 400μM almost exclusively being the only concentration to result in a significant decrease. Given the involvement of QS in protease production, this result was surprising as we would have predicted their production to be the most affected phenotype of the different virulence factors tested. Another important observation was the difference in the results seen for the two *B. cenocepacia* isolates where K56-2 was more affected by the presence of DKPs compared to H111 at both early and late stationary phase. Given that the secondary CciIR QS system of *B. cenocepacia* K56-2 has also been characterized as being involved with the positive regulation of proteases (Malott *et al.* 2005; O'Grady *et al.* 2009), our results indicate the possibility of DKPs also interfering with this QS system thus resulting in the greater decrease that was observed. This is a result that has not yet been documented in literature and would therefore be an interesting point for further inquiry.

Bcc species, particularly *B. multivorans,* also produce lipases under the regulation of QS as an important virulence factor involved in lung epithelial cell invasion and the evasion of host immunity (Carvalho *et al.* 2007; Mullen *et al.* 2007; O'Grady *et al.* 2009). Despite the extensive utilization of Bcc lipases in industry (Sanchez *et al.* 2018; Padilha *et al.* 2019), relatively little has been documented on their production in the context of bacterial infection. This is what led to our interest in examining lipase production in this study. Much like proteases, lipase genes are also positively regulated by the CepIR QS system, therefore explaining why there was also a decrease in their production while in the presence of DKPs. Unexpectedly, however, the production of lipases was affected to a greater extent than proteases as a 25-40% decrease was recorded for many of the Bcc species tested. These results could indicate that the lipase genes

of Bcc species are more reliant on QS regulation than once thought. Another noteworthy observation was the varying results seen between the different DKP molecules used. Out of the four DKPs, cyclo(-phe-pro) had the greatest inhibitory effect on the production of lipases as even the smallest concentration tested (25μM) resulted in significant decreases in lipase production at both early and late stationary phase. Recent work conducted by Scoffone and colleagues (2016), looked at a number of larger DKP molecules on the virulence of *B. cenocepacia* J2315 and identified two DKPs, which also contain phenylalanine groups, to hold the greatest inhibitory effects. Taken together, these findings along with our observations indicate that the inhibitory function of these molecules could be highly dependent on the presence of larger functional groups like phenylalanine. Additionally, this could also explain why cyclo(-D-ala-val), the smallest DKP under investigation, was the least effective at altering extracellular virulence factor production.

To gain a broader understanding of the inhibitory function of our DKP molecules, we chose to also look at the production of siderophores which are iron acquisition molecules known to be negatively regulated by QS in Bcc species as a means of preventing cytoplasmic iron overload (Lewenza and Sokol, 2001; O'Grady *et al.* 2009; Butt and Thomas, 2017). Consequently, the production of siderophores has been shown to be highly growth-phase dependent where the production of siderophores, particularly ornibactin, tends to increase much later in late stationary phase unlike other positively regulated factors (Lewenza and Sokol, 2001). This production pattern was evident in our CAS assay results as a significant increase in siderophores was detected from early to late stationary phase in all of the Bcc species tested. With the addition of DKPs, however, this increase was even larger, indicating DKPs to interfere with the down-regulation that is normally employed by the CepIR QS system.

The reliance on QS for the regulation of siderophore production was further highlighted by the results seen for K56-2 where the presence of DKPs increased siderophore detection to levels similar to that of the QS double mutant, K56-*cepR,cciIR.* This once again highlights the importance of QS regulation for the coordinated expression of various virulence factors that contribute to the overall phenotype of Bcc species.

In addition to AHL-based QS regulation, there are a number of regulatory mechanisms that are currently known to influence the production of extracellular virulence factors, such as the BDSF-dependent QS system (Schmid *et al.* 2012), the c-di-GMP pathway (Fazli *et al.* 2011), and the recently described RqpSR two-component system (Cui *et al.* 2018), to name a few. Therefore the significant changes seen in the production of proteases, lipases and siderophores could have potentially been the result of DKPs interfering with any of these systems, both directly or indirectly. However, considering the pattern we have observed in the data presented and what has been put forth by Buroni and colleagues (2018), we believe DKPs to be functioning as predicted, by interfering with the CepIR QS system of Bcc species leading to a decreased detection of proteases and lipases along with an increased detection of siderophores. Based on these results, we were then interested in determining the extent to which DKPs could function as antibiofilm agents given the significant role that QS also plays in the production of important biofilm-associated factors.

6.2 DKPs limit the production of biofilm-associated factors

The second part of this study focused on investigating the antibiofilm properties of DKPs cyclo(-D-ala-val), cyclo(-pro-val), cyclo(-leu-pro) and cyclo(-phe-pro) against Bcc species by measuring biofilm biomass production and viable biofilm cells over time (Chapter 4). The first described link between biofilm production and QS regulation in Bcc species came from Huber

and colleagues in 2001, where *cepR* and *cepI* mutants of *B. cenocepacia* H111 were both shown to have structural defects in their biofilms, particularly at the later stages of biofilm development. Tomlin *et al.* (2005) also demonstrated this trend to occur with mutants of the CciIR QS in *B. cenocepacia* K56-2. This link has since been further characterized, with multiple studies showing the production of many different biofilm-associated factors including various adhesins, exopolysaccharides (EPS), and the indispensable BapA large surface protein to all be regulated in part by the CepIR and CciIR QS systems in Bcc species (Huber *et al.* 2002; Holden *et al.* 2009; Inhulsen *et al.* 2012; Fazli *et al.* 2014). These factors together with extracellular DNA, amyloidogenic proteins and lipids collectively make up the extracellular matrix (ECM), the highly characteristic, protective barrier that holds bacterial cells together and accounts for the majority of the biofilm's biomass (Ferreira *et al.* 2011; Messiaen *et al.* 2014). Therefore, given the involvement of QS in the formation of the biofilm ECM in Bcc species, we originally hypothesized that the presence of DKPs would result in the decreased production of biofilm biomass with a subsequent decrease in the number of viable biofilm cells embedded in the biofilm. The data we collected from this part of the study, however, showed some unexpected trends that only partially supported this hypothesis.

The role of QS regulation has been previously shown to vary throughout biofilm development in Bcc species as QS mutants exhibit much greater impairment in biofilm formation and stability during the later stages of maturation and dispersal compared to the initial stages of attachment and growth (Huber *et al.* 2001; Tomlin *et al.* 2005; Brackman *et al.* 2009). This pattern was also indicated by our results as the biofilm biomass formed by the K56-*cciIR* and K56-*cepR,cciIR* mutant strains were similar to that of K56-2 at the earlier time points of 4, 8, or 12 hours of incubation, but significantly inhibited by 3-4 times after 24 hours

of growth. Given that these differences were not observed until the latest time tested, it would have been interesting to measure beyond this time point to hypothetically see an even greater difference at 48 hours. Nevertheless, the data we obtained indicated that QS-regulated biofilm factors were more strongly expressed and critical during the later stages of biofilm formation. Surprisingly, the data we collected from our viable biofilm cell counts did not show this trend as both of the QS mutant strains did not exhibit any decrease in viability over time in comparison to the wild-type K56-2. This was an interesting observation as no apparent change in viable biofilm cell numbers alongside a significantly reduced amount of biofilm biomass led us to infer that the loss of proper QS regulation decreased the amount of self-produced biofilm-associated factors. Based on these unexpected experimental results, we were then interested in determining whether the presence of DKPs would result in these trends as well.

With the addition of DKPs to the starting cultures of each of the Bcc species, our hypothesis was generally supported as only a few experimental treatments limited the production of biofilm biomass at the earlier time points of 4 and 8 hours. While at the later time points of 12 and 24 hours, an even greater amount of inhibition was observed, particularly while in the presence of cyclo(-leu-pro) and cyclo(-phe-pro). The higher level of inhibition seen at the later stages of biofilm development align with what has been reported previously, suggesting DKPs to be interfering with the QS-mediated formation of biofilm in Bcc species (Huber *et al.* 2001; Tomlin *et al.* 2005). Another noteworthy observation was the extent of inhibition by DKPs seen between the different Bcc species tested. While the two *B. cepacia* isolates seemed to be the most affected at the higher concentrations of DKPs, resulting in 20-40% less biofilm biomass, it is also interesting to note that significant inhibition in biomass production of the two *B. multivorans* isolates was seen even in the presence of the smallest

concentration tested of 1μM. These findings suggest that the degree to which QS systems regulate the production of biofilm-associated factors, like EPS and structural proteins, likely differs among Bcc species. This is a hypothesis that could possibly hold true given the differences that have been previously documented for other virulence traits; however, further experimentation would need to be carried out to determine this (Wopperer *et al.* 2006; Carvalho *et al.* 2007; Mullen *et al.* 2007).

Considering the role that QS plays in the production of various factors that contribute to biofilm ECM, quite notably at the later stages of its formation, we had predicted that a decrease in the structural integrity of the ECM via QS interference would consequently result in a lower number of cells embedded in the biofilm. As shown previously in our untreated control experiments, however, this was not the case as both K56-*cciIR* and K56-*cepR,cciIR* mutants did not have any change in the number of viable cells from the wild-type, K56-2. The addition of DKPs also followed this trend as no change was observed in the viability of any of the Bcc species over 24 hours under the defined experimental conditions. Although there were a couple of incidences where a significant decrease in viable cells was recorded, the overall lack of change in biofilm viability among Bcc species mirrored the results we obtained in the untreated control experiments described above. These results indicate that despite the suspected reduction in the production of biofilm-associated factors, the resulting amount of ECM formed must still be great enough to hold a similar number of viable cells to the untreated controls which maintain uninterrupted QS regulation.

Given the importance of biofilm formation in the adaptability and pathogenicity of Bcc species, there are a number of regulatory mechanisms that are involved in its formation (Udine *et al.* 2013; Suppiger *et al.* 2013; Fazli *et al.* 2014). Much like in the case of extracellular

virulence factor production, this means that there are a number of possible pathways that these DKPs could be altering, leading to the observed phenotype. Considering the patterns observed in our data thus far, however, the results indicate an interference with QS regulation in Bcc species. Although the specific mechanism may require further inquiry, the suspected decrease in ECM with the addition of DKPs suggests that embedded biofilm cells are more vulnerable to external manipulations, such as exposure to antibiotic treatments. Therefore, based on the combined observations of our virulence factor assays and biofilm assays, we then hypothesized that DKPs would potentiate the activity of clinically relevant antibiotics, being ceftazidime, meropenem and tobramycin, in the treatment of Bcc biofilms.

6.3 DKPs potentiate the activity of antibiotics

In the final part of this study, we were interested in further expanding on our results to investigate whether DKPs cyclo(-D-ala-val), cyclo(-pro-val), cyclo(-leu-pro) and cyclo(-phe-pro) could function as antibiotic potentiators in the treatment of Bcc biofilms, *in vitro* (Chapter 5). Treating pre-existing Bcc biofilm infections often requires the use of complex combination treatments that involve high dosage antibiotics over an extended period of time, consequently increasing the selective pressure for the development of resistance (Zhou *et al.* 2007; Abbott *et al.* 2016; Garcia *et al.* 2018). The use of antivirulence molecules with no antimicrobial activity of their own, like DKPs, therefore offers an ideal solution for recovering antibiotic efficacy (Allen *et al.* 2014; Scoffone *et al.* 2019). Specifically, Brackman and colleagues (2011), demonstrated the use of two separate QSIs, baicalin hydrate (BH) and cinnamaldehyde, to potentiate the antimicrobial activity of tobramycin in the treatment of *B. multivorans* and *B. cenocepacia* biofilms. While more recently, an arginine derivative of the glycopolymer PNAG was also shown to sensitize various species of the Bcc to commonly administered antibiotics by

directly targeting biofilm structural integrity and thus increasing antibiotic penetration (Narayanaswamy *et al.* 2017, 2019). The data we collected from our combination treatment experiments adds to these published reports as DKPs, particularly cyclo(-leu-pro) and cyclo(-phe-pro), were shown to potentiate the activity of each of the three antibiotics under investigation. The extent to which these DKP molecules enhanced antimicrobial activity differed between the different classes of antibiotics used, suggesting that their potentiating activity could be dependent on the specific activity of the antibiotic.

The use of β-lactams, such as ceftazidime and meropenem, are commonly used in a clinical setting as a means of controlling Bcc biofilm infections by inhibiting bacterial cell-wall biosynthesis (Peeters *et al.* 2009). On their own, high concentrations ranging from ≤256μg/mL to >512μg/mL were needed to observe a 3 $\log_{10}$ reduction in *B. cepacia* 16192, *B. multivorans* C5393 and *B. cenocepacia* K56-2 viable biofilm cells, otherwise referred to as the minimum biofilm eradication concentration (MBEC) (Harrison *et al.* 2010). In combination with DKPs, however, the MBEC values decreased by two to three doubling dilutions, indicating clinically significant shifts in sensitivity as defined by Tomlin *et al.* (2005). These observations could be the result of a number of factors taking place, one of which is supported by the observations we made in our previous experiments. By functioning as QSIs, the suspected decrease in the production of various biofilm-associated factors which comprise the protective ECM layer could have allowed for greater antibiotic penetration, resulting in the increased killing of Bcc biofilm-embedded cells (Messiaen *et al.* 2014). Additionally, other mechanisms of antibiotic resistance, including the synthesis of efflux pumps, drug modifying enzymes and drug neutralizing proteins, have all been shown to be regulated in part by QS (O'Grady *et al.* 2009). These changes could have also left Bcc species more susceptible to the antimicrobial activity of

the different antibiotics used in this study. Taken together, these suspected physiological changes as a result of DKP exposure could account for the decrease in MBEC values that were observed for each of the β-lactam antibiotics used in this study.

While the use of tobramycin to treat Bcc infections may not be prescribed as often due to many species of the Bcc showing relatively high levels of resistance to aminoglycosides (Abbott *et al.* 2016; Kennedy *et al.* 2016), we were still interested in determining if DKPs could potentiate its activity. Much like in the case of the β-lactams, high concentrations of tobramycin ranging from ≤256μg/mL to >512μg/mL were also needed to result in a 3 $\log_{10}$ reduction in Bcc biofilm cells when used on its own. Surprisingly, with the addition of DKPs not only did we see a change in the MBEC by two to three doubling dilutions, but there were also a number of experimental replicates where complete eradication was observed. The explanation behind this could be due to the reasons listed above, with interference of QS decreasing mechanisms of antibiotic resistance and biofilm ECM. However, recent work put forth by Slachmuylders and colleagues (2018), who investigated the mechanism behind the potentiating activity of the QSI BH, highlights the need for continued investigation into the inhibitory mechanism of DKPs. Although BH is a known QSI previously shown to enhance the antimicrobial activity of tobramycin (Brackman *et al.* 2011), the molecular mechanism of potentiation was only recently elucidated, showing its effects to be due to reasons unrelated to QS inhibition (Slachmuylders *et al.* 2018). Through the use of several biofilm models and transcriptomic analyses, BH was shown to affect cellular respiration, impacting several pathways involved in the oxidative stress response of Bcc species. Given that ROS-mediated killing is considered as one mode of antimicrobial activity of tobramycin, the addition of BH was shown to increase this activity and thus increase the susceptibility of the targeted clinical isolates. Based on these findings, it is

important to note that although DKPs demonstrated an interference with QS regulation, the exact mechanism behind their antibiotic potentiating activity requires further experimentation and analysis.

6.4 Summary of Findings

With the need for identifying alternative therapeutic methods for the treatment of chronic and recurrent infections caused by species of the Bcc, investigating the use of QSIs offers an ideal approach for recovering antibiotic efficacy without an increase in selective pressure. Recognized as a novel class of QSIs, DKPs hold many important physiochemical properties that have collectively led to recent inquiries into their effects towards limiting the pathogenicity of Bcc species. Therefore, understanding the phenotypic effects of these molecules offers a first step with regard to their potential role in alternative therapeutics. To this end, we were interested in further characterizing the ability of DKPs cyclo(-D-ala-val), cyclo(-pro-val), cyclo(-leu-pro) and cyclo(-phe-pro) to function as antivirulence agents, as antibiofilm agents, and as antibiotic potenitators in the treatment of Bcc biofilms, *in vitro.* Based on previous work in our lab and recently published data, we hypothesized that by interfering with QS regulation, DKPs would alter Bcc extracellular virulence factor production and limit the formation of biofilm with a subsequent increase in antibiotic susceptibility when grown as a biofilm.

Taken together, the results obtained in this study supported our hypothesis, illustrating the capacity of DKPs to function as QSIs towards *B. cepacia, B. multivorans,* and *B. cenocepacia* clinical isolates. Through the use of various phenotypic assays, our work demonstrated DKPs to result in a significant decrease in the production of extracellular proteases and lipases with an increase in the detection of secreted siderophores, consistent with inhibition of QS regulation.

The results of these assays also provided context to the extent to which DKPs functioned as antivirulence agents, showing varying results depending on the DKP molecule and its concentration, the bacterial growth-phase, and the Bcc isolate under examination. Overall, the effects of DKPs were greater with higher DKP concentrations and cylco(-phe-pro) was generally the most inhibitory DKP which could be ascribed to the presence of its phenylalanine group based on the recent work of Scoffone *et al.* (2016).

Further investigation into the potential of these molecules to act as antibiofilm agents involved determining their effects on the production of biofilm biomass and on the number of viable biofilm cells. Interestingly, we observed no apparent change in viability alongside a significantly inhibited level of biofilm biomass production, leading us to infer that interference with QS regulation decreased the amount of the self-produced biofilm-associated factors that comprise the biofilm ECM. By altering the integrity of the biofilm structure, we wanted to then determine whether these effects would result in an increased susceptibility to treatment with ceftazidime, meropenem, or tobramycin. The combination treatments led to observing MBEC values that were two to three doubling dilutions less than treatment with antibiotics alone, indicating clinically significant shifts in susceptibility. We believe these shifts to be due to the altered ECM structure and the inhibited expression of resistance mechanisms as a result of QS inhibition. However, in light of recent evidence put forth by Slachmuylders and colleagues (2018), the mechanism behind the potentiating activity of DKPs may be more complex than what has been demonstrated in this study, leaving us interested in further experimentation.

6.5 Future Directions

With the aim of gaining an initial insight into the QSI properties of DKPs cyclo(-D-ala-val), cyclo(-pro-val), cyclo(-leu-pro) and cyclo(-phe-pro), the data we collected in this study highlighted a number of areas for continued scientific inquiry. Carrying out additional analyses could therefore provide further supporting evidence, leading to the next steps towards understanding their potential use in a clinical setting.

6.5.1 Transcriptomic analyses to assess the effects of DKPs at the molecular level

In the current study, we utilized a number of phenotypic assays as a means of demonstrating the effects of DKPs on the QS-regulated virulence phenotype of different species of the Bcc. Although the patterns we observed in our data supported our hypothesis, further characterization into the molecular alterations could provide insight into the changes occurring at the genetic level. Furthermore, transcriptomic analyses could also reveal other patterns in the data that were not identifiable within the experimental parameters we chose to employ, such as what was uncovered regarding the potentiating activity of BH (Slachmuylders *et al.* 2018). Therefore, quantifying changes at the genetic level would provide us with a more complete and clear understanding of the mechanism behind the phenotypic observations that were made in this study.

6.5.2 Confocal laser scanning microscopy to visualize Bcc biofilms

The Calgary Biofilm Device (CBD) and the MBEC assay protocol were both used in this study as a way of cultivating and treating Bcc biofilms (Ceri *et al.* 1999; Harrison *et al.* 2010). By doing so, this allowed us to collect meaningful data regarding the different DKP and antibiotic combinations of interest in a high through-put manner. In addition to this method of biofilm analysis, however, obtaining more qualitative data by visualizing Bcc biofilms through

the use of confocal laser scanning microscopy (CLSM) could offer further evidence regarding the effects of DKPs on the structural integrity of Bcc biofilms. Similar to the methods described by Doroshenko and colleagues (2014), we would be interested in staining biofilm biomass that was grown with or without the presence of DKPs as a means of visualizing the level of disruption in the formation of biofilm ECM. Furthermore, the use of antibiotic fluorescent conjugates could then provide quantitative data towards determining the distance to which antibiotics are capable of penetrating through the biofilm ECM (Stone *et al.* 2018). With this, we would then hypothesize a greater distance of antibiotic penetration in biofilm ECM that was formed in the presence of DKPs, supporting the increased antimicrobial activity that was seen in the combination treatments explored in this study.

6.5.3 Examining the potentiating activity of DKPs in vivo

As data collected through *in vitro* methods do not always correlate to the outcomes observed using *in vivo* methods, we could further investigate the antivirulence and antibiofilm properties of DKPs through the use of an infection model. Both *Galleria mellonella* and *Caenorhabditis elegans* are model organisms that are commonly used to study disease progression of chronic Bcc infections given their convenience in tracking Bcc pathogenesis while obtaining a large sum of data over a relatively short span of time (Balla and Troemel, 2013; Ramarao *et al.* 2012). Therefore, utilizing the *in vitro* results that we collected in this study as a guide for predicting the most effective combination treatments, we would then treat one of these species following infection with Bcc species. Measuring the percent survival of these model organisms over time could offer insight into the clinical significance of using DKPs in combination with antibiotics while also providing a clearer understanding of the pathogenicity of the different Bcc species under examination.

6.5.4 Investigating different treatment combinations on a larger panel of clinical isolates

As described previously, the treatment of Bcc infections often involves a complex combination of different classes of antibiotics as a means of combining several modes of action against multiple bacterial targets (Abbott *et al.* 2016). Therefore, to take our antibiotic potentiating experiments one step further it would be interesting to utilize different treatment combinations that include two antibiotics, such as ceftazidime + tobramycin or meropenem + tobramycin, co-administered with DKPs. To this, we would continue using the CBD to cultivate Bcc biofilms and the MBEC assay protocol to treat them with different combinations of interest in a checkerboard style setup (Ceri *et al.* 1999; Harrison *et al.* 2010; Narayanaswamy *et al.* 2017). Furthermore, to gain a more complete analysis of the effects of these combination treatments on Bcc species, it would be important to examine a larger panel of clinical isolates. In this study we included the use of two clinical isolates from three of the most prevalent Bcc species found to infect patients with CF, *B. cepacia, B. multivorans* and *B. cenocepacia* (Cystic Fibrosis Canada, 2018). However, the inclusion of more isolates in future studies would allow for a greater understanding of the clinical significance that DKPs could potentially hold.

6.5.5 Evolutionary trajectory assessment of DKPs as antibiotic potentiators

One of the defining characteristics that make QSI molecules so attractive for use in alternative therapeutics is their lack of direct antimicrobial activity on the targeted species which limits the likelihood for developing resistance. However, given that their ideal use in a clinical setting would be through co-administration with one or more antibiotics, it is important to consider their evolutionary trajectory while in the presence of said antibiotic(s). A recent study by Sass and colleagues (2019), demonstrated the QSI BH to lose its tobramycin-potentiating activity while treating *B. cenocepacia* J2315 biofilms over several successive

treatment cycles. Additional whole-genome sequencing identified mutations in genes involved in central metabolism, oxidative stress response pathways and mechanisms related to tobramycin uptake, indicating the development of resistance. These findings highlight an interesting concept that has generally been overlooked in regard to identifying antibiotic potentiator molecules for use in a clinical setting to treat multi-drug resistant bacterial infections. Herein, we would then propose conducting a similar study in order to determine the evolutionary trajectory of DKPs in combination with antibiotics in the treatment of Bcc biofilms.

6.6 Concluding Remarks

Identifying antivirulence molecules that hold the capacity to potentiate antibiotics is a growing area of research that has over recent years demonstrated promise towards recovering antibiotic efficacy in the treatment of multi-drug resistant bacterial infections. Here we provided evidence towards the first steps in investigating the use of DKPs as such agents in the treatment of Bcc biofilms. DKPs cyclo(-D-ala-val), cyclo(-pro-val), cyclo(-leu-pro) and cyclo(-phe-pro) all demonstrated varying levels of antivirulence, antibiofilm and antibiotic potentiating activity as shown through the use of several phenotypic assays. Together these data provide the initial groundwork for further scientific inquiry involving transcriptomic analyses, *in vivo* studies and evolutionary trajectory assessments as methods for characterizing the inhibitory mechanism of DKPs towards the pathogenicity of Bcc species. The continued study of these molecules could uncover clinically significant modes of action that are highly beneficial towards enhancing our knowledge of alternative therapeutics.

References

Abbott FK, Milne KEN, Stead DA, Gould IM. 2016. Combination antimicrobial susceptibility testing of *Burkholderia cepacia* complex: significance of species. *International Journal of Antimicrobial Agents.* 48(5): 521-527

Abraham WR. 2016. Going beyond the control of quorum-sensing to combat biofilm infections. *Antibiotics.* 5(3): 1-16

Adler C, Corbain NS, Seyedsayamdost MR, Pomares MF, de Cristobal RE, Clardy J, Kolter R, Vincent PA. 2012. Catecholate siderophores protect bacteria from pyochelin toxicity. *PLoS ONE.* 7(10): 1-7

Allen RC, Popat R, Diggle SP, Brown SP. 2014. Targeting virulence: can we make evolution-proof drugs? *Nature Reviews Microbiology.* 12(4): 300-308

Arora NK, Verma M. 2017. Modified microplate method for rapid and efficient estimation of siderophores produced by bacteria. *3 Biotech.* 7: 381

Avgeri SG, Matthaiou DK, Dimopoulos G, Grammatikos AP, Falagas ME. 2009. Therapeutic options for *Burkholderia cepacia* infections beyond co-trimoxazole: a systematic review of the clinical evidence. *International Journal of Antimicrobial Agents.* 33: 394–404

Baldwin A, Sokol PA, Parkhill J, Mahenthiralingam E. 2004. The *Burkholderia cepacia* epidemic strain marker is part of a novel genomic island encoding both virulence and metabolism-associated genes in *Burkholderia cenocepacia. Infection and Immunity.* 72(3): 1537-1547

Balla KM, Troemel ER. 2013. *Caenorhabditis elegans* as a model for intracellular pathogen infection. *Cellular Microbiology.* 15(8): 1313-1322

Belin P, Moutiez M, Lautru S, Seguin J, Pernodet JL, Gondry M. 2012. The nonribosomal synthesis of diketopiperazines in tRNA-dependent cyclodipeptide synthase pathways. *Natural Product Reports.* 29(9): 961-979

Borthwick AD, Liddle J. 2011. The design of orally bioavailable 2,5-diketopiperazine oxytocin antagonists: from concept to clinical candidate for premature labor. *Medicinal Research Reviews.* 31(4): 576-604

Borthwick AD. 2012. 2,5-Diketopiperazines: synthesis, reactions, medicinal chemistry, and bioactive natural products. *Chemical Reviews.* 112: 3641-3716

Brackman G, Coenye T. 2015. Quorum sensing inhibitors as anti-biofilm agents. *Current Pharmaceutical Designs.* 21(00): 1-7

Brackman G, Cos P, Maes L, Neils HJ, Coenye T. 2011. Quorum sensing inhibitors increase the susceptibility of bacterial biofilms to antibiotics *in vitro* and *in vivo. Antimicrobial Agents and Chemotherapy.* 55(6): 2655-2661

Brackman G, Hillaert U, Calenbergh SV, Neils HJ, Coenye T. 2009. Use of quorum sensing inhibitors to interfere with biofilm formation and development in *Burkholderia multivorans* and *Burkholderia cenocepacia. Research in Microbiology.* 160(2): 144-151

Brackman G, Risseeuw M, Celen S, Cos P, Maes L, Neils HJ, Van Calenbergh S, Coenye T. 2012. Synthesis and evaluation of the quorum sensing inhibitory effect of substituted triazolydihydrofuanones. *Bioorganic & Medicinal Chemistry.* 20(15): 4737-4743

Bragonzi A, Horati H, Kerrigan L, Lore NI, Scholte BJ, Weldon S. 2018. Inflammation and host-pathogen interaction: cause and consequence in cystic fibrosis lung disease. *Journal of Cystic Fibrosis.* 17(2): S40-S45

Bringmann G, Lang G, Steffens S, Schaumann K. 2004. Petrosifungins A and B, novel cyclodepsipeptides from a sponge-derived strain of *Penicillium brevicompactum. Journal of Natural Products.* 67(3): 311-315

Brown D. 2015. Antibiotic resistance breakers: can repurposed drugs fill the antibiotic discovery void? *Nature Reviews Drug Discovery.* 14(12): 821-832

Buroni S, Scoffone VC, Fumagalli M, Makarov V, Cagnone M, Trespidi G, De Rossi E, Forneris F, Riccardi G, Chiarelli LR. 2018. Investigating the mechanism of action of diketopiperazines

inhibitors of *Burkholderia cenocepacia* quorum sensing synthase CepI: a site-directed mutagenesis study. *Frontiers in Pharmacology.* 9: 836

Butt A, Thomas M. 2017. Iron acquisition mechanisms and their role in the virulence of *Burkholderia* species. *Frontiers in Cellular and Infection Microbiology.* 7(460): 1-21

Bylund J, Burgess LA, Cescutti P, Ernst RK, Speert DP. 2006. Exopolysaccharides from *Burkholderia cenocepacia* inhibit neutrophil chemotaxis and scavenge reactive oxygen species. *Journal of Biological Chemistry.* 281(5): 2526-2532

Campbell J, Lin Q, Geske GD, Blackwell HE. 2009. New and unexpected insights into the modulation of LuxR-type quorum sensing by cyclic dipeptides. *ACS Chemical Biology.* 4(12): 1051-1059

Carvalho AP, Ventura GM, Pereira CB, Leão RS, Folescu TW, Higa L, Teixeira LM, Plotkowski MC, Merquior VL, Albano RM, Marques EA. 2007. *Burkholderia cenocepacia, B. multivorans, B. ambifaria* and *B. vietnamiensis* isolates from cystic fibrosis patients have different profiles of exoenzyme production. *APMIS*. 115(4): 311-318

Carvalho MP, Abraham WR. 2012. Antimicrobial and biofilm inhibiting diketopiperazines. *Current Medicinal Chemistry.* 19(21): 3564-3577

Castonguay-Vanier J, Vial L, Tremblay J, Deziel E. 2010. *Drosophila melanogaster* as a model host for the *Burkholderia cepacia* complex. *PLoS ONE.* 5(7): 1-10

Cerantola S, Lemassu-Jacquier A, Montrozier H. 1999. Structural elucidation of a novel exopolysaccharide produced by a mucoid clinical isolate of *Burkholderia cepacia.* Characterization of a trisubstituted glucuronic acid residue in a heptasaccharide repeating unit. *European Journal of Biochemistry.* 260: 373-383

Ceri H, Olson M, Morck D, Storey D, Read R, Buret A, Olson B. 2001. The MBEC assay system: multiple equivalent biofilms for antibiotic and biocide susceptibility testing. *Methods in Enzymology.* 337(2201): 377-385

Ceri H, Olson ME, Stremick C, Read RR, Morck D, Buret A. 1999. The Calgary biofilm device: new technology for rapid determination of antibiotic susceptibilities of bacterial biofilms. *Journal of Clinical Microbiology.* 37(6): 1771-1776

Cescutti P, Bosco M, Picotti F, Impallomeni G, Leitao JH, Richau JA, Sa-Correia I. 2000. Structural study of the exopolysaccharide produced by a clinical isolate of *Burkholderia cepacia. Biochemical and Biophysical Research Communications.* 273: 1088-1094

Chambers CE, Visser MB, Schwab U, Sokol PA. 2005. Identification of *N*-acylhomoserine lactones in mucopurulent respiratory secretions from cystic fibrosis patients. *FEMS Microbiology Letters.* 244(2): 297-304

Cohen TS, Prince A. 2012. Cystic fibrosis: a mucosal immunodeficiency syndrome. *Nature Medicine.* 18(4): 509-519

Conway BA, Chu KK, Bylund J, Altman E, Speert DP. 2004. Production of exopolysaccharide by *Burkholderia cenocepacia* results in altered cell surface interactions and altered bacterial clearance in mice. *Journal of Infectious Diseases*. 190:957–966

Corey RB. 1938. The crystal structure of diketopiperazine. *Journal of the American Chemical Society.* 60(7): 1598-1604

Courney JM, Dunbar KEA, McDowell A, Moore JE, Warke TJ, Stevenson M, Elborn JS. 2004. Clinical outcome of *Burkholderia cepacia* complex infection in cystic fibrosis adults. *Journal of Cystic Fibrosis.* 3(2): 93-98

Coutinho CP, dos Santos SC, Madeira A, Mira NP, Moreira AS, Sa-Correia I. 2011. Long-term colonization of the cystic fibrosis lung by *Burkholderia cepacia* complex bacteria: epidemiology, clonal variation, and genome-wide expression alterations. *Frontiers in Cellular and Infection Microbiology.* 1(12): 1-11

Cui C, Yang C, Song S, Fu S, Sun X, Yang L, He F, Zhang LH, Zhang Y, Deng Y. 2018. A novel two-component system modulates quorum sensing and pathogenicity in *Burkholderia cenocepacia. Molecular Microbiology.* 108(1): 32-44

Cunha MV, Silvia AS, Leitao JH, Moreira LM, Videira PA, Sa-Correia I. 2004. Studies on the involvement of the exopolysaccharide produced by cystic fibrosis-associated isolates of the *Burkholderia cepacia* complex in biofilm formation and in persistence of respiratory infections. *Journal of Clinical Microbiology.* 42(7): 3052-3058

Cuzzi B, Cescutti P, Furlanis L, Lagatolla C, Sturiale L, Garozzo D, Rizzo R. 2012. Investigation of bacterial resistance to the immune system response: cepacian depolymerisation by reactive oxygen species. *Innate Immunity.* 18(4): 661-671

Cystic Fibrosis Canada. 2018. The Canadian Cystic Fibrosis Registry 2018 Annual Data Report. Toronto, Canada: Cystic Fibrosis Canada

D'Argenio D, Wu M, Hoffman LR, Kulasekara HD, Deziel E, Smith EE, Nguyen H, Ernst RK, Freeman TJL, Spencer DH, Brittnacher M, Hayden HS, Selgrade S, Klausen M, Goodlett DR, Burns JL, Ramsey BW, Miller SI. 2007. Growth phenotypes of *Pseudomonas aeruginosa lasR* mutants adapted to the airways of cystic fibrosis patients. *Molecular Microbiology.* 64(2): 512-533

Daugan A, Grondin P, Ruault C, Le Monnier de Gouville AC, Coste H, Linget JM, Kirilovsky J, Hyafil F, Labaudiniere R. 2003. The discovery of tadalafil: a novel and highly selective PDE5 inhibitor. 2:2,3,6,7,12,12a-hexahydropyrazino[1',2':1,6]pyrido[3,4-*b*]indole-1,4-dione analogues. *Journal of Medicinal Chemistry.* 46(21): 4533-4542

David J, Bell RE, Clark GC. 2015. Mechanisms of disease: host-pathogen interactions between *Burkholderia* species and lung epithelial cells. *Frontiers in Cellular and Infection Microbiology.* 5: 1-13

Delhaes L, Monchy S, Frealle E, Hubans C, Salleron J, Leroy S, Prevotat A, Wallet F, Wallaert B, Dei-Cas E, Sime-Ngando T, Chabe M, Viscogliosi E. 2012. The airway microbiota in cystic fibrosis: a complex fungal and bacterial community - implications for therapeutic management. *PLoS ONE.* 7(4): e36313

Denman CC, Brown AR. 2013. Mannitol promotes adherence of an outbreak strain of *Burkholderia multivorans* via an exopolysaccharide-independent mechanism that is

associated with upregulation of newly identified fimbrial and afimbrial adhesins. *Microbiology.* 159(4): 771-781

Ding Z, Li F, Zhong C, Li F, Liu Y, Wang S, Zhao J, Li W. 2020. Structure-based design and synthesis of novel furan-diketopiperazine-type derivatives as potent microtube inhibitors for treating cancer. *Bioorganic and Medicinal Chemistry.* 28(10): 115435

Doroshenko N, Tseng BS, Howlin RP, Deacon J, Wharton JA, Thurner PJ, Gilmore BF, Parsek MR, Stoodley P. 2014. Extracellular DNA impedes the transport of vancomycin in *Staphylococcus epidermidis* biofilms pre-exposed to subinhibitory concentrations of vancomycin. *Antimicrobial Agents and Chemotherapy.* 58(12): 7273-7282

Elborn JS. 2016. Cystic fibrosis. *The Lancet.* 388(10059): 19-25

Ernst J, Klinger-Strobel M, Arnold K, Thamm J, Hartung A, Pletz MW, Makarewicz O, Fischer D. 2018. Polyester-based particles to overcome the obstacles of mucus and biofilms in the lung for tobramycin application under static and dynamic fluidic conditions. *European Journal of Pharmaceutics and Biopharmaceutics.* 131: 120-129

Fazli M, Almblad H, Rybtke ML, Givskov M, Eberl L, Tolker-Nielsen T. 2014. Regulation of biofilm formation in *Pseudomonas* and *Burkholderia* species. *Environmental Microbiology.* 16(7): 1961-1981

Fazli M, McCarthy Y, Givskov M, Ryan RP, Tolker-Nielsen T. 2013. The exopolysaccharide gene cluster Bcam1330-Bcam1341 is involved in *Burkholderia cenocepacia* biofilm formation, and its expression is regulated by c-di-GMP and Bcam1349. *MicrobiologyOpen.* 2: 105-122

Fazli M, O'Connell A, Nilsson M, Niehaus K, Dow JM, Givskov M, Ryan RP, Tolker-Nielsen T. 2011. The CRP/FNR family protein Bcam1349 is a c-di-GMP effector that regulates biofilm formation in the respiratory pathogen *Burkholderia cenocepacia. Molecular Microbiology.* 82(2): 327-341

Ferreira AS, Leitão JH, Silva IN, Pinheiro PF, Sousa SA, Ramos CG, Moreira LM. 2010. Distribution of cepacian biosynthesis genes among environmental and clinical Burkholderia

strains and role of cepacian exopolysaccharide in resistance to stress conditions. *Applied and Environmental Microbiology.* 76:441– 450

Ferreira AS, Silva IN, Oliveira VH, Cunha R, Moreira LM. 2011. Insights into the role of extracellular polysaccharides in *Burkholderia* adaptation to different environments. *Frontiers in Cellular and Infection Microbiology.* 1(16): 1-9

Ferreira MR, Gomes SC, Moreira LM. 2019. Mucoid switch in *Burkholderia cepacia* complex bacteria: triggers, molecular mechanisms and implications in pathogenesis. *Advances in Applied Microbiology.* 107: 113-140

Flemming HC, Wingender J. 2010. The biofilm matrix. *Nature Reviews Microbiology.* 8(9): 623-633

Fraser-Pitt D, Mercer D, Lovie E, Robertson J, O'Neil D. 2016. Activity of cysteamine against the cystic fibrosis pathogen *Burkholderia cepacia* complex. *Antimicrobial Agents and Chemotherapy.* 60(10): 6200-6206

Gadsby DC, Vergani P, Csanady L. 2006. The ABC protein turned chloride channel whose failure causes cystic fibrosis. *Nature.* 440: 477-483

Gaglione R, Cesaro A, Dell'Olmo E, Di Girolamo R, Tartaglione L, Pizzo E, Arciello A. 2020. Cryptides identified in human apolipoprotein B as new weapons to fight antibiotics resistance in cystic fibrosis disease. *International Journal of Molecular Sciences.* 21(6): 1-18

Gahl WA, Balog JZ, Kleta R. 2007. Nephropathic cystinosis in adults: natural history and effects of oral cysteamine therapy. *Annals of Internal Medicine.* 147(4): 242-251

Galie N, Brundage BH, Ghofrani HA, Oudiz RJ, Simonneau G, Safdar Z, Shapiro S, White RJ, Chan M, Beardsworth A, Frumkin L, Barst RJ. 2008. Tadalafil therapy for pulmonary arterial hypertension. *Circulation.* 119(22): 2894-2903

Ganesh PS, Vishnupriya S, Vadivelu J, Mariappan V, Vellasamy KM, Shankar EM. 2020. Intracellular survival and innate immune evasion of *Burkholderia cepacia*: improved

understanding of quorum sensing-controlled virulence factors, biofilm, and inhibitors. *Microbiology and Immunology.* 64(2): 87-98

Garcia BA, Carden JL, Goodwin DL, Smith TA, Gaggar A, Leon K, Antony VB, Rowe SM, Solomon GM. 2018. Implementation of successful eradication protocol for *Burkholderia cepacia* complex in cystic fibrosis patients. *BMC Pulmonary Medicine.* 18(35): 1-5

Giessen TW, Marahiel MA. 2015. Rational and combinatorial tailoring of bioactive cyclic dipeptides. *Frontiers in Microbiology.* 6: 785

Gingues S, Kooi C, Visser MB, Subsin B, Sokol PA. 2005. Distribution and expression of the ZmpA metalloprotease in the *Burkholderia cepacia* complex. *Journal of Bacteriology.* 187(24): 8247-8255

Gonzalez JF, Ortin I, de la Cuesta E, Menendez JC. 2012. Privileged scaffolds in synthesis: 2,5-piperazinediones as templates for the preparation of structurally diverse heterocycles. *Chemical Society Reviews.* 41: 6902-6915

Gu B, He S, Yan X, Zhang L. 2013. Tentative biosynthetic pathways of some microbial diketopiperazines. *Applied Microbiology and Biotechnology.* 97(19): 8439-8453

Guilhen C, Forestier C, Balestrino D. 2017. Biofilm dispersal: multiple elaborate strategies for dissemination of bacteria with unique properties. *Molecular Microbiology.* 105(2): 188-210

Hamad, M. A., Di Lorenzo, F., Molinaro, A., and Valvano, M. A. 2012. Aminoarabinose is essential for lipopolysaccharide export and intrinsic antimicrobial peptide resistance in *Burkholderia cenocepacia*. *Molecular Microbiology*. 85(5): 962–974

Harrison JJ, Stremick CA, Turner RJ, Allan ND, Olson ME, Ceri H. 2010. Microtiter susceptibility testing of microbes growing on peg lids: a miniaturized biofilm model for high-throughput screening. *Nature Protocols.* 5(7): 1236-1254

Hinsa SM, Espinosa-Urgel M, Ramos JL, O'Toole GA. 2003. Transition from reversible to irreversible attachment during biofilm formation by *Pseudomonas fluorescens* WCS365

requires an ABC transporter and a large secreted protein. *Molecular Microbiology.* 49(4): 905-918

Holden MT, Ram Chhabra S, de Nys R, Stead P, Bainton NJ, Hill PJ, Manefield M, Kumar N, Labatte M, England D, Rice S, Givskov M, Salmond GP, Stewart GS, Bycroft BW, Kjelleberg S, and Williams P. 1999. Quorum-sensing cross talk: isolation and chemical characterization of cyclic dipeptides from *Pseudomonas aeruginosa* and other gram-negative bacteria. *Molecular Microbiology.* 33: 1254-1266.

Holden MTG, Seth-Smith HMB, Crossman LC, Sebaihia M, Bentley SD, Cerdeno-Tarraga AM, Thomson NR, Bason N, Quail MA, Sharp S, Cherevach I, Churcher C, Goodhead I, Hauser H, Holroyd N, Mungall K, Scott P, Walker D, White B, Rose H, Iversen P, Mil-Homens D, Rocha EPC, Fialho AM, Baldwin A, Dowson C, Barrell BG, Govan JR, Vandamme P, Hart AC, Mahenthiralingam E, Parkhill J. 2009. The genome of *Burkholderia cenocepacia* J2315 an epidemic pathogen of cystic fibrosis patients. *Journal of Bacteriology.* 191(1): 261-277

Houston DR, Eggleston I, Synstad B, Eijsink VGH, Van Aalten DMF. 2002. The cyclic dipeptide CI-4 [cyclo-(L-Arg-D-Pro)] inhibits family 18 chitinases by structural mimicry of a reaction intermediate. *Biochemical Journal.* 27(368): 23-27

Huber B, Riedel K, Hentzer M, Heydorn A, Gotschlich A, Givskov M, Molin S, Eberl L. 2001. The *cep* quorum-sensing system of *Burkholderia cepacia* H111 controls biofilm formation and swarming motility. *Microbiology.* 147(9): 2517-2528

Huber B, Riedel K, Kothe M, Givskov M, Molin S, Eberl L. 2002. Genetic analysis of functions involved in the late stages of biofilm development in *Burkholderia cepacia* H111. *Molecular Microbiology.* 46(2): 411-426

Inhulsen S, Aguilar C, Schmid N, Suppiger A, Riedel K, Eberl L. 2012. Identification of functions linking quorum sensing with biofilm formation in *Burkholderia cenocepacia* H111. *MicrobiologyOpen.* 1(2): 225-242

Isles A, Maclusky I, Corey M, Gold R, Prober C, Fleming P, Levison H. 1984. *Pseudomonas cepacia* infection in cystic fibrosis: an emerging problem. *The Journal of Pediatrics.* 104(2): 206-210

Jiang Y, Geng M, Bai L. 2020. Targeting biofilms therapy: current research strategies and development hurdles. *Microorganisms.* 8(1222): 1-34

Jorgensen S, Skov KW, Diderichsen B. 1991. Cloning, sequencing, and expression of a lipase gene from *Pseudomonas cepacia:* lipase production in heterologous hosts requires two *Pseudomonas* genes. *Journal of Bacteriology.* 173: 559-567

Kanoh K, Kohno S, Katada J, Takahashi J, Uno I, Hayashi Y. 1999. Synthesis and biological activities of phenylahistin derivatives. *Bioorganic & Medicinal Chemistry.* 7(7): 1451-1457

Kennedy S, Beaudoin T, Yau YCW, Caraher E, Zlonsnik JEA, Spreet DP, LiPuma JJ, Tullis E, Waters V. 2016. Activity of tobramycin against cystic fibrosis isolates of *Burkholderia cepacia* complex grown as biofilms. *Antimicrobial Agents and Chemotherapy.* 60(1): 348-355

Koo H, Allan RN, Howlin RP, Stoodley P, Hall-Stoodley L. 2017. Targeting microbial biofilms: current and prospective therapeutic strategies. *Nature Reviews Microbiology.* 15(12): 740-755

Kooi C, Subsin B, Chen R, Pohorelic B, Sokol PA. 2006. *Burkholderia cenocepacia* ZmpB is a broad-specificity zinc metalloprotease involved in virulence. *Infection and Immunity.* 74(7): 4083-4093

Kostakioti M, Hadjifrangiskou M, Hultgren SJ. 2013. Bacterial biofilms: development, dispersal, and therapeutic strategies in the dawn of the postantibiotic era. *Cold Spring Harbor Perspectives in Medicine.* 3(4): a010306

Kothe M, Antl M, Huber B, Stoecjer K, Ebrecht D, Steinmetz I, Eberl L. 2003. Killing of *Caenorhabditis elegans* by *Burkholderia cepacia* is controlled by the *cep* quorum-sensing system. *Cell Microbiology.* 5(5): 343-351

Lameignere E, Malinovska L, Slavikova M, Duchaud E, Mitchell EP, Varrot A, Sedo O, Imberty A, Wimmerova M. 2008. Structural basis for mannose recognition by a lectin from opportunistic bacteria *Burkholderia cenocepacia. Biochemical Journal.* 411(2): 307-318

Lasa I, Penades JR. 2006. Bap: a family of surface proteins involved in biofilm formation. *Research in Microbiology.* 157(2): 99-107

Lautru S, Gondry M, Genet R, and Pernodet JL. 2002. The albonoursin gene cluster of *S. noursei* biosynthesis of diketopiperazine metabolites independent of nonribosomal peptide synthetases. *Chemistry & Biology.* 9: 1355–1364

Lewenza S, Conoway B, Greenberg EP, Sokol PA. 1999. Quorum sensing in *Burkholderia cepacia*: identification of the LuxRI homologs CepIR. *Journal of Bacteriology.* 181(3): 748-756

Lewenza S, Sokol PA. 2001. Regulation of ornibactin biosynthesis and *N*-Acyl-L-Homoserine lactone production by CepR in *Burkholderia cepacia. Journal of Bacteriology.* 183(7): 2212-2218

Liao S, Qin X, Li D, Tu Z, Li J, Zhou X, Wang J, Yang B, Lin X, Liu J, Yang X, Liu Y. 2014. Design and synthesis of novel soluble 2,5-diketopiperazine derivatives as potential anticancer agents. *European Journal of Medicinal Chemistry.* 83: 236-244

Lonon MK, Woods DE, Straus DC. 1988. Production of lipase by clinical isolates of *Pseudomonas cepacia. Journal of Clinical Microbiology.* 26(5): 979-984

Macia MD, Rojo-Molinero E, Oliver A. 2014. Antimicrobial susceptibility testing in biofilm-growing bacteria. *Clinical Microbiology and Infection.* 20(10): 981-990

Maeda K, Nakata H, Koh Y, Miyakawa T, Ogata H, Takaoka Y, Shibayama S, Sagawa K, Fukushima D, Moravek J, Koyanagi Y, Mitsuya H. 2004. Spirodiketopiperazine-based CCR5 inhibitor which preserves CC-chemokine/CCR5 interactions and exerts potent activity against R5 human immunodeficiency virus type 1 *in vitro. Journal of Virology.* 78(16): 8654-8662

Mahenthiralingam E, Coenye T, Chung JW, Speert DP, Govan JR, Taylor P, Vandamme P. 2000. Diagnostically and experimentally useful panel of strains for *Burkholderia cepacia* complex. *Journal of Clinical Microbiology.* 38: 910-913

Mahenthiralingam E, Urban TA, Goldberg JB. 2005. The multifarious, multireplicon *Burkholderia cepacia* complex. *Nature Reviews Microbiology.* 3(2): 144-156

Malott RJ, Baldwin A, Mahenthiralingam E, Sokol PA. 2005. Characterization of the *cciIR* quorum-sensing system in *Burkholderia cenocepacia. Infection and Immunity.* 73(8): 4982-4992

Mariappan V, Vellasamy KM, Hshim OH, Vadivelu J. 2011. Profiling of *Burkholderia cepacia* secretome at mid-logarithmic and early-stationary phases of growth. *PLoS ONE.* 6(10): 1-9

Mathew A, Eberl L, Carlier AL. 2014. A novel siderophore-independent strategy of iron uptake in the genus *Burkholderia. Molecular Microbiology.* 91(4): 805-820

Matsui H, Grubb BR, Tarran R, Randell SH, Gatzy JT, Davis CW, Boucher RC. 1998. Evidence for periciliary liquid layer depletion, not abnormal ion composition, in the pathogenesis of cystic fibrosis airways disease. *Cell.* 95: 1005-1015

McCafferty GP, Pullen MA, Wu C, Edwards RM, Allen MJ, Woodlard PM, Borthwick AD, Liddle J, Hickey DMB, Brooks DP, Westfall TD. 2007. Use of a novel and highly selective oxytocin receptor antagonist to characterize uterine contractions in the rat. *American Journal of Physiology – Regulatory, Integrative and Comparative Physiology.* 293: R299-R305

McClean S, Callaghan M. 2009. *Burkholderia cepacia* complex: epithelial cell-pathogen confrontations and potential for therapeutic intervention. *Journal of Medical Microbiology.* 58(1): 1-12

McKeon SA, Nguyen DT, Viteri DF, Zlosnik JEA, Sokol PA. 2011. Functional quorum sensing systems are maintained during chronic *Burkholderia cepacia* complex infections in patients with cystic fibrosis. *Journal of Infectious Diseases.* 203(3): 383-392

Messiaen AS, Neils H, Coenye T. 2014. Investigating the role of matrix components in protection of *Burkholderia cepacia* complex biofilms against tobramycin. *Journal of Cystic Fibrosis.* 13(1): 56-62

Miyoshi T, Miyairi N, Aoki H, Kohsaka M, Sakai H, Imanaka H. 1972. Bicyclomycin, a new antibiotic: taxonomy, isolation and characterization. *Journal of Antibiotics.* 25(10): 569-575

Mullen T, Markey K, Murphy P, McClean S, Callaghan M. 2007. Role of lipase in *Burkholderia cepacia* complex (Bcc) invasion of lung epithelial cells. *European Journal of Clinical Microbiology and Infectious Diseases.* 26(12): 869-877

Munkholm M, Mortensen J. 2014. Mucociliary clearance: pathophysiological aspects. *Clinical Physiology and Functional Imaging.* 34(3): 171-177

Narayanaswamy VP, Duncan AP, LiPuma JJ, Wiesmann WP, Baker SM, Townsend SM. 2019. *In vitro* activity of a novel glycopolymer against biofilms of *Burkholderia cepacia* complex cystic fibrosis clinical isolates. *Antimicrobial Agents and Chemotherapy.* 63(6): 1-11

Narayanaswamy VP, Giatpaiboon S, Baker SM, Wiesmann WP, LiPuma JJ, Townsend SM. 2017. Novel glycopolymer sensitizes *Burkholderia cepacia* complex isolates from cystic fibrosis patients to tobramycin and meropenem. *PLoS ONE.* 12(6): 1-12

Nicholson B, Lloyd GK, Miller BR, Palladino MA, Kiso Y, Hayashi Y, Neuteboom STC. 2006. NPI-2358 is a tubulin-depolymerizing agent: in vitro evidence for activity as a tumor vascular-disrupting agent. *Anti-Cancer Drugs.* 17(1): 25-31

O'Grady EP, Viteri DF, Malott RJ, Sokol PA. 2009. Reciprocal regulation by the CepIR and CciIR quorum sensing systems in *Burkholderia cenocepacia. BMC Genomics.* 10: 441

O'Toole GA. 2011. Microtiter dish biofilm formation assay. *Journal of Visualized Experiments.* 47: 2437

Ortiz A, Sansinenea E. 2017. Cyclic dipeptides: secondary metabolites isolated from different microorganisms with diverse biological activities. *Current Medicinal Chemistry.* 24(25): 2773-2780

Padilha G, Osorio W. 2019. Economic method for extraction/purification of a *Burkholderia cepacia* lipase with potential biotechnology application. *Applied Biochemistry and Biotechnology.* 189(4): 1108-1126

Palmer KL, Aye LM, Whiteley M. 2007. Nutritional cues control *Pseudomonas aeruginosa* multicellular behavior in cystic fibrosis sputum. *Journal of Bacteriology.* 189(22): 8079-808

Peeters E, Nelis HJ, Coenye T. 2009. *In vitro* activity of ceftazidime, ciprofloxacin, meropenem, minocycline, tobramycin and trimethoprim/sulfamethoxazole against planktonic and sessile *Burkholderia cepacia* complex bacteria. *Journal of Antimicrobial Chemotherapy*. 64(4): 801-809

Perzborn M, Syldatk C, Rudat J. 2013. Enzymatical and microbial degradation of cyclic dipeptides (diketopiperazines). *AMB Express.* 3: 51

Pope CF, Gillespie SH, Pratten JR, McHugh TD. 2008. Fluoroquinolone- resistant mutants of *Burkholderia cepacia*. *Antimicrobial Agents and Chemotherapy.* 52(3): 1201–1203

Purighalla S. 2011. Interactions between *Pseudomonas aeruginosa* and *Burkholderia* spp. in cystic fibrosis. (MSc Thesis) University of Calgary, Canada

Ramarao N, Nielsen-Leroux C, Lereclus D. 2012. The insect *Galleria mellonela* as a powerful infection model to investigate bacterial pathogenesis. *Journal of Visualized Experiments.* 70: 1-7

Reihill JA, Moreland M, Jarvis GE, McDowell A, Einarsson GG, Elborn JS, Martin SL. 2017. Bacterial proteases and haemostasis dysregulation in the CF lung. *Journal of Cystic Fibrosis.* 16(1): 49-57

Ressurreicao ASM, Delatouche R, Gennari C, Piarulli U. 2011. Bifunctional 2,5-Diketopiperazines as rigid three-dimensional scaffolds in receptors and peptidomimetics. *European Journal of Organic Chemistry.* 2: 217-228

Rhodes KA, Schweizer HP. 2017. Antibiotic resistance in *Burkholderia* species. *Physiology & Behavior.* 176(5): 139-148

Riordan JR, Rommens JM, Kerem B, Alon N, Rozmahel R, Grzelckak Z. 1989. Identification of the cystic fibrosis gene: cloning and characterization of complementary DNA. *Science.* 245: 1066-1072

Romling U, Fiedler B, Bosshammer J, Grothues D, Greipel J, von der Hardt H, Tummler B. 1994. Epidemiology of chronic *Pseudomonas aeruginosa* infections in cystic fibrosis. *Journal of Infectious Diseases.* 170: 1616-1621

Rudilla H, Merlos A, Sans-Serramitjana E, Fuste E, Sierra JM, Zalacain A, Vinuesa T, Vinas M. 2018. New and old tools to evaluate new antimicrobial peptides. *AIMS Microbiology.* 4(3): 522-540

Rushton L, Sass A, Baldwin A, Dowson CG, Donoghue D, Mahenthiralingam E. 2013. Key role for efflux in the preservative susceptibility and adaptive resistance of *Burkholderia cepacia* complex bacteria. *Antimicrobial Agents and Chemotherapy*. 57(7): 2972–2980

Sanchez DA, Tonetto GM, Ferreira ML. 2018. *Burkholderia cepacia* lipase: a versatile catalyst in synthesis reactions. *Biotechnology and Bioengineering.* 115(1): 6-24

Saruwatari T, Yagishita F, Mino T, Noguchi H, Hotta K, Watanabe K. 2014. Cytochrome P450 as dimerization catalyst in diketopiperazine alkaloid biosynthesis. *ChemBioChem.* 15: 656-659

Sass A, Slachmuylders L, Van Acker H, Vandenbussche, Ostyn L, Bove M, Crabbe A, Chiarelli LR, Buroni S, Van Nieuwerburgh F, Abatih E, Coenye T. 2019. Various evolutionary trajectories lead to loss of the tobramycin-potentiating activity of the quorum-sensing inhibitor baicalin hydrate in *Burkholderia cenocepacia* biofilms. *Antimicrobial Agents and Chemotherapy.* 63(4): 1-14

Sathyanarayanan MB, Balachandranath R, Srinivasulu YG, Kannaiyan SK, Subbiahdoss G. 2013. The effect of gold and iron-oxide nanoparticles on biofilm-forming pathogens. *ISRN Microbiology.* 2013: 272086

Saucer K, Cullen MC, Rickard AH, Zeef LAH, Davies DG, Gilbert. 2004. Characterization of nutrient-induced dispersion in *Pseudomonas aeruginosa* PAO1 biofilm. *Journal of Bacteriology.* 186(21): 7312-7326

Schmid N, Pessi G, Deng Y, Aguilar C, Carlier AL, Grunau A, Omasits Zhang LH, Ahrens CH, Eberl L. 2012. The AHL- and BDSF-dependent quorum sensing systems control specific and overlapping sets of genes in *Burkholderia cenocepacia* H111. *PLoS ONE.* 7(11): 1-12

Schwyn B, Neilands JB. 1987. Universal chemical assay for the detection and determination of siderophores. *Analytical Biochemistry.* 160: 47–56

Scoffone VC, Chiarelli LR, Makarov V, Brackman G, Israyilova A, Azzalin A, Forneris F, Riabova O, Savina S, Coenye T, Riccardi G, Buroni S. 2016. Discovery of new diketopiperazines inhibiting *Burkholderia cenocepacia* quorum sensing *in vitro* and *in vivo. Scientific Reports.* 6: 32487.

Scoffone VC, Chiarelli LR, Trespidi G, Mentasti M, Riccardi G, Buroni S. 2017. *Burkholderia cenocepacia* infections in cystic fibrosis patients: drug resistance and therapeutic approaches. *Frontiers in Microbiology.* 8(1592): 1-13

Scoffone VC, Trespidi G, Chiarelli LR, Barnieri G, Buroni S. 2019. Quorum sensing as antivirulence target in cystic fibrosis pathogens. *International Journal of Molecular Sciences.* 20(8): 1-38

Sfeir MM. 2018. *Burkholderia cepacia* complex infection: more complex than the bacterium name suggests. *Journal of Infection.* 77(3): 166-170

Sharma D, Misba L, Khan AU. 2019. Antibiotics versus biofilm: an emerging battleground in microbial communities. *Antimicrobial Resistance and Infection Control*. 8(1): 76

Shaw E, Wuest WM. 2020. Virulence attenuating combination therapy: a potential multi-target synergy approach to treat *Pseudomonas aeruginosa* infections in cystic fibrosis patients. *RSC Medicinal Chemistry.* 11(3): 358-369

Shimazaki N, Shima I, Okamoto M, Yoshida K, Hemmi K, Hashimoto M. 1991. PAF inhibitory activity of diketopiperazines: structure-activity relationships. *Lipids.* 26(12): 1175-1178

Silva IN, Santos PM, Santos MR, Zlosnik JEA, Speert DP, Buskirk SW, Bruger EL, Waters CM, Cooper VS, Moreira LM. 2016. Long-term evolution of *Burkholderia multivorans* during a

chronic cystic fibrosis infection reveals shifting forces of selection. *mSystems.* 1(3): e00029-16

Singh AV, Bandi M, Raje N, Richardson P, Palladino MA, Chauhan D, Anderson KC. 2011. A novel vascular disrupting agent plinabulin triggers JNK-mediated apoptosis and inhibits angiogenesis in multiple myeloma cells. *Blood.* 117(21): 5692-5700

Slachmuylders L, Van Acker H, Brackman G, Sass A, Van Nieuwerburgh F, Coenye T. 2018. Elucidation of the mechanism behind the potentiating activity of baicalin against *Burkholderia cenocepacia* biofilms. *PLoS ONE.* 13(1): 1-18

Slinger BL, Deay JJ, Chandler JR, Blackwell HE. 2019. Potent modulation of the CepR quorum sensing receptor and virulence in a *Burkholderia cepacia* complex member using non-native lactone ligands. *Scientific Reports.* 9: 13449

Smith EE, Buckley DG, Wu Z, Saenphimmachak C, Hofman LR, D-Argenio DA, Miller SI, Ramsey BW, Speert DP, Moskowitz SM, Burns JL, Kaul R, Olson MV. 2006. Genetic adaptation by *Pseudomonas aeruginosa* to the airways of cystic fibrosis patients. *Proceedings of the National Academy of Sciences of the United States of America.* 103(22): 8487-8492

Sokol PA, Darling P, Woods DE, Mahenthiralingam E, Kooi C. 1999. Role of ornibactin biosynthesis in the virulence of *Burkholderia cepacia:* characterization of pvdA, the gene encoding L-ornithine N(5)-oxygenase. *Infection and Immunity.* 67: 4443-4455

Sokol PA, Malott RJ, Riedel K, Eberl L. 2007. Communication systems in the genus *Burkholderia:* global regulators and targets for novel antipathogenic drugs. *Future Microbiology.* 2(5): 555-563

Sokol PA, Sajjan U, Visser MB, Gingues S, Forstner J, and Kooi C. 2003. The CepIR quorum-sensing system contributes to the virulence of *Burkholderia cenocepacia* respiratory infections. *Microbiology.* 149: 3649-3658

Sousa SA, Ramos CG, Leitao JH. 2011. *Burkholderia cepacia* complex: emerging multihost pathogens equipped with a wide range of virulence factors and determinants. *International Journal of Microbiology.* 2011: 1-9

Sousa SA, Ulrich M, Bragonzi A, Burke M, Worlitzsch D, Leitão JH, Meisner C, Eberl L, Sá-Correia I, Döring G. 2007. Virulence of *Burkholderia cepacia* complex strains in gp91$^{phox-/-}$ mice. *Cellular Microbiology.* 9:2817–2825

Stone MRL, Butler MS, Phestsang W, Cooper MA, Blaskovich MAT. 2018. Fluorescent antibiotics: new research tools to fight antibiotic resistance. *Trends in Biotechnology.* 36(5): 523-536

Straus DC, Lonon MK, Huston JC. 1992. Inhibition of rat alveolar macrophage phagocytic function by a *Pseudomonas cepacia* lipase. *Journal of Medical Microbiology.* 37(5): 335-340

Subramoni S, Sokol PA. 2012 Quorum sensing systems influence *Burkholderia cenocepacia* virulence. *Future Microbiology.* 7(12): 1373-1387

Subsin B, Chambers CE, Visser MB, Sokol PA. 2007. Identification of genes regulated by the *cepIR* quorum-sensing system in *Burkholderia cenocepacia* by high-throughput screening of a random promoter library. *Journal of Bacteriology.* 189(3): 968-979

Sulak O, Cioci G, Delia M, Lahmann M, Varrot A, Imberty A, Wimmerova M. 2010. A TNF-like trimeric lectin domain from *Burkholderia cenocepacia* with specificity for fucosylated human histo-blood group antigens. *Structure.* 18(1): 59-72

Suppiger A, Schmid N, Aguilar C, Pessi G, Eberl L. 2013. Two quorum sensing systems control biofilm formation and virulence in members of the *Burkholderia cepacia* complex. *Virulence.* 4(5): 400-409

Thieme L, Hartung A, Tramm K, Klinger-Strobel M, Jandt KD, Makarewicz O, Pletz MW. 2019. MBEC versus MBIC: the lack of differentiation between biofilm reducing and inhibitory effects as a current problem in biofilm methodology. *Biological Procedures Online.* 21(1): 1-5

Tomlin KL, Malott RJ, Ramage G, Storey DG, Sokol PA, Ceri H. 2005. Quorum-sensing mutations affect attachment and stability of *Burkholderia cenocepacia* biofilms. *Applied and Environmental Microbiology.* 71(9): 5208-5218

Traverse CC, Mayo-Smith LM, Poltak SR, Cooper VS. 2012. Tangled bank of experimentally evolved *Burkholderia* biofilms reflects selection during chronic infections. *Proceedings of the National Academy of Sciences of the United States of America.* 110(3): E250-E259

Tseng SP, Tsai WC, Liang CY, Lin YS, Huang JW, Chang CY, Tyan YC, Lu PL. 2014. The contribution of antibiotic resistance mechanisms in clinical *Burkholderia cepacia* complex isolates: an emphasis on efflux pump activity. *PLoS ONE.* 9(8): 1-10

Tyers M, Wright GD. 2019. Drug combinations: a strategy to extend the life of antibiotics in the 21st century. *Nature Reviews Microbiology.* 17(3): 141-155

Udine C, Brackman G, Bazzini S, Buroni S, Van Acker H, Pasca MR, Riccardi G, Coenye T. 2013. Phenotypic and genotypic characterization of *Burkholderia cenocepacia* J2315 mutants affected in homoserine lactone and diffusible signal factor-based quorum sensing systems suggests interplay between both types of systems. *PLoS ONE.* 8(1): 1-12

Uehlinger S, Schwager S, Bernier SP, Riedel K, Nguyen DT, Sokol PA, Eberl L. 2009. Identification of specific and universal virulence factors in *Burkholderia cenocepacia* strains by using multiple infection hosts. *Infection and Immunity.* 77(9): 4102-4110

Vior NM, Lacret R, Chandra G, Dorai-Raj S, Trick M, Truman AW. 2018. Discovery and biosynthesis of the antibiotic bicyclomycin in distantly related bacterial classes. *Applied and Environmental Microbiology.* 84(9): e02828-17

Visser MB, Majumdar S, Hani E, Sokol PA. 2004. Importance of the ornibactin and pyochelin siderophore transport systems in *Burkholderia cenocepacia* lung infections. *Infection and Immunity.* 72(5): 2850-2857

Wopperer J, Cardona ST, Huber B, Jacobi CA, Valvano MA, Eberl L. 2006. A quorum-quenching approach to investigate the conservation of quorum-sensing-regulated functions within the *Burkholderia cepacia* complex. *Applied and Environmental Microbiology.* 72(2): 1579-1587

Wright GD. 2016. Antibiotic adjuvants: rescuing antibiotics from resistance. *Trends in Microbiology.* 24(11): 862-871

Zhao P, Xue Y, Li J, Li X, Zu X, Zhao Z, Quan C, Gao W, Feng S. 2019. Non-lipopeptide fungi-derived peptide antibiotics developed since 2000. *Biotechnology Letters.* 41: 651-673

Zhou J, Chen Y, Tabibi S, Alba L, Garber E, Saiman L. 2007. Antimicrobial susceptibility and synergy studies of *Burkholderia cepacia* complex isolated from patients with cystic fibrosis. *Antimicrobial Agents and Chemotherapy.* 51(3): 1085-1088

Supplementary Information

Supplementary Figure 1: Growth curves of Bcc species

Bacterial strains **(a)** *B. cepacia* 15862, **(b)** *B. cepacia* 16192, **(c)** *B. multivorans* C5393, **(d)** *B. multivorans* LMG13010, **(e)** *B. cenocepacia* H111, **(f)** *B. cenocepacia* K56-2, **(g)** *B. cenocepacia* K56-*cciIR*, **(h)** *B. cenocepacia* K56-*cepR,cciIR* were grown in 15mL culture tubes containing SCFM (3mL) at 37 ˚ C and 250 rpm. Optical density readings (at 600nm) were recorded every two hours for 24 hours. The light grey dashed line indicates the early stationary phase time point assessed in this study, while the dark grey dashed line indicates the late stationary phase time point.

a)

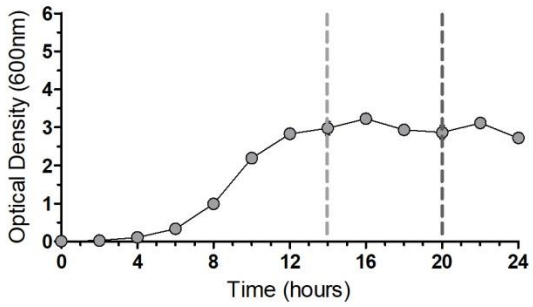
Optical Density (600nm)
Time (hours)

b)

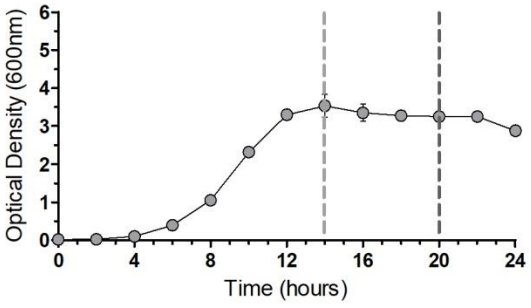
Optical Density (600nm)
Time (hours)

c)

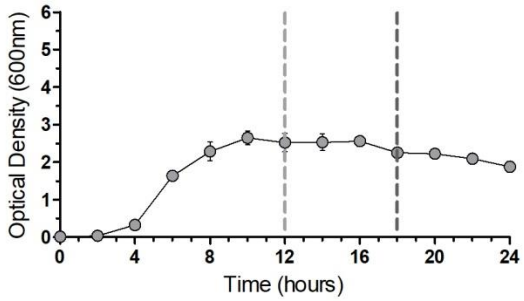
Optical Density (600nm)
Time (hours)

d)

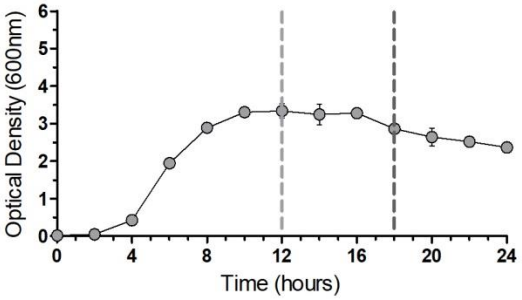
Optical Density (600nm)
Time (hours)

e)

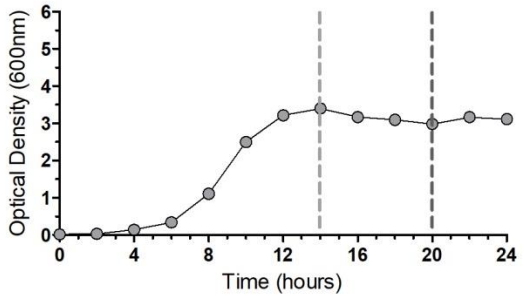
Optical Density (600nm)
Time (hours)

f)

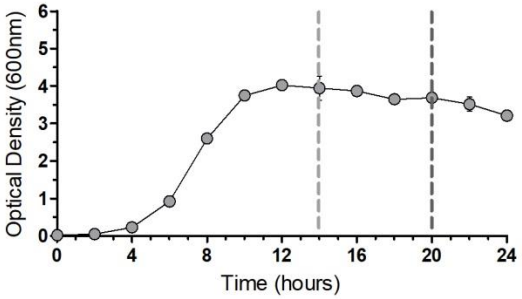
Optical Density (600nm)
Time (hours)

g)

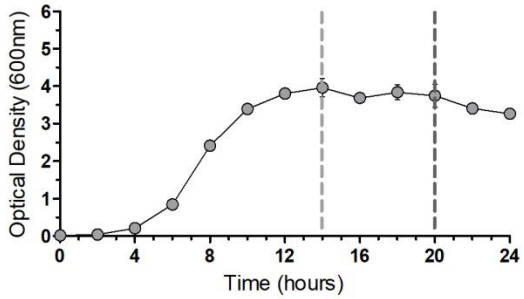
Optical Density (600nm)
Time (hours)

h)

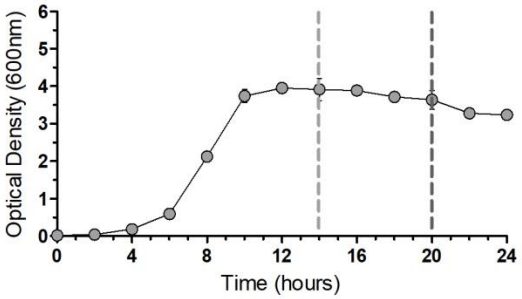
Optical Density (600nm)
Time (hours)

Supplementary Figure 2: Biofilm equivalency test

(a) A diagram of a 96-well plate indicating the different components added to each well for the assessment of equivalent biofilm formation. Biofilms were grown for 24 hours at 37 ° C and 120 rpm prior to each form of assessment. **(b)** Results of the biofilm biomass equivalency test using the crystal violet (CV) staining method. **(c)** Results of the viable biofilm cell count test utilizing the CBD and viable cell enumeration techniques. These tests were each carried out two times with each data point representing the average of six wells (n=6). Significance was determined by one-way ANOVA and the Tukey post-hoc test where no significance was seen between any of the data points. Bars indicate ± SD.

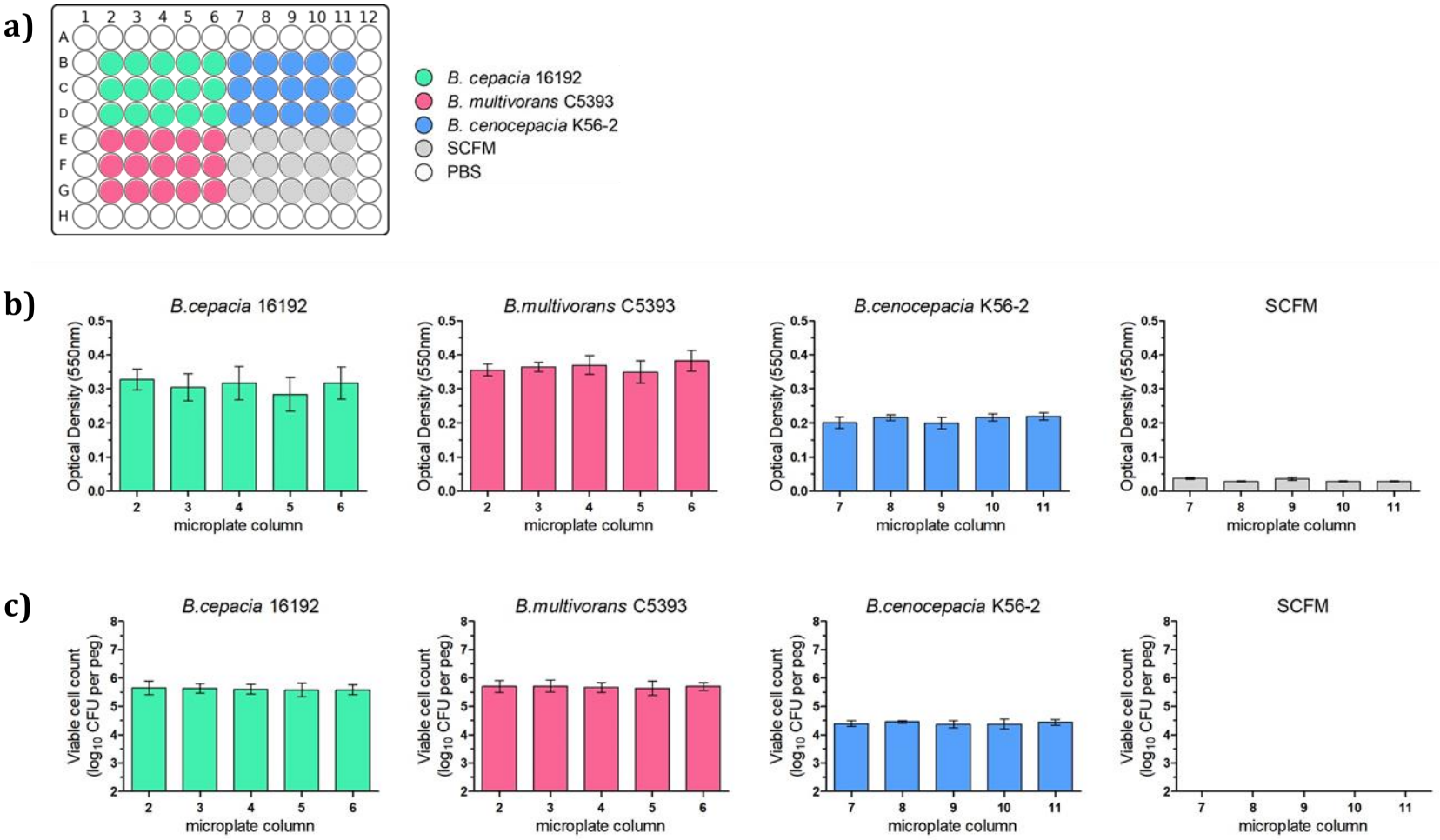
a)
1 2 3 4 5 6 7 8 9 10 11 12
A
B
C
D
E
F
G
H
B. cepacia 16192
B. multivorans C5393
B. cenocepacia K56-2
SCFM
PBS
b)
B.cepacia 16192
B.multivorans C5393
B.cenocepacia K56-2
SCFM
Optical Density (550nm)
microplate column
c)
Viable cell count (log10 CFU per peg)
microplate column